



Feasibility and benefit of different lashing arrangements for sea transport of containers on weather deck

Antonio Guimaraes

Master Thesis

presented in partial fulfillment

of the requirements for the double degree:

“Advanced Master in Naval Architecture” conferred by University of Liege
"Master of Sciences in Applied Mechanics, specialization in Hydrodynamics, Energetics and Propulsion" conferred by Ecole Centrale de Nantes

developed at West Pomeranian University of Technology, Szczecin
in the framework of the

“EMSHIP”

Supervisors: Dr. Tadeusz Graczyk, West Pomeranian University of Technology, Szczecin
Dipl. Ing. Viktor Wolf, Germanischer Lloyd SE

Reviewer: Dr. Robert Bronsart, University of Rostock

Szczecin, February 2013



Universität Rostock



Traditio et Innovatio



Zachodniopomorski
Uniwersytet
Technologiczny
w Szczecinie

DRAFT

ABSTRACT

Nowadays, seagoing container ships carry cargo containers stowed on weather deck up to eight or even nine tiers high. In heavy sea conditions or in case of improper stowage, deck containers and their securing equipment are exposed to extreme forces caused by sea induced ship motions, gravity, wind, and green water. An inadequate dimensioning of container securing system may result in container damages and losses. An effort has been made by shipping industry and classification societies to prevent failure of container securing systems and, thus, to minimize container damages and losses at sea. On the other hand, due to economic reasons, shipping companies aspire to optimize the utilization of their fleet. Consequently, suppliers of container lashing equipment develop alternative methods for container securing on weather deck, such as external lashing, promising higher container capacity of existing ships. To ensure safe and reliable container transport on board ships, a particular verification of those novel container securing systems is required for approval of container stowage and lashing plans by classification societies.

The basic difference between the often used internal lashing to the alternative external lashing system is that the first one secures the compressed side of the stack, while the second one secures the lifted side of stack. Thus, with internal lashing the compressive load acting on container posts is increased by the vertical component of the lashing force, limiting the allowable stack weight. This limitation does not occur when external lashing is used, allowing higher stack weights and better cargo distribution. In the other hand, the lashing force can be a limiting point due to the overloading caused on the lashing rod by uplifting, especially when high vertical clearance is allowed on the locks.

Parametric studies were conducted with FEM models of container stacks using external lashing system. Parameters as lashing rod pre-tension, twist lock stiffness, lashing rod and lashing bridge stiffness and vertical clearance of twist locks were analyzed. The effect of these parameters on the operational loads acting on containers and lashing equipments was studied, and the parameters of influence and their sensitivities were determined.

Using the outputs of the parametric studies, practical design criteria for stowage systems using external lashing were derived. The vertical clearance of twist locks was the most relevant design criteria for single stacks, having a strong influence especially on the lashing forces due to the uplifting. The determination of the lashing forces as a function of relevant system parameters, e.g. height of lashing bridge and twist lock type, was necessary.

Comparative analyses of internal and external lashing regarding allowable stack weights and cargo distribution were performed. The comparison was made for each stack configuration (stack height and lashing bridge configuration), showing the benefits and drawbacks of each lashing system for the shipping companies.

DRAFT

DECLARATION OF AUTHORSHIP

I declare that this thesis and the work presented in it are my own and have been generated by me as the result of my own original research.

Where I have consulted the published work of others, this is always clearly attributed.

Where I have quoted from the work of others, the source is always given. With the exception of such quotations, this thesis is entirely my own work.

I have acknowledged all main sources of help.

Where the thesis is based on work done by myself jointly with others, I have made clear exactly what was done by others and what I have contributed myself.

This thesis contains no material that has been submitted previously, in whole or in part, for the award of any other academic degree or diploma.

I cede copyright of the thesis in favour of the West Pomeranian University of Technology.

Date:

Signature

DRAFT

CONTENTS

1. INTRODUCTION.....	1
1.1. Motivation	3
1.2. Objectives.....	4
1.2.1. Parametric Studies.....	5
1.2.2. Design Criteria Definition.....	5
1.2.3. Comparison Between Internal and External Lashing Arrangements.....	5
1.2.4. Additional Studies.....	5
2. PROBLEM DESCRIPTION.....	7
2.1. The Evolution on the Design of Container Ships.....	7
2.2. Container Dimensions and Types	8
2.3. Container Stowage on Weather Deck	10
2.4. Lashing Components.....	11
2.4.1. Lashing Plate.....	12
2.4.2. Base Socket.....	13
2.4.3. Lashing Assemblies – Lashing Rod and Turnbuckle.....	13
2.4.4. Twist Locks.....	15
2.5. Lashing Bridge.....	16
2.6. Container Securing Arrangements	17
2.6.1. Internal Lashing.....	19
2.6.2. External Lashing	20
2.7. Ship Behaviour and Loading.....	22

2.8. Permissible Loads on Containers and Lashing Components	24
2.9. Cargo Securing Manual.....	25
2.10. Containers Lost Overboard	26
3. BIBLIOGRAPHICAL REVIEW	29
4. METHODOLOGY	33
5. PARAMETRIC STUDIES.....	41
5.1. Ship Dimensions	41
5.2. Studied Parameters	43
5.2.1. Lashing assembly pre-tension	43
5.2.2. Twist lock vertical stiffness.....	44
5.2.3. Lashing stiffness (lashing assembly and lashing bridge).....	44
5.2.4. Vertical clearance of locks	45
5.3. Nominal Values.....	45
5.3.1. Bay 74 – Row 02.....	45
5.3.2. Bay 30 – Row 02.....	48
5.3.3. Additional Stack.....	49
5.4. Lashing Rod Pre-Tension Variation.....	50
5.5. Twist Lock Vertical Stiffness.....	53
5.6. Lashing Stiffness Variation.....	55
5.6.1. Bay 74 – Row 02.....	56
5.6.2. Bay 30 – Row 02.....	59
5.7. Variation of the Vertical Clearance of Locks.....	62
5.7.1. Bay 74 – Row 02.....	62
5.7.2. Bay 30 – Row 02.....	68

5.7.3. Additional Stack	75
6. DESIGN CRITERIA	83
7. COMPARISON BETWEEN LASHING ARRANGEMENTS	89
7.1. Maximum Cargo Capacity	89
7.1.1. 8-Tier High Stack with 2-Tier High Lashing Bridge	90
7.1.2. 6-Tier High Stack with 1-Tier High Lashing Bridge	93
7.1.3. 4-Tier High Stack with no Lashing Bridge	95
7.2. Linear Cargo Distribution	97
7.2.1. 8-Tier High Stack with 2-Tier High Lashing Bridge	97
7.2.2. 6-Tier High Stack with 1-Tier High Lashing Bridge	99
7.2.3. 4-Tier High Stack with no Lashing Bridge	101
7.3. Additional Calculation	102
8. ADDITIONAL STUDIES	105
8.1. Lashing Assembly Stiffness	105
8.2. Lashing Bridge Stiffness	108
9. CONCLUSIONS	111
9.1. Future Work	113
10. ACKNOWLEDGEMENTS	115
11. BIBLIOGRAPHY	117
12. APPENDIX I – TRADE STATISTICS	121
13. APPENDIX II – CONTAINER TYPES	125
14. APPENDIX III – OPERATIONAL LOAD LIMITS	127
15. APPENDIX IV – DESIGN CRITERIA WORKFLOW	129

DRAFT

LIST OF FIGURES

Figure 1.1 – Far East – North Europe trade line from Hanjin Shipping Company (Hanjin 2013).....	1
Figure 1.2. <i>CMA CGM Marco Polo</i> , the biggest container ship in the world (Wikipedia 2013).	2
Figure 1.3. Containers stowed in holds and on weather deck. Code of container position and definition of bays (longitudinal position), rows (transverse position) and tiers (vertical position) for stack (A) and container (B) positioning (GL 2012).	3
Figure 1.4 – Internal (left) and external (right) lashing arrangements.	4
Figure 2.1 – Evolution of the Panamax container ships (US Army 2013).....	8
Figure 2.2 – Containers stacked on weather deck (Murdoch and Tozer n.d.).	10
Figure 2.3 - Containers stacked on weather deck with lashing bridge (Murdoch and Tozer n.d.).....	11
Figure 2.4 – Lashing components on deck: twist lock (1), turnbuckle (2), lashing rod (3), single (4) and double (5) base socket and lashing plate (6) (Murdoch and Tozer n.d.).....	12
Figure 2.5 – Lashing plate (left) and scheme for welding on deck, hatch cover or lashing bridge (right). The angle depends on the distance between the lashing plate and the container front (SEC 2007).	12
Figure 2.6 – D-ring, alternative design for the lashing plate (ABS 2010).	12
Figure 2.7 – Double base socket placing two containers and twist locks.	13
Figure 2.8 – Example of a lashing rod with four attachment positions (SEC 2007).	14
Figure 2.9 – Example of turnbuckle design (ABS 2010).	15
Figure 2.10 – Examples of twist lock designs: manual lock (left), fully-automatic lock (middle) and semi-automatic lock (right) (ABS 2010).	15

Figure 2.11 - Example of a SAL design and its dimensions.	16
Figure 2.12 - Lashing bridge or raised lashing platform (ABS 2010).	17
Figure 2.13 – Two different combinations of lashing arrangements against lateral wind forces (ABS 2010).	18
Figure 2.14 – Internal lashing arrangement (ABS 2010).	20
Figure 2.15 – External lashing arrangement (ABS 2010).	21
Figure 2.16 – Deformed behaviour of the end walls of a container frame when subjected to lateral acceleration: in the left, racking deformation at the door end; in the right, uplifting at the front end.	21
Figure 2.17 – Free body diagram of a ship during rolling motion.	22
Figure 2.18 – Forces acting on container posts. Uplifting force (left) and container post load (right) (GL 2012).	24
Figure 2.19 – Racking forces acting on container frames (GL 2012).	25
Figure 3.1 – FE models of 20-foot container and FAL used in the calculations of (Rathje, Darie and Schnorrer 2008).	30
Figure 3.2 - Deformation mode of a multi-stack configuration at the maximum rolling angle (Wolf and Rathje, Motion Simulation of Container Stacks on Deck 2009).	31
Figure 3.3 – Experimental and numerical analyses performed with a 20-foot ISO container (Wolf, Darie and Rathje, Rule Development for Container Stowage on Deck 2011).	32
Figure 4.1 – FEM model of the 40-foot HQ container modelled with shell elements.	33
Figure 4.2 – Visual representation of the superelement of the 40-foot HQ container. At each corner casting, the 5 black dots represent the master nodes.	34
Figure 4.3 – Detailed solid model of a SAL placed between two corner castings (Rathje, Darie and Schnorrer 2008).	35
Figure 4.4 – FEM model of a 8-tier high container stack with 2-tier high lashing bridge used in the study. Containers are modelled with superelements; locks, lashing assemblies and	

lashing bridge are represented by linear springs; contact elements are modelled between containers to represent friction effects; and hull and hatch cover are considered rigid. 37

Figure 4.5 – Heeling angle and the transversal component of the acceleration. 37

Figure 4.6 – Schematic description of the results obtained using the FE model. 40

Figure 5.1 – Container stowage plan. 41

Figure 5.2 – Container stacks taken from the stowage plan. 42

Figure 5.3 – Additional stack used for the parametric studies. 43

Figure 5.4 – Association of springs in series. 44

Figure 5.5 – Container stack from bay 74 and row 2. 46

Figure 5.6 – Stack deformation using the nominal values for the stack from bay 74 and row 2.
..... 47

Figure 5.7 – Container stack from bay 30 and row 2. 48

Figure 5.8 – Stack deformation using the nominal values for the stack from bay 30 and row 2.
..... 49

Figure 5.9 – Lashing Force x Pre-Tension for bay 74 and row 2. 51

Figure 5.10 – Uplifting Force x Pre-Tension for bay 74 and row 2. 51

Figure 5.11 – Transverse Forces on Twistlocks x Pre-Tension for bay 74 and row 2. 52

Figure 5.12 – Container Post Load x Pre-Tension for bay 74 and row 2. 52

Figure 5.13 – Lashing Force x Twist Lock Stiffness for bay 74 and row 2. 53

Figure 5.14 – Uplifting Force x Twist Lock Stiffness for bay 74 and row 2. 54

Figure 5.15 – Transverse Forces on Twistlocks x Twist Lock Stiffness for bay 74 and row 2.
..... 54

Figure 5.16 – Container Post Load x Twist Lock Stiffness for bay 74 and row 2. 55

Figure 5.17 – Lashing Force x Lashing Stiffness for bay 74 and row 2. 57

Figure 5.18 – Uplifting Force x Lashing Stiffness for bay 74 and row 2.	57
Figure 5.19 – Racking Force x Lashing Stiffness for bay 74 and row 2.....	58
Figure 5.20 – Container Post Load x Lashing Stiffness for bay 74 and row 2.	58
Figure 5.21 – Lashing Force x Lashing Stiffness for bay 30 and row 2.	60
Figure 5.22 – Uplifting Force x Lashing Stiffness for bay 30 and row 2.	60
Figure 5.23 – Racking Force x Lashing Stiffness for bay 30 and row 2.....	61
Figure 5.24 – Container Post Load x Lashing Stiffness for bay 30 and row 2.	61
Figure 5.25 – Lashing Force x Vertical Clearance for bay 74 and row 2 ($E_{rod} = 70$ GPa).	62
Figure 5.26 – Uplifting Force x Vertical Clearance for bay 74 and row 2 ($E_{rod} = 70$ GPa). ...	63
Figure 5.27 – Racking Force x Vertical Clearance for bay 74 and row 2 ($E_{rod} = 70$ GPa).....	63
Figure 5.28 – Container Post Load x Vertical Clearance for bay 74 and row 2 ($E_{rod} = 70$ GPa).	64
Figure 5.29 – Lashing Force x Vertical Clearance for bay 74 and row 2 ($E_{rod} = 140$ GPa). ...	64
Figure 5.30 – Uplifting Force x Vertical Clearance for bay 74 and row 2 ($E_{rod} = 140$ GPa). .	65
Figure 5.31 – Racking Force x Vertical Clearance for bay 74 and row 2 ($E_{rod} = 140$ GPa)....	65
Figure 5.32 – Container Post Load x Vertical Clearance for bay 74 and row 2 ($E_{rod} = 140$ GPa).....	66
Figure 5.33 – Lashing Force x Vertical Clearance for bay 74 and row 2 ($E_{rod} = 210$ GPa). ...	66
Figure 5.34 – Uplifting Force x Vertical Clearance for bay 74 and row 2 ($E_{rod} = 210$ GPa). .	67
Figure 5.35 – Racking Force x Vertical Clearance for bay 74 and row 2 ($E_{rod} = 210$ GPa)....	67
Figure 5.36 – Container Post Load x Vertical Clearance for bay 74 and row 2 ($E_{rod} = 210$ GPa).....	68
Figure 5.37 – Lashing Force x Vertical Clearance for bay 30 and row 2 ($E_{rod} = 70$ GPa).	69
Figure 5.38 – Uplifting Force x Vertical Clearance for bay 30 and row 2 ($E_{rod} = 70$ GPa). ...	69
Figure 5.39 – Racking Force x Vertical Clearance for bay 30 and row 2 ($E_{rod} = 70$ GPa).....	70

Figure 5.40 – Container Post Load x Vertical Clearance for bay 30 and row 2 ($E_{rod} = 70$ GPa).
..... 70

Figure 5.41 – Lashing Force x Vertical Clearance for bay 30 and row 2 ($E_{rod} = 140$ GPa). ... 71

Figure 5.42 – Uplifting Force x Vertical Clearance for bay 30 and row 2 ($E_{rod} = 140$ GPa). . 71

Figure 5.43 – Racking Force x Vertical Clearance for bay 30 and row 2 ($E_{rod} = 140$ GPa)... 72

Figure 5.44 – Container Post Load x Vertical Clearance for bay 30 and row 2 ($E_{rod} = 140$ GPa).
..... 72

Figure 5.45 – Lashing Force x Vertical Clearance for bay 30 and row 2 ($E_{rod} = 210$ GPa). ... 73

Figure 5.46 – Uplifting Force x Vertical Clearance for bay 30 and row 2 ($E_{rod} = 210$ GPa). . 73

Figure 5.47 – Racking Force x Vertical Clearance for bay 30 and row 2 ($E_{rod} = 210$ GPa)... 74

Figure 5.48 – Container Post Load x Vertical Clearance for bay 30 and row 2 ($E_{rod} = 210$ GPa).
..... 74

Figure 5.49 – Lashing Force x Vertical Clearance for the additional stack ($E_{rod} = 70$ GPa)... 75

Figure 5.50 – Uplifting Force x Vertical Clearance for the additional stack ($E_{rod} = 70$ GPa). 76

Figure 5.51 – Racking Force x Vertical Clearance for the additional stack ($E_{rod} = 70$ GPa). . 76

Figure 5.52 – Container Post Load x Vertical Clearance for the additional stack ($E_{rod} = 70$ GPa).
..... 77

Figure 5.53 – Lashing Force x Vertical Clearance for the additional stack ($E_{rod} = 140$ GPa). 77

Figure 5.54 – Uplifting Force x Vertical Clearance for the additional stack ($E_{rod} = 140$ GPa).
..... 78

Figure 5.55 – Racking Force x Vertical Clearance for the additional stack ($E_{rod} = 140$ GPa). 78

Figure 5.56 – Container Post Load x Vertical Clearance for the additional stack ($E_{rod} = 140$ GPa).
..... 79

Figure 5.57 – Lashing Force x Vertical Clearance for the additional stack ($E_{rod} = 210$ GPa). 79

Figure 5.58 – Uplifting Force x Vertical Clearance for the additional stack ($E_{rod} = 210$ GPa).	80
Figure 5.59 – Racking Force x Vertical Clearance for the additional stack ($E_{rod} = 210$ GPa).	80
Figure 5.60 – Container Post Load x Vertical Clearance for the additional stack ($E_{rod} = 210$ GPa).	81
Figure 6.1 – Lashing force variation versus vertical clearance for several stack configurations.	84
Figure 6.2 – Sensitivity of the lashing force variation as a function of the lashing stiffness...	84
Figure 6.3 – Uplifting force variation versus vertical clearance for several stack configurations.	86
Figure 6.4 – Sensitivity of the uplifting force variation as a function of the lashing stiffness.	86
Figure 7.1 - Maximum cargo capacity for 8-tier high stack with 2-tier high lashing bridge, using external lashing arrangement.	90
Figure 7.2 - Maximum cargo capacity for 8-tier high stack with 2-tier high lashing bridge, using internal lashing arrangement.	92
Figure 7.3 – Maximum cargo capacity for 6-tier high stack with 1-tier high lashing bridge, using external lashing arrangement.	93
Figure 7.4 – Maximum cargo capacity for 6-tier high stack with 1-tier high lashing bridge, using internal lashing arrangement.	94
Figure 7.5 – Maximum cargo capacity for 4-tier high stack with no lashing bridge, using external lashing arrangement.	95
Figure 7.6 – Maximum cargo capacity for 4-tier high stack with no lashing bridge, using internal lashing arrangement.	96
Figure 7.7 – Configuration for 8-tier high stack with 2-tier high lashing bridge and external lashing.	97
Figure 7.8 – Configuration for 8-tier high stack with 2-tier high lashing bridge and internal lashing.	98

Figure 7.9 – Configuration for 6-tier high stack with 1-tier high lashing bridge and external lashing	100
Figure 7.10 – Configuration for 6-tier high stack with 1-tier high lashing bridge and internal lashing	101
Figure 7.11 – Configuration for 4-tier high stack with no lashing bridge and external lashing.	101
Figure 7.12 – Top lashed 4-tier high stack with no lashing bridge and external lashing.....	102
Figure 7.13 – Top lashed 4-tier high stack with no lashing bridge and internal lashing.	103
Figure 8.1 – Lashing assembly geometry.....	106
Figure 8.2 – Axial displacement applied in the base of the turnbuckle.	107
Figure 8.3 – Force x Deformation curve of the lashing assembly.	108
Figure 8.4 – FE model of the 2-tier high lashing bridge.....	108

DRAFT

DRAFT

LIST OF TABLES

Table 2.1 – Standard sizes for ISO Series 1 freight containers.....	9
Table 4.1 – Twist lock stiffness values.	35
Table 4.2 – Load steps summary for the numerical analyses.....	39
Table 5.1 – Ship dimensions for the parametric studies.	42
Table 5.2 – Semi-automatic lock dimensions.	46
Table 5.3 – Operational loads for the nominal case with the stack from bay 74 and row 2. ...	47
Table 5.4 – Operational loads for the nominal case with the stack from bay 30 and row 2. ...	48
Table 5.5 – Operational loads for the nominal case with the additional stack.....	50
Table 5.6 – Lashing stiffness values for the container stack from bay 74 and row 2.	56
Table 5.7 – Lashing stiffness values for the container stack from bay 30 and row 2.	59
Table 7.1 – Numerical results of the maximum cargo capacity for 8-tier high stack with 2-tier high lashing bridge, using external lashing arrangement.	91
Table 7.2 – Numerical results of the maximum cargo capacity for 8-tier high stack with 2-tier high lashing bridge, using internal lashing arrangement.....	92
Table 7.3 – Numerical results of the maximum cargo capacity for 6-tier high stack with 1-tier high lashing bridge, using external lashing arrangement.	94
Table 7.4 – Numerical results of the maximum cargo capacity for 6-tier high stack with 1-tier high lashing bridge, using internal lashing arrangement.....	95
Table 7.5 – Numerical results of the maximum cargo capacity for 4-tier high stack with no lashing bridge, using external lashing arrangement.	96
Table 7.6 – Numerical results of the maximum cargo capacity for 4-tier high stack with no lashing bridge, using internal lashing arrangement.....	96

Table 7.7 - Numerical results for 8-tier high stack and 2-tier high lashing bridge with linear cargo distribution, using external lashing arrangement.	98
Table 7.8 – Numerical results for 8-tier high stack and 2-tier high lashing bridge using internal lashing arrangement.	99
Table 7.9 – Numerical results for 6-tier high stack and 1-tier high lashing bridge with linear cargo distribution, using external lashing arrangement.	99
Table 7.10 – Numerical results for 6-tier high stack and 1-tier high lashing bridge using internal lashing arrangement.	100
Table 7.11 – Numerical results for 4-tier high stack and no lashing bridge using external lashing arrangement.	102
Table 7.12 – Numerical results for 4-tier high stack and no lashing bridge using external lashing arrangement for top lashed configuration.	103
Table 7.13 – Numerical results for 4-tier high stack and no lashing bridge using internal lashing arrangement for top lashed configuration.	104
Table 8.1 – Material properties for the lashing assembly analysis.	106
Table 8.2 – Numerical result of the 1-tier high lashing bridge stiffness.	109
Table 8.3 – Numerical result of the 2-tier high lashing bridge stiffness.	110
Table 12.1 – Top 20 exporters of containerized cargo from 2009 and 2010 (WSC 2013)...	121
Table 12.2 – Top 20 importers of containerized cargo from 2009 and 2010 (WSC 2013). ..	122
Table 12.3 – Top 20 European Union exporters of containerized cargo from 2010 (WSC 2013).	123
Table 12.4 – Top 20 European Union importers of containerized cargo from 2010 (WSC 2013).	124
Table 13.1 – Container types.	125
Table 14.1 – Operational load limits for containers and lashing components according (GL 2012).	127

1. INTRODUCTION

Since Malcolm McLean developed the metal shipping container in 1956, replacing the traditional break bulk method of handling dry goods and revolutionizing the cargo transport worldwide (Transportation Research Board 2006), intermodal transport using cargo containers has been growing every year.

Nowadays, about 90% of the non-bulk cargo worldwide is transported on containers (Ebeling 2009). According to the World Shipping Council (WSC 2013), China was the top exporter country of containerized cargo in the world in 2010 (31.3 mi TEU) and the European Union (EU) was the second importer region in the world (16.8 mi TEU), just below United States (17.6 mi TEU). With an increasing on the number of cargo transported on containers, the size of the vessels has been increasing as well.



Figure 1.1 – Far East – North Europe trade line from Hanjin Shipping Company (Hanjin 2013).

On the export side, liner trade is dominated by countries in East Asia. Liner exports are also highly concentrated, with the top ten exporting nations accounting for more than two-thirds of the total liner export value, and Greater China (including mainland China, Hong Kong S.A.R. and Taiwan) account for 28% of the value of liner exports and 30% of the global volume of containerized exports. On both the export and import side, EU's liner trade is dominated by Germany, which accounts for 20% of EU liner exports and 17% of EU liner imports. The top four exporters and importers of the European Union (which include Germany, Italy, Netherlands, and the United Kingdom) also rank within the top 20 globally.

Section 12 presents the trade statistics generated by the World Shipping Council (WSC 2013).

The so called Ultra Large Container Ships (ULCS) are already in operation, especially on the route North Europe – Far East (Figure 1.1). The largest container ship in operation at this moment is *Maersk Emma*, 397 meters long and able to carry 15,500 TEU (twenty-foot equivalent unit). The container ship with the maximum cargo capacity is *CMA CGM Marco Polo* (Figure 1.2), which is able to carry 16,000 TEU along its 396 meters (Wikipedia 2013).



Figure 1.2. *CMA CGM Marco Polo*, the biggest container ship in the world (Wikipedia 2013).

The shipping company *Maersk* has a project to launch in 2014 a class of ships named *Triple-E Maersk*. These ships will be 400 meters long and able to carry 18,000 TEU (Maersk 2013). Comparing to *Emma Maersk*, which is only 3 meters shorter, the cargo capacity was increased on 16% (2,500 TEU). The overall dimensions of the ships are limited by harbour conditions, but designers increased the beam, changed the hull shape and modified the configuration of the superstructure in order to increase the cargo efficiency of the ship. Those ULCS can transport containers on weather deck stacked up to 8 or even 9 tiers high (Figure 1.3).

The increasing on the size of container ships results in some engineering problems: structural issues (Schellin, Rathje and Kahl Vol. 22, No. 2, June 2012), as twisting, springing and warping; and cargo securing problems, as container lashing on deck (Rathje, Darie and Schnorrer 2008). Ship design has developed but container lashing systems have not. As a consequence, many containers from container ships were reported lost overboard during the last years. Estimates of 2,000 to 10,000 annually damaged and lost containers were published in the maritime press (see section 2.10).

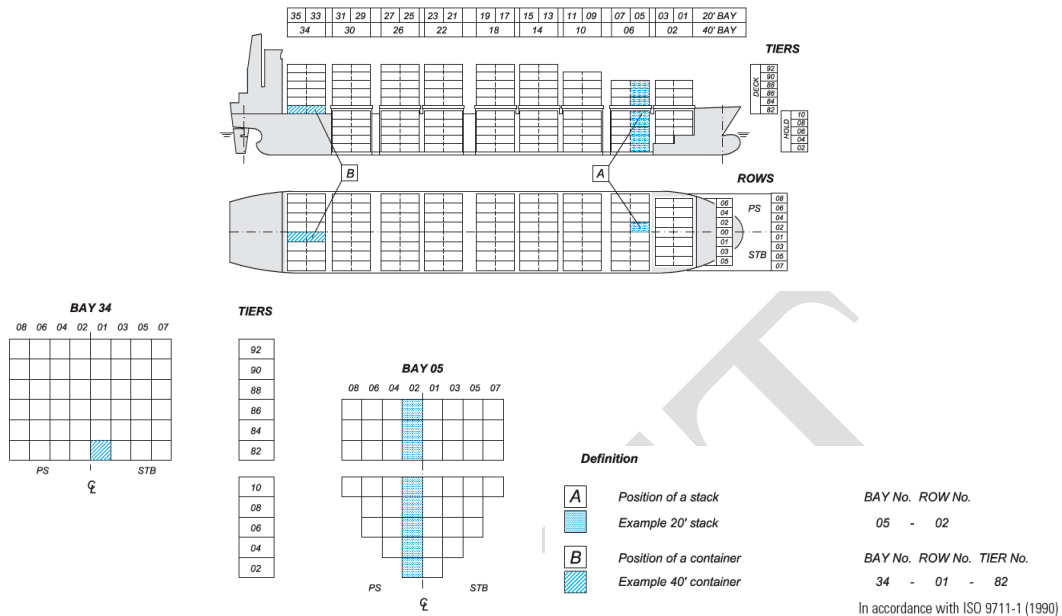


Figure 1.3. Containers stowed in holds and on weather deck. Code of container position and definition of bays (longitudinal position), rows (transverse position) and tiers (vertical position) for stack (A) and container (B) positioning (GL 2012).

In the occurrence of some structural problem on a ship, as a hull collapse, for example, lives of the crew members are in danger. If a cargo securing system fails and containers are lost overboard, lives are not directly in danger and the economic losses are covered by insurance companies. However, containers lost overboard are more than an economic issue; lost containers floating on the sea surface are hard to be detected and can be a hazard for other ships, especially small crafts. Besides, if the containers are carrying dangerous goods, there is an additional risk of environmental pollution.

1.1. Motivation

An effort is being made by shipping industry and classification societies to prevent failure of container securing systems and, thus, to minimize container damages and losses at sea. On the other hand, due to economic reasons, shipping companies aspire to optimize the utilization of their fleet. Consequently, suppliers of container lashing components develop alternative methods for container securing on weather deck, such as external lashing, promising higher

container capacity of existing ships. To ensure safe and reliable container transport on board ships, a particular verification of those novel container securing systems is required for approval of container stowage and lashing plans by classification societies.

In this work, feasibility of external lashing for container securing on weather deck is to be examined observing the Classification Rules for Stowage and Lashing of Containers, from Germanischer Lloyd (GL 2012). Potential restrictions of external lashing due to system parameters and effects, such as clearance in twist locks and relative longitudinal displacement of adjacent stacks are to be analyzed. Observing results from these investigations, in second step, possible practical benefit of external lashing, i.e., higher container capacity, higher stack weights or better weight distribution compared to internal lashing is to be estimated. Figure 1.4 shows a comparison between internal and external lashing arrangements.

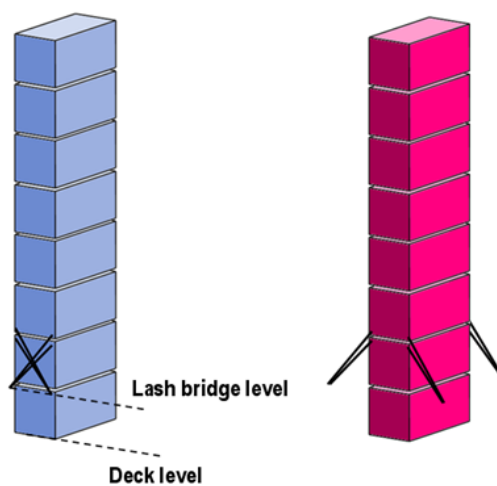


Figure 1.4 – Internal (left) and external (right) lashing arrangements.

1.2. Objectives

The main tasks of this study are the investigation of the use of external lashing arrangement to secure container stacks on deck of ships and compare its performance with the often used internal lashing arrangement. The material obtained at the end of the study will be a complement to the cargo securing research activities previously performed at GL and will possibly be used for the updating of classification rules. The main steps of the study are listed below:

1.2.1. Parametric Studies

Parametric studies of single deck stacks with external lashing arrangement are to be performed. Relevant system parameters, such as twist lock clearance, stiffness of lashing assemblies and lashing bridge, etc. are to be identified. The effect of those parameters on operational loads acting on containers and lashing components is to be quantified.

1.2.2. Design Criteria Definition

Practical design criteria for stowage systems with external lashing arrangement are to be derived from outcomes of the first task. A limit value for twist lock vertical clearance is expected to be the most relevant design criteria for single stacks. The determination of the limit values for twist lock vertical clearance as a function of relevant system parameters, e.g. height of lashing bridge, may be necessary.

1.2.3. Comparison Between Internal and External Lashing Arrangements

Comparative analyses of internal and external lashing arrangements regarding container capacity, i.e., allowable stack weights, cargo distribution, etc., are to be performed considering restrictions for external lashing arrangement determined in previous step. Preferably, these analyses should be carried out in form of a general comparison of container capacity for internal and external lashing. Optionally, a possible benefit of external lashing is to be demonstrated for an individual case based on an existing cargo securing plan.

1.2.4. Additional Studies

During the execution of the main tasks, additional studies can be performed to investigate important characteristics of cargo securing systems. The dynamic behavior of the stack can be examined, for example. Another important point which can be studied is the stack interaction and the possible interference of lashing rods connected to adjacent stacks.

DRAFT

2. PROBLEM DESCRIPTION

Many shipping containers are lost overboard every year, basically during storms and extreme sea conditions. A series of incidents involving container losses during heavy seas was registered in the Bay of Biscay in 2006 and motivated several studies in order to better understand their causes (Wolf, Darie and Rathje, Rule Development for Container Stowage on Deck 2011).

Although damage records reveal that smaller containerships suffer substantial losses and damages, Post-Panamax ships are suspected to be even more vulnerable because of immature technical standards that do not reflect the rapid growth of these ships and because of the associated lack of sufficient experience with these ships. Consequently, the motivation to better understand and enhance safety matters of container transport at sea became apparent, and the commitment to analyze and assess rule related technical aspects of safe and sound container shipping initiated various Research and Development (R&D) activities at GL (Wolf and Rathje, Motion Simulation of Container Stacks on Deck 2009).

2.1. The Evolution on the Design of Container Ships

Since the introduction of the intermodal container until the release of Post-Panamax type of ships, ship dimensions were limited by the lock chambers of the Panama Canal, i.e. a maximum ship breadth (beam) of 32.3 m, a maximum overall ship length of 294.1 m and a maximum draught of 12.0 m. Ships limited by these dimensions are called Panamax container ships. Panama Canal lock chambers are 305 m long and 33.5 m wide, and the largest depth of the canal is 12.5-13.7 m. The canal is about 86 km long, and passage takes eight hours (Containertech 2008). The corresponding cargo capacity was around 4,500 TEU (Figure 2.1). These ships were able to carry stacks up to eight tiers high in the holds and four tiers high on the deck.

In 1996, APL navigation company developed a new transportation net without using the Panama Canal (Containertech 2008). This marked the creation of the new type of container

ships called Post-Panamax (Figure 2.1). The cargo capacity started to rapidly increase, as well as the height of the stacks stowed on the weather deck. Post-Panamax ships carry up to eight tiers high stacks on the deck.

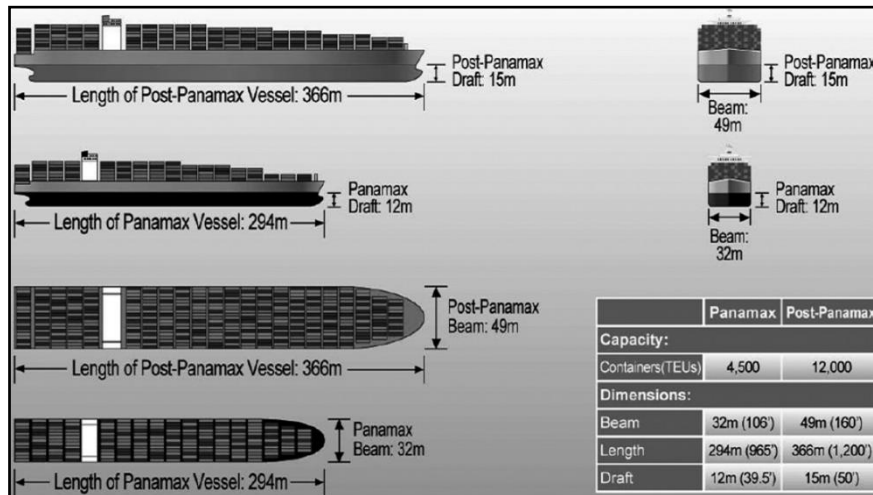


Figure 2.1 – Evolution of the Panamax container ships (US Army 2013).

After the Post-Panamax type of ships, ship dimensions were limited by the Suez Canal, which connects the Mediterranean Sea to the Red Sea and is used on the trade line between Europe and Asia, and by harbour dimensions. As previously mentioned, ULCS are already able to carry around 16,000 TEU with nine tiers high stacks (Wikipedia 2013).

2.2. Container Dimensions and Types

Containers are standardized cargo units. They are manufactured in a large variety of sizes and types, each designed to meet specific cargo and transportation requirements. Their length is usually 20 or 40 feet, although longer containers are used, especially in the US trade; these containers are 45, 48 and 53 feet long. Their width is always 8 feet although their height can vary. The term *high cube container* (HQ) usually refers to a standard-sized container that has a height of 9 feet 6 inches. Container heights can be 8 feet, 8 feet 6 inches, 9 feet 6 inches or 10 feet 6 inches (Murdoch and Tozer n.d.).

The International Organization for Standardization (ISO) standard for containers defines dimensions, both internal and external (Table 2.1), and load ratings. All containers have a

framework and corner posts fitted with corner castings. The castings at each corner of the container support the container's weight (Murdoch and Tozer n.d.).

Table 2.1 – Standard sizes for ISO Series 1 freight containers.

<i>Designation</i>	<i>Length</i>	<i>Width</i>	<i>Height</i>
1AAA	40'0"	8'0"	9'6"
1AA			8'6"
1A			8'0"
1AX			< 8'0"
1BBB	30'0"	8'0"	9'6"
1BB			8'6"
1B			8'0"
1BX			< 8'0"
1CC	20'0"	8'0"	8'6"
1C			8'0"
1CX			< 8'0"
1D	10'0"	8'0"	8'0"
1DX			< 8'0"

The corner castings are the only points at which a container should be supported, and are used to attach securing fittings, such as lashing rods (section 2.4.3) and twist locks (section 2.4.4).

The position and spacing of corner castings are carefully controlled. Containers that are longer than 40 feet usually have additional support points at the 40-foot position so that they can be stowed over a standard 40-foot container (Murdoch and Tozer n.d.).

Cargo containers are available in several types, depending on the carried cargo and the access. The external dimensions and the load ratings are basically the same for every configuration, but containers especially used to carry liquids and refrigerated cargo, for example, are available. APPENDIX II – CONTAINER TYPES shows the most common types of cargo containers.

2.3. Container Stowage on Weather Deck

Cargo containers can be stowed both inside the holds and on deck of container ships, which are designed exclusively for the transport of containers (Murdoch and Tozer n.d.). When stowed in holds, containers are secured by cell guides. On deck, container stacks are placed on hatch covers, above the deck line, and lashing elements and locks must ensure the cargo securing (Figure 2.2). Generally, containers are stowed above and below deck with their sides or longest dimension oriented in the fore-and-aft direction.

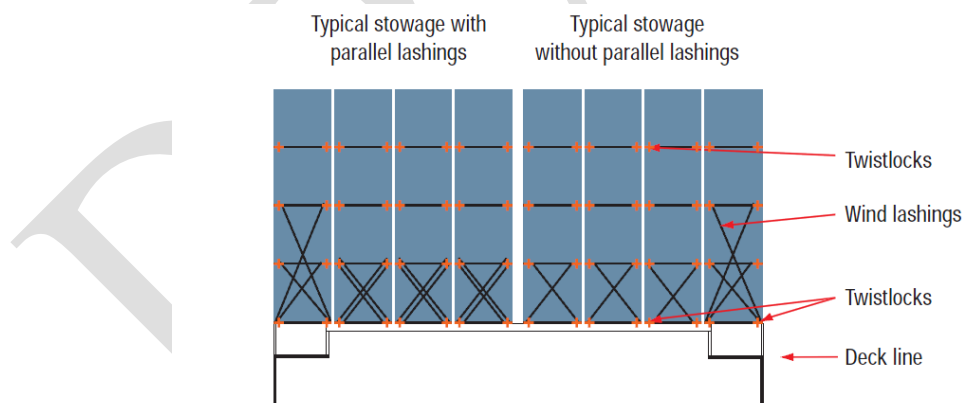


Figure 2.2 – Containers stacked on weather deck (Murdoch and Tozer n.d.).

In Panamax container ships container stacks on the weather deck could be up to four or five tiers high. In this case, lashing rods can be connected up to the bottom of the second tier and wind lashing can be connected to the bottom of the third tier (Figure 2.2). Above this point, twist locks must ensure the stack integrity.

In case of larger container ships, such as Post-Panamax and ULCS, where containers are stacked on deck up to eight or nine tiers high, stacks are much more flexible and there is a need to lash containers above the third tier. With the use of a lashing bridge (section 2.5) it is possible to move the lashing point one or two tiers higher. In this case, lashing rods can be connected the bottom of the fourth tier and wind lashing to the bottom of the fifth tier (Figure 2.3).

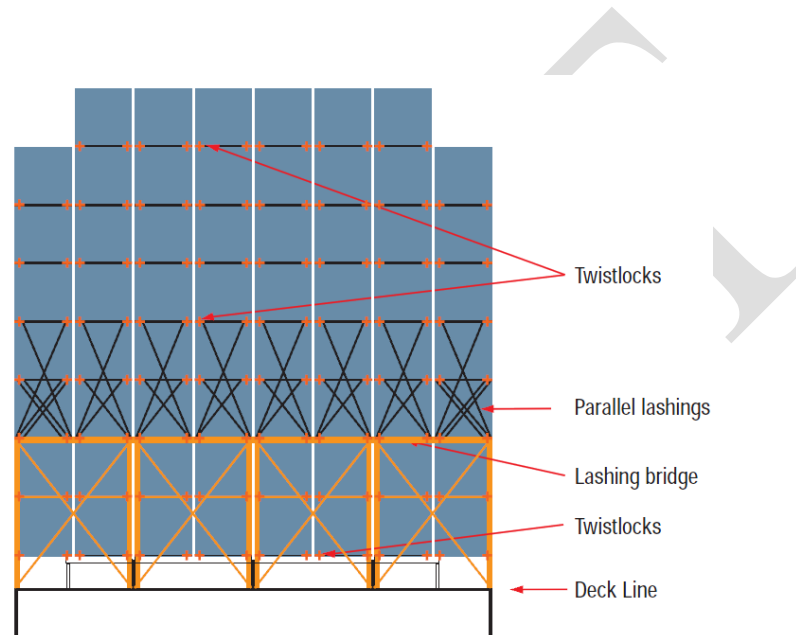


Figure 2.3 - Containers stacked on weather deck with lashing bridge (Murdoch and Tozer n.d.).

2.4. Lashing Components

Lashing components are used to secure containers stowed on deck. For some time, P&I (Protection and Indemnity) insurance clubs have recommended the use of a system based on twist locks, lashing rods, turnbuckles and lashing plates (Murdoch and Tozer n.d.). Additionally, base sockets are welded to the deck or hatch cover and are used to place the base twist locks. Lashing components are divided in two groups: fixed fittings – lashing plates and base sockets – and loose fittings – lashing rods, turnbuckles and twist locks. Figure 2.4 shows the disposition of lashing components on deck.

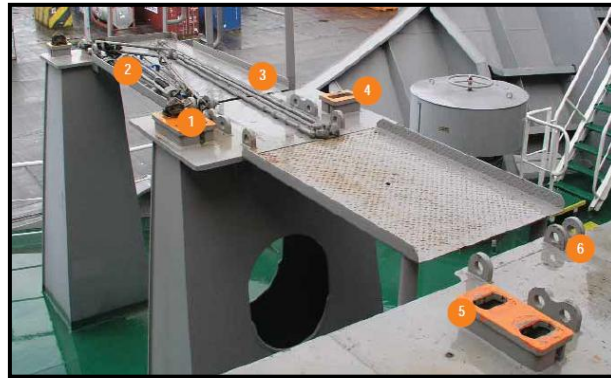


Figure 2.4 – Lashing components on deck: twist lock (1), turnbuckle (2), lashing rod (3), single (4) and double (5) base socket and lashing plate (6) (Murdoch and Tozer n.d.).

2.4.1. Lashing Plate

The lashing plate, also known as “pad-eye”, is the tie down point for the turnbuckle on deck or hatch cover. It is designed only for in plane loading, so an out-of-plane loading could bend the plate and may crack the connecting weld (Figure 2.5).

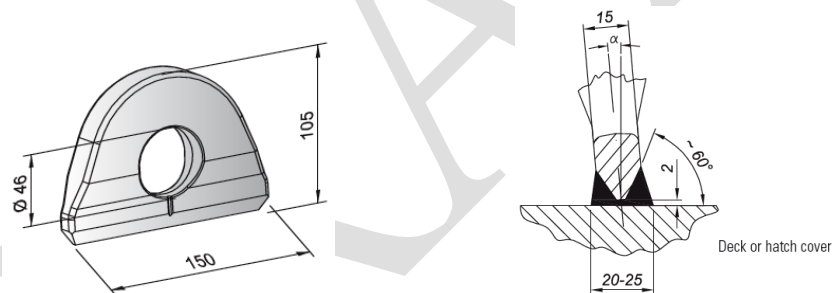


Figure 2.5 – Lashing plate (left) and scheme for welding on deck, hatch cover or lashing bridge (right).

The angle depends on the distance between the lashing plate and the container front (SEC 2007).

An alternative tie down point for the turnbuckle is the D-ring, a variation of the lashing plate. This design allows out-of-plane loading with free rotation of the turnbuckle (Figure 2.6).



Figure 2.6 – D-ring, alternative design for the lashing plate (ABS 2010).

2.4.2. Base Socket

The base socket, also known as twist lock foundation or raised socket, is a device attached directly to the deck or hatch cover and used to place the base twist locks of the stack (Figure 2.7). Base sockets are manufactured in single and double configurations. For locations where the containers must span hatch covers, or are supported partly on hatch covers and partly on pedestals, sliding base sockets are often used. These allow relative movement in the underlying hull structure while still providing tension, transverse shear, and compression restraints (ABS 2010).

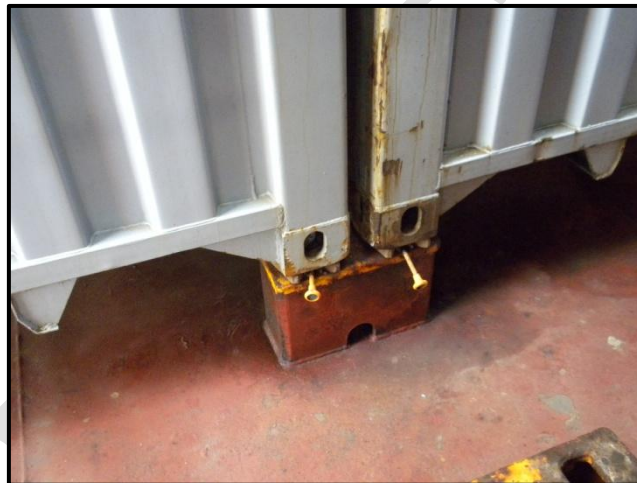


Figure 2.7 – Double base socket placing two containers and twist locks.

2.4.3. Lashing Assemblies – Lashing Rod and Turnbuckle

Lashing assemblies are utilized to resist the overturning moment of a free standing stack. Typically, they consist of a tension element (for example, steel rod, chain or wire rope) and a tensioning device (for example, a turnbuckle). Modern container lashing assemblies typically use a steel rod as the tension element (ABS 2010).

The upper end of the lashing rod is designed to fit the openings in the container corner castings and to engage or secure the rod to the corner casting when rotated to the intended angle of application. They are commonly designed to only support tensile loads, not compressive loads. Slack is removed, and the assembly is tightened with a threaded element

in the tensioning device (lashing pre-tension). Repetitive container stack movements that occur in a seaway can cause the lashing assembly to alternate between slack and taut conditions. This may cause the tensioning device to loosen if not fitted with a locking device to prevent the threaded portion from backing off (ABS 2010).

Usually, high tensile steel is used in the manufacturing of lashing rods that have the appropriate strength and length while remaining light enough for one person to handle. The end fittings must be easily installed in a corner casting several meters above the access platform and also mate with the tensioning device (turnbuckle). Flexibility to handle containers of different heights (standard and HQ containers) can be provided with additional links or attachment points on the lashing rod (ABS 2010), as it can be seen in Figure 2.8. According Cargotec (Cargotec 2005), a lashing equipment manufacturer, lashing rod diameter is usually between 25 and 27 mm.

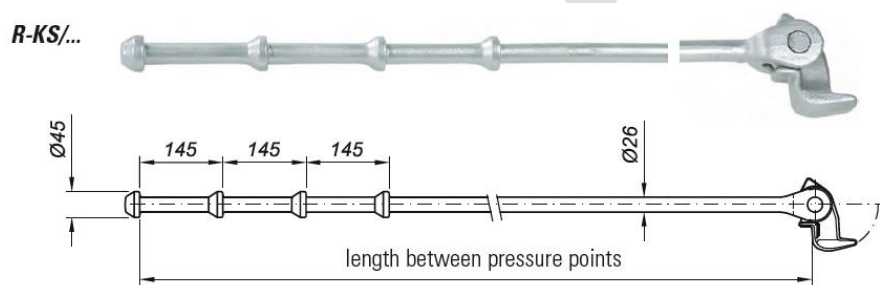


Figure 2.8 – Example of a lashing rod with four attachment positions (SEC 2007).

Chain and wire rope are not typically used on pure container ships because they are more difficult to install and maintain. They can, however, be useful for non-standardized cargo stowage arrangements (ABS 2010).

Turnbuckles, or tensioning devices, usually require an additional rod or tool to turn the barrel or body of the turnbuckle as it is tightened or loosened. It is important that it also be fitted with a locking mechanism to reduce the likelihood that lashing assemblies will slacken in a seaway due to the cyclical loading and unloading associated with the ship's motions (ABS 2010).

The maximum range of operation (minimum to maximum working length) is one of the primary factors determining the working length of the entire lashing assembly (ABS 2010). Figure 2.9 shows an example of turnbuckle design.

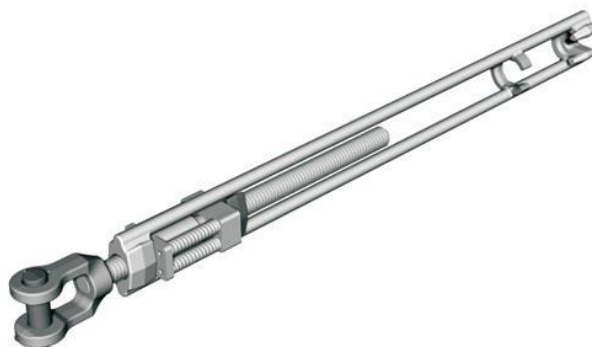


Figure 2.9 – Example of turnbuckle design (ABS 2010).

2.4.4. Twist Locks

These fittings are designed to fit the openings in the container corner castings and connect adjacent containers in the stack or to connect the base container to the base socket. They are designed to pass compression, shear and tensile loads.

Twist locks are available in manual, semi-automatic and fully-automatic types (Figure 2.10). The manual locks (ML) require an operator to lock and unlock the fitting. Semi-automatic locks (SAL) can be locked automatically when the containers are set in place, but must be manually unlocked. The fully-automatic locks (FAL) do not require manual locking or unlocking, relying instead on slight tipping/rotation of the container above to disengage the fitting.



Figure 2.10 – Examples of twist lock designs: manual lock (left), fully-automatic lock (middle) and semi-automatic lock (right) (ABS 2010).

Twist locks allow containers to slide horizontally before the fittings engage and restrain horizontal movement – both in the longitudinal and in the transversal directions. Likewise,

there are gaps between the tension elements and the corner castings that allow some vertical separation of containers to occur before the tension is restrained (ABS 2010). These gaps are called twist lock clearance and their values can change the load distribution between containers and lashing components. Due to the way they are designed, FAL tend to allow a bigger clearance than ML and SAL. The clearance values can be determined based on the dimensions of the twist lock and the corner casting. As an example, a SAL design is shown in Figure 2.11. The corner casting dimensions can be obtained in (IACS 2004).

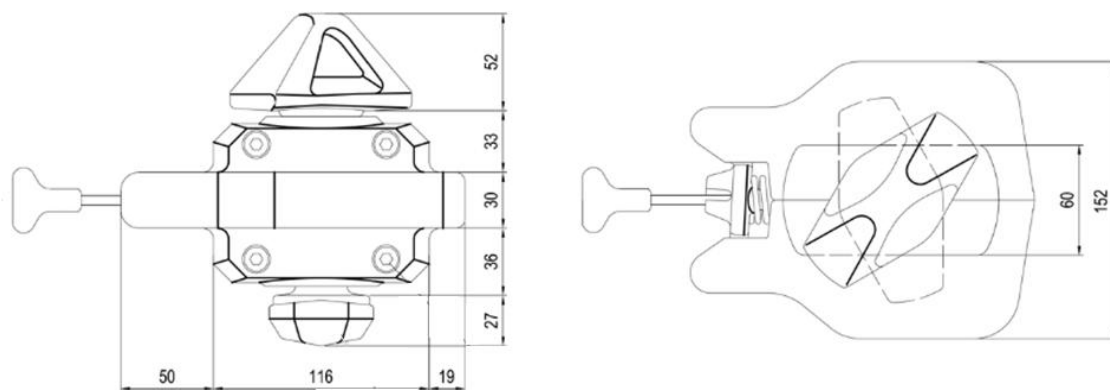


Figure 2.11 - Example of a SAL design and its dimensions.

2.5. Lashing Bridge

Flexible lashing systems are more effective when the horizontal restraining component can be applied at a higher point in the container stack. Because of their weight and size, long lashing rods are more difficult to handle and install. Long lashing assemblies have less stiffness, and due to the steeper angle of application, the resulting horizontal force is reduced. For these reasons, lashing bridges – or raised lashing platforms – are often used when container stack heights and weight are not constrained by vessel stability or visibility (ABS 2010). A raised lashing platform such as that shown in Figure 2.12 can offer the following benefits:

- Better lashing angles for shorter and more manageable lashing assemblies;
- Higher allowable stack weights for given container and lashing assembly strength ratings;
- Good access to monitor and maintain reefer containers in 1st and 2nd tiers;
- Options for handy stowage of lashing rods and turnbuckles.

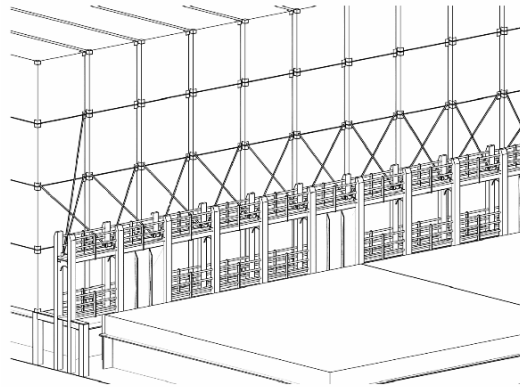


Figure 2.12 - Lashing bridge or raised lashing platform (ABS 2010).

2.6. Container Securing Arrangements

Container stacks may be secured with systems employing fixed and flexible restraints or combinations of both. Several arrangements for container securing on deck are possible, depending on the height of the stack, the stack weight and the loading acting on the containers and lashing components.

It is possible to have container stacks secured only by twist locks, both between the four corners of adjacent containers of a stack and between the base container and the hatch cover. According (ABS 2010), this system may be used for securing stacks with one or more containers depending on the location, accelerations, and the wind load. Permissible stack weights are based on the vertical strength of the twist locks and corner posts, in tension and compression, and by the end wall racking strength of the containers (see section 2.8).

When higher and/or heavier stacks are stowed on weather deck and permissible load limits acting on container frames or twist locks are exceeded, in case of stacks secured only by twist locks, flexible lashing assemblies can be used. Lashing assemblies may be used to provide the stack vertical and/or lateral movement restraint. They are connected to fixed points at the deck, hatch covers or lashing bridges, by means of lashing plates, and to the openings in the container corner castings, as described in section 2.4.3. Twist locks are still used in combination to lashing assemblies. This type of securing system is generally used for container stacks on the weather deck.

Securing systems for deck stowage of containers are generally designed so that each stack is independent and may be loaded or unloaded without impact to the adjacent stack (ABS 2010). Lashing assemblies can be used both in the vertical direction, restraining uplifting of the stack, and in the diagonal direction, restraining both uplifting and racking (see section 2.8). Container stacks are generally secured by diagonal lashing assemblies, in order to restrain both vertical and lateral movements. Vertical lashings can be used in a combination with diagonal lashing in stacks with high values of uplifting, like the outermost stacks of a bay subjected to lateral wind forces. Single diagonal lashings, due to the wind action in only one side of the stack, can also be used in this case, restraining the lateral movement of the stack (racking deformation). In Figure 2.13, two different combinations of lashing arrangements against lateral wind forces in the starboard side. In the left, paired internal lashing is combined to a vertical lashing assembly connected to the 3rd tier container to restrain uplifting. In the right, paired internal lashing is combined to diagonal lashing to restrain lateral deformation of the stack (racking).

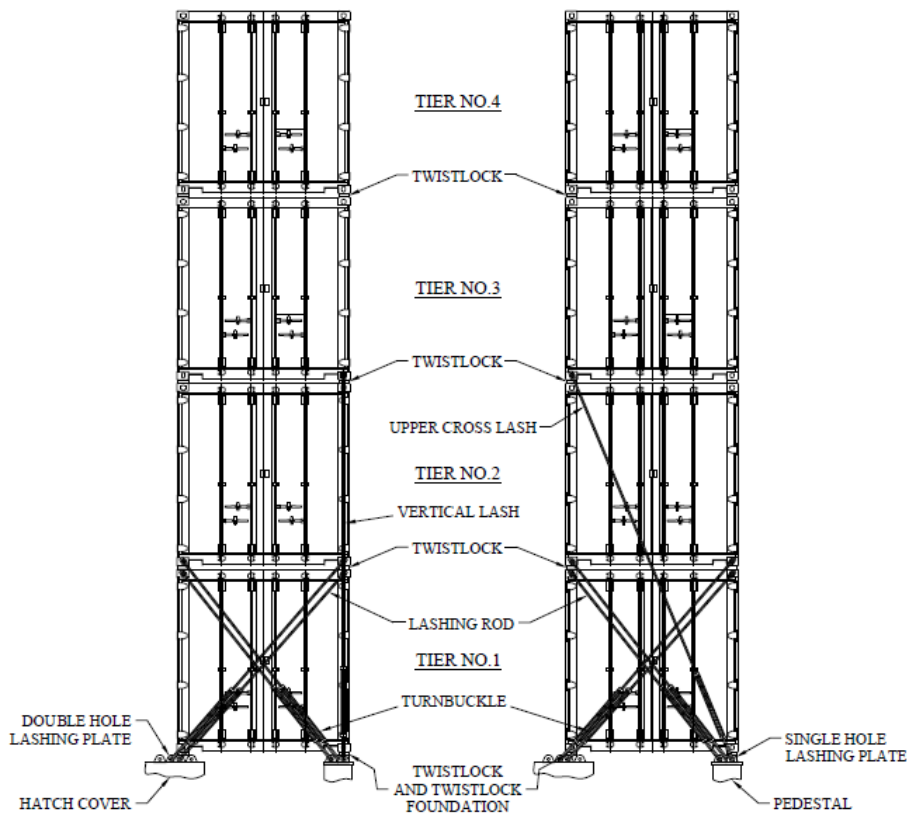


Figure 2.13 – Two different combinations of lashing arrangements against lateral wind forces (ABS 2010).

There are basically two different arrangements of diagonal lashing in use: the often used internal lashing, also known as cross lash, and the external lashing, also known as side lash. Lashing assemblies are flexible bars with tension only resistance – there is no compression stiffness due to the way the head of the lashing rod is connected to the corner casting.

When a container stack is subjected to a lateral acceleration, the loaded lashing assemblies can be connected to the lifted or to the compressed side of the stack, depending on the lashing arrangement. Figure 1.4 shows a comparison between internal and external lashing arrangement.

2.6.1. Internal Lashing

With internal lashing arrangement, the loaded lashing assemblies are connected to the compressed side of the stack. At this side, the lashing assembly constrains basically the lateral movement of the stack, while the uplifting forces at the other side are basically supported by the twist locks.

The lashing tension force has a vertical component acting on the compressed side of the stack, increasing the container post load acting on the lowermost container. If this load exceeds the limit established by the classification society, the stack weight must be decreased – which is not very interesting for the operational point of view. When internal lashing arrangement is used, the stack weight and cargo distribution are usually limited by the container post load and the racking forces acting on container frames (see section 7). This system was already studied by Wolf (Wolf, Darie and Rathje, Rule Development for Container Stowage on Deck 2011).

Figure 2.14 shows two different lashing arrangements; the left stack uses paired internal lashing, the most common arrangement – short lashing rods connected to the top of the 1st tier and bottom of the 2nd tier. The right stack uses an alternative arrangement with internal lashing – short lashing rods connected to the bottom of the 2nd tier and long lashing rods connected to the bottom of the 3rd tier.

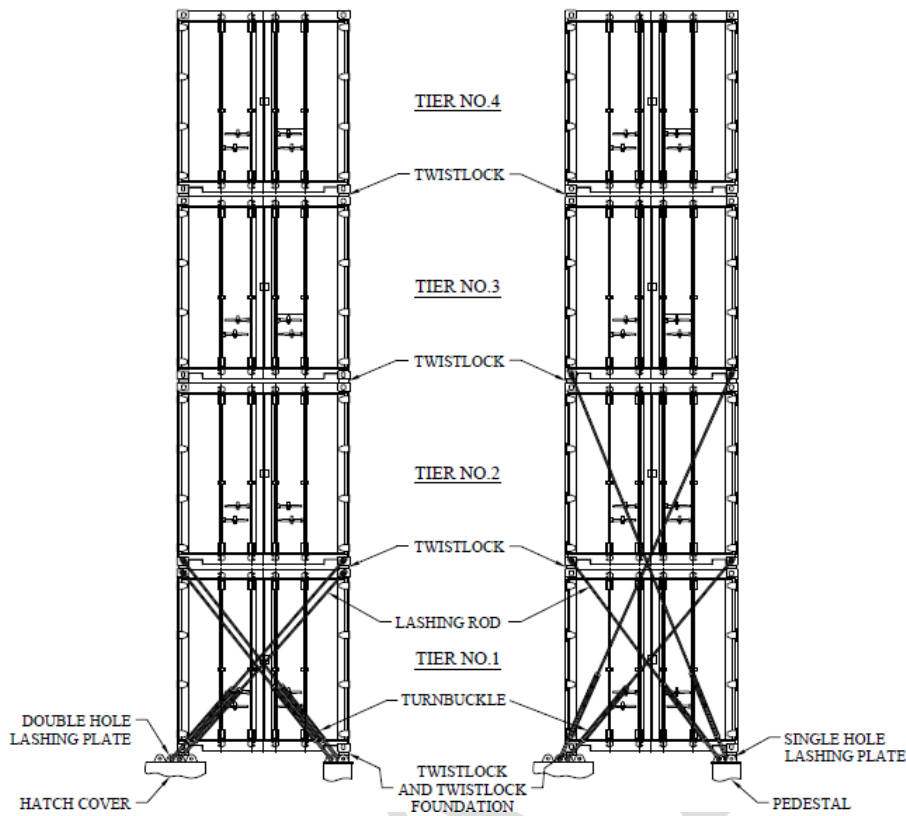


Figure 2.14 – Internal lashing arrangement (ABS 2010).

2.6.2. External Lashing

Differently of internal lashing, when external lashing arrangement is used the loaded lashing assemblies are connected to the lifted side of the stack. In this case, both the lateral and vertical (uplifting) movement of the stack are constrained. The uplifting force is shared both by the twist locks and the lashing assemblies. Due to the absence of a vertical component of the lashing force acting on the compressed side of the stack, the container post loads tend to be smaller at the base of the stack when this system is used. It means that the stack weights can be greater and heavier containers can be carried upper in the stack, which is very interesting from the operational point of view.

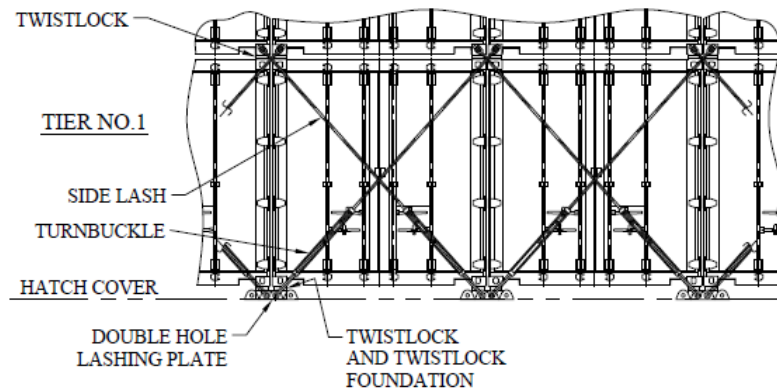


Figure 2.15 – External lashing arrangement (ABS 2010).

However, the lashing rod connected to the corner casting located at the lifted side of the front end of the top lashed container (bottom of the 2nd tier, when lashing bridge is not used) can be overloaded. Due to the difference in racking stiffness between the two end frames of the container (GL 2012), the deformed behavior of the containers from a lateral loaded stack can be seen in Figure 2.16. In the door end, racking deformation is more significant, while at the front end uplifting is more significant. At the front end, in the lifted side, there is a vertical trend of separation between the corner castings (Wolf, Darie and Rathje, Rule Development for Container Stowage on Deck 2011). This movement is restrained both by the twist lock and the lashing assembly, and the proportion depends on the lashing stiffness and the vertical clearance of the twist lock, as it will be studied in section 5.

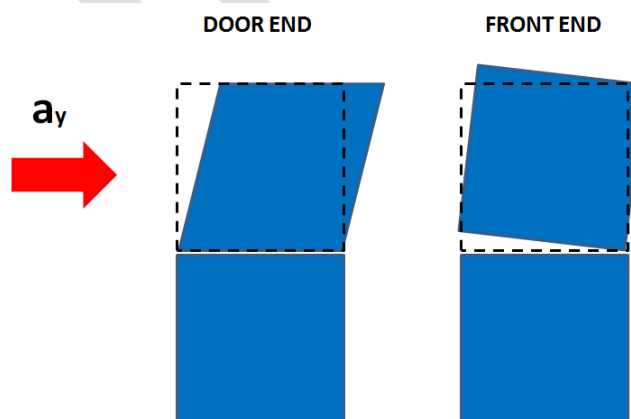


Figure 2.16 – Deformed behaviour of the end walls of a container frame when subjected to lateral acceleration: in the left, racking deformation at the door end; in the right, uplifting at the front end.

Besides, lashing assemblies connected to adjacent stacks in the same bay can have an interference one on each other when the stacks are subjected to relative longitudinal displacement. For example, when the adjacent stacks are supported by different hatch covers the relative longitudinal displacement between them can be significant to cause interference between the lashing rods and damage them.

2.7. Ship Behaviour and Loading

Container stacks stowed on the weather deck are exposed to dynamic forces caused basically by ship motions, gravity acceleration, green water and lateral wind forces, in the case of outermost rows (Rathje, Darie and Schnorrer 2008). Lateral forces are the most significant for the container stacks, causing both tensile and compressive forces on the container posts, racking forces on the container frames and loading lashing equipments, as it is described in section 2.8.

The largest part of the lateral acceleration acting on container stacks on deck is due to ship's inclination during roll motion (static component). However, the total transverse acceleration, which is obtained from Equation (2-1), is also composed by dynamic components due to roll, heave, sway, yaw and pitch, as it can be seen in the free body diagram from Figure 2.17.

$$\ddot{y} = (g + b_v) \sin(\phi) + b_h \cos(\phi) + \left(\frac{2\pi}{T_\phi}\right)^2 \phi (z - z_\phi) \quad (2-1)$$

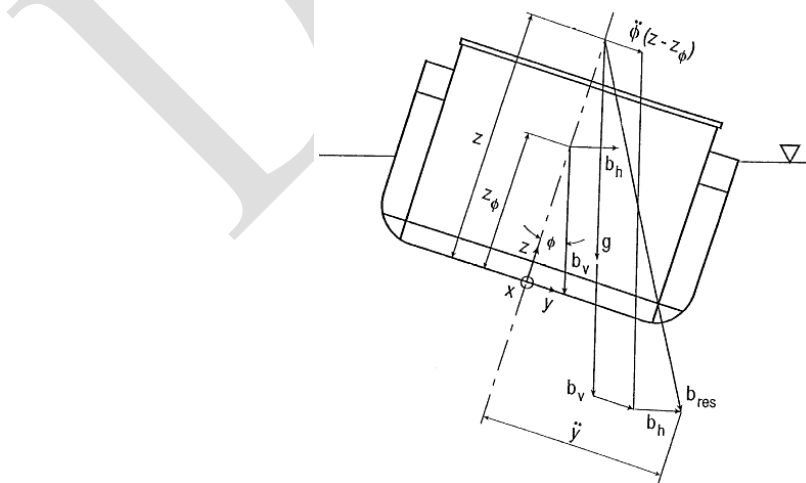


Figure 2.17 – Free body diagram of a ship during rolling motion.

Where:

z	= vertical position of the calculation point
z_ϕ	= vertical position of the roll axis
ϕ	= roll angle
T_ϕ	= roll period
g	= gravity acceleration
b_v	= vertical acceleration due to ship motion
b_h	= horizontal acceleration due to ship motion
b_{res}	= resultant acceleration
\ddot{y}	= resultant transverse acceleration

The roll period can be obtained from the Weiss formula (Equation (2-2)), which correlates the roll period (T_ϕ) to the ship's breadth (B) and the metacentric height (\overline{GM}).

$$T_\phi = \frac{0.78B}{\overline{GM}} \quad (2-2)$$

The larger the metacentric height, the shorter the roll period (the larger the roll frequency). It means more initial stability to the ship and larger values of the roll acceleration ($\ddot{\phi}$), increasing the total lateral acceleration (\ddot{y}) for the same roll angle (ϕ).

For container positions far from the ship's rolling axis, both in the longitudinal, transverse and vertical directions, the lateral acceleration values tend to be greater than at the rolling axis. According (Rathje, Darie and Schnorrer 2008), dynamic accelerations depend on the following governing parameters:

- ship's loading condition
- ship's hull form
- ship's speed
- ship's route and associated wave climates
- hull and hatch cover flexibility

Due to limitations of computer capacity and lack of appropriate physical formulations and corresponding computer routines, traditional seakeeping programs to determine dynamic accelerations treat the ship's hull as a rigid body (Rathje, Darie and Schnorrer 2008).

From the point of view of design of cargo securing systems and container stowage on weather deck, classification societies provide simplified diagrams for the determination of transverse accelerations on each position of the ship based on ship dimensions and \overline{GM} values (GL 2012).

2.8. Permissible Loads on Containers and Lashing Components

Longitudinal, transverse and vertical accelerations acting on container stacks on weather deck result in forces and deformations on container frames and lashing components. Classification societies have load limits established on rules for classification and construction of cargo securing systems, which are verified for the approval of the Container Stowage and Lashing Plan, part of the Cargo Securing Manual – CSM – which is described in section 2.9.

For (GL 2012), container posts can have a maximum compressive load of 848 kN and a maximum tensile load of 250 kN (Figure 2.18). The container post compressive load can be reduced by the stack weight reduction or by changing the lashing arrangement, as described in section 2.8. Excessive container post tensile load, or uplifting force, can be reduced by the application of vertical lashing or diagonal lashing with external arrangement.

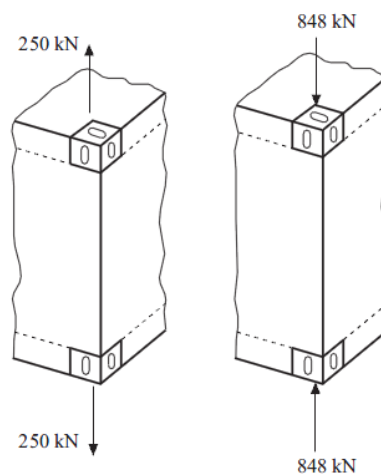


Figure 2.18 – Forces acting on container posts. Uplifting force (left) and container post load (right) (GL 2012).

According (GL 2012), the maximum allowable racking force acting on container end walls is 150 kN and on side walls is 125 kN (Figure 2.19). Transverse racking loads (acting on end walls) can be reduced by the use of diagonal lashing to restrain the lateral movement of the container frame.

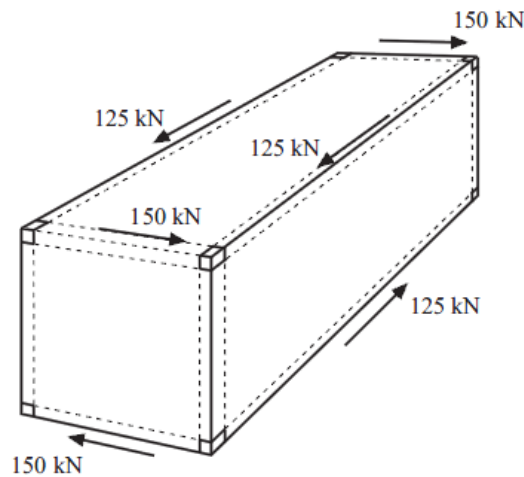


Figure 2.19 – Racking forces acting on container frames (GL 2012).

Twist locks have an operational load limit of 210 kN in the horizontal direction (GL 2012), when they work in shear. In the vertical direction, tensile forces are limited by the uplifting force (250 kN) and compressive forces by the container post load (848 kN).

The tensile load limit acting on the lashing assembly established by (GL 2012) is 230 kN. If this value is exceeded, additional lashing can be used. Besides, the lashing arrangement can be modified or the stack weight and cargo distribution can be changed.

The load limits on container frames and lashing components can be different for each classification society. Table 14.1 summarizes the operational load limits established by (GL 2012).

2.9. Cargo Securing Manual

The Cargo Securing Manual (CSM) is an official document for the ship as required by the International Convention for the Safety Life at Sea (SOLAS) from the International Maritime

Organization (IMO). All containers shall be stowed and secured throughout the voyage in accordance with the CSM. A copy of this document, approved by a classification society on behalf of the Flag Administration, must be retained onboard the vessel for examination and/or reference by classification society surveyors, port and Flag State inspectors, and those involved with safe stowage and securing of cargoes carried.

Each container stowage location on the vessel must be identified in the CSM and the characteristics of each cell provided. This can be done in the form of drawings, sketches or tables of information. At a minimum, the following should be included:

- Container Stowage and Lashing Plan showing IMO bay/stack/tier numbering and all possible container stowage configurations (optional lengths, heights, overstows, etc.);
- Capacity tables giving total slot capacities in applicable container stowage configurations;
- Visibility restrictions at a range of drafts and trim;
- Hazardous cargo stowage locations, limitations and required segregations as applicable;
- Clear heights in holds;
- Location of refrigerated container stowage locations and outlets;
- Section diagrams showing each unique stack configuration and stack base height.

Besides, the CSM contains a detailed description of every lashing component used in the ship, which must also be approved by the classification society.

An example of a Container Stowage and Lashing Plan is given in Figure 5.1 and Figure 5.2.

2.10. Containers Lost Overboard

When the operational load limits are exceeded, container frame or lashing equipments can failure by one of the failure modes presented in Table 14.1. An individual failure can result in the collapse of the whole stack or even the whole bay. Cargo containers and the goods inside them can be damaged or even lost overboard. According (Rathje, Darie and Schnorrer 2008), estimates of 2,000 to 10,000 annually damaged and lost containers were published in the maritime press.

Even with the requirement of a CSM with a Container Stowage and Lashing Plan approved by a classification society, using design loads with a low probability of occurrence, failures of containers and lashing components are still reported resulting in cargo lost overboard. They can happen especially in case of heavy seas or parametric rolling (Murdoch and Tozer n.d.). Besides heavy sea conditions, which, in extreme cases, imply green water on deck, improper container stowing, like heavy container on stack top, and container overweight are known as a common cause for damage of lower stacked container or twist locks and even loss of containers overboard (Wolf and Rathje, Motion Simulation of Container Stacks on Deck 2009), which is more than an economic issue. Containers lost overboard and floating at the surface represent a hazard for ships and, in particular, smaller craft. On top of this, deck containers may be loaded with dangerous goods. Thus, container losses also represent remarkable environmental implications (Wolf, Darie and Rathje, Rule Development for Container Stowage on Deck 2011).

DRAFT

3. BIBLIOGRAPHICAL REVIEW

There are not so many publications related to container stowage and lashing systems. As mentioned earlier, there was a great development of the container industry and an evolution on the design of container ships but not on cargo securing systems. Specifically for external lashing arrangement, no publications were found and this master thesis is expected to be the state of the art.

Classification societies have specific rules for container stowage and cargo securing. GL was the first classification society to introduce specific rules for stowage and lashing of containers (GL 2012). American Bureau of Shipping (ABS) has a complete guide for certification of container securing systems (ABS 2010) with well done descriptions of lashing components and lashing arrangements. Lloyd's Register (LR) published, besides its rules for cargo securing arrangements (LR 2011), a master's guide to container securing (Murdoch and Tozer n.d.). This document was developed with The Standard P&I Club to discuss container securing systems, the causes of lashing failure and to offer advice as to how losses can be minimized. Besides the three classification societies already mentioned, Det Norske Veritas (DNV) (DNV 2011) and Bureau Veritas (BV) also have rules for cargo securing system with rule based design principles and load limits.

In February 2006, three container ships lost about 180 containers in heavy seas in the Bay of Biscay within two days. Subsequently, the project "Seaborne Container Losses and Damages" was initiated to analyze the causes of those damage series (Rathje, Darie and Schnorrer 2008).

An 8,400 TEU Post-Panamax container ship was investigated and GL determined container racking, uplifting, and post loads at locations of interest, taking into account the wave induced hull pressures, the ship's response including the flexible hull vibrations, the resulting container accelerations and, finally, the container weight information from the loading computer. Further, loading capacity of the FAL was comprehensively investigated in finite element analyses. The numerical results proved that the combined racking, uplifting, and post loads on containers exceeded the locks' bearing capacity in the investigated case. In addition, full-scale test series with FAL and a common 20-foot container were performed and

confirmed thoroughly the results of the numerical calculations (Rathje, Darie and Schnorrer 2008).

The investigations revealed that the container loses in the Bay of Biscay in 2006 happened in extreme sea conditions, which occurs about 23 hours during 25 years exposure time in the North Atlantic Ocean. Such extremely rare events can hardly be covered by reasonably practicable design values for stowage and lashing of containers laid down in the classification rules. Thus, the FAL were likely to fail due to the exceptional dynamic load combinations in those storm conditions. A basic malfunction of the FAL was not observed. However, numerical calculations and experiments showed that the performance of the FAL can be significantly affected by various parameters, such as the condition of container corner castings. Moreover, identified failure mechanisms specific for FAL revealed that the actual combinations of the simultaneously acting dynamic racking, uplifting and container post loads are, besides their respective maximum values, essential for lock bearing capacity, especially for that lock type. Consequently, the increasing relevance of the reliable prediction of the sea induced container and lashing loads and, thus, the need of better understand the complex container stack dynamics became apparent (Rathje, Darie and Schnorrer 2008).

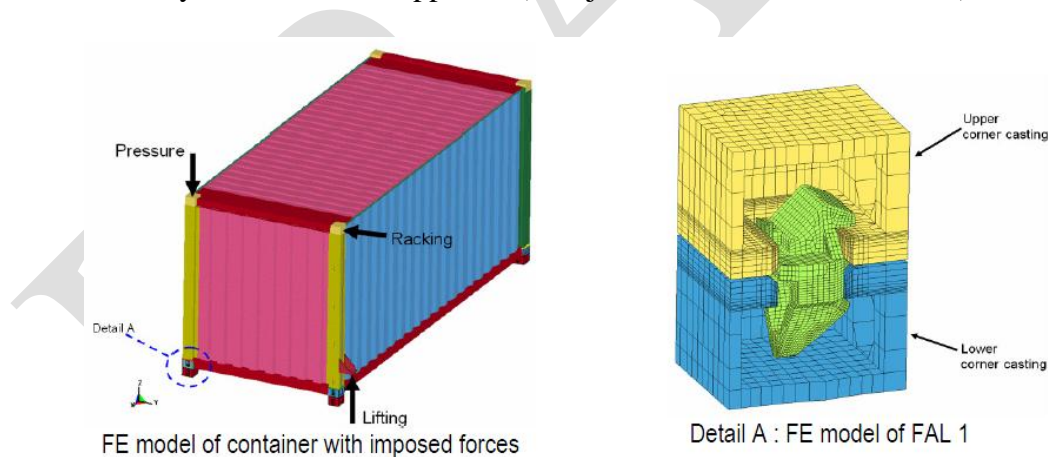


Figure 3.1 – FE models of 20-foot container and FAL used in the calculations of (Rathje, Darie and Schnorrer 2008).

The container stack dynamics was studied as a part of the joint industry project *Lashing@Sea*, which involved shipping companies, research institutes, classification societies and lashing manufacturers (MARIN 2009). In (Wolf and Rathje, Motion Simulation of Container Stacks on Deck 2009), GL developed a numerical approach for time domain simulation of deck

container stacks subjected to sea induced loads. Numerical calculations using FEM and model validation using full-scale test data are presented. Due to the nonlinearities present in the model, as friction, damping effects and large displacements, a simplified global FE model was used in order to reduce the computational effort. Submodeling techniques were used to represent the twist locks and substructuring method was used to model the containers.

With the simplified global model, the model verification was performed for various single and multi-stack configurations and the stack's motion and container and lashing loads were taken. To validate the FE model, full-scale bench tests were performed with a 2-tier high stack. The accelerations were measured on several corners of the containers and a good correlation was obtained. Additionally, parametric studies were performed varying the cargo distribution, twist lock stiffness, stack damping and stack interaction (Figure 3.2) in order to gain insight into the dynamics of containers stowed on the weather deck.

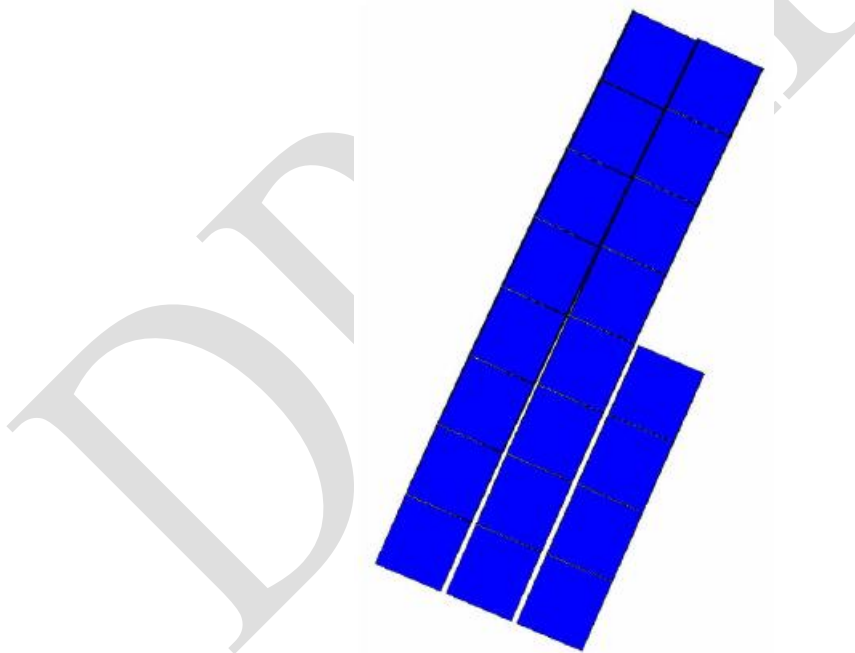


Figure 3.2 - Deformation mode of a multi-stack configuration at the maximum rolling angle (Wolf and Rathje, Motion Simulation of Container Stacks on Deck 2009).

Also as a part of the *Lashing@Sea* project (MARIN 2009), Souza et al. (Souza, et al. 2012) developed a scaled experimental model of a 7-tier high stack of 20-foot containers connected

by twist locks. The physical and structural characteristics of the scaled models were calibrated using numerical and experimental approaches. A series of experiments with controlled parameters were performed using a shaking table test to understand the effects of each variable in the container stack dynamics and present enough data to validate a numerical model.

As a continuation of the research and rule development studies performed by GL, Wolf et al. (Wolf, Darie and Rathje, Rule Development for Container Stowage on Deck 2011) performed global analyses on 8-tier high stacks of 40-foot standard ISO containers connected by SAL and lashed with internal lashing arrangement raised to the 1st tier (1-tier high lashing bridge). Racking, uplifting and container post loads were measured in the time domain for a roll angle of 24.2° and a roll period of 17.0 seconds. Different results were observed in the door and front end walls of the containers, and numerical and experimental analyses were performed with a 20-foot ISO container under constant racking load. The deformed behavior observed in the container frames is similar to the description of Figure 2.16, due to the much higher stiffness at the front end than at the door end (Figure 3.3).

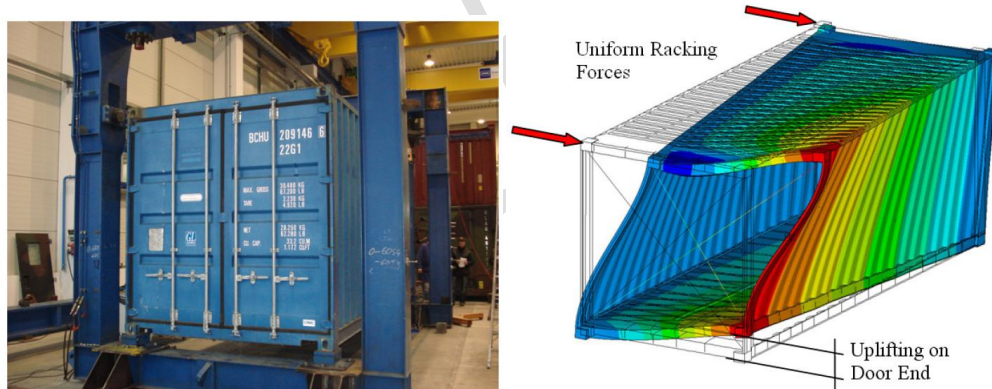


Figure 3.3 – Experimental and numerical analyses performed with a 20-foot ISO container (Wolf, Darie and Rathje, Rule Development for Container Stowage on Deck 2011).

4. METHODOLOGY

In order to achieve the goals established in section 1.2, it was decided to investigate individual container stacks stowed on the weather deck of container ships. Using the same methodology and adapting the model proposed by (Wolf and Rathje, Motion Simulation of Container Stacks on Deck 2009), a FEM model of the container stack was generated using APDL language and the software *ANSYS Mechanical 14.0*. The stack model is composed by:

- Containers
- Twist locks
- Lashing assemblies
- Lashing bridge

The containers were modeled using substructuring technique. With this method, the container structure, which was modeled using shell elements to represent its stiffness and mass inertia (Figure 4.1), was reduced in one superelement with a smaller set of degrees of freedom – DOF. The container model used was minutely studied by GL and validated by experimental analyses (Wolf, Darie and Rathje, Rule Development for Container Stowage on Deck 2011).



Figure 4.1 – FEM model of the 40-foot HQ container modelled with shell elements.

The mass of each empty container is 3.94 tons (m_{box}) and the maximum allowable weight for the fully loaded container is 30.5 tons (m_{max}) – cargo and empty box. The cargo mass was

inputted in the model by the density of shell plates with no stiffness, in order to give the model the inertia properties of the cargo. For the inertia force estimation, the vertical position of the center of gravity of the cargo on each container was estimated at 45% of the container height.

The superelement (*MATRIX50*, in *ANSYS Mechanical*) of the container contains the stiffness matrix of the shell model (Figure 4.2). Master nodes are located in the 8 corner castings of the container (5 nodes per corner). Using this technique, it is possible to take into account the structural properties of the containers with low computational cost.

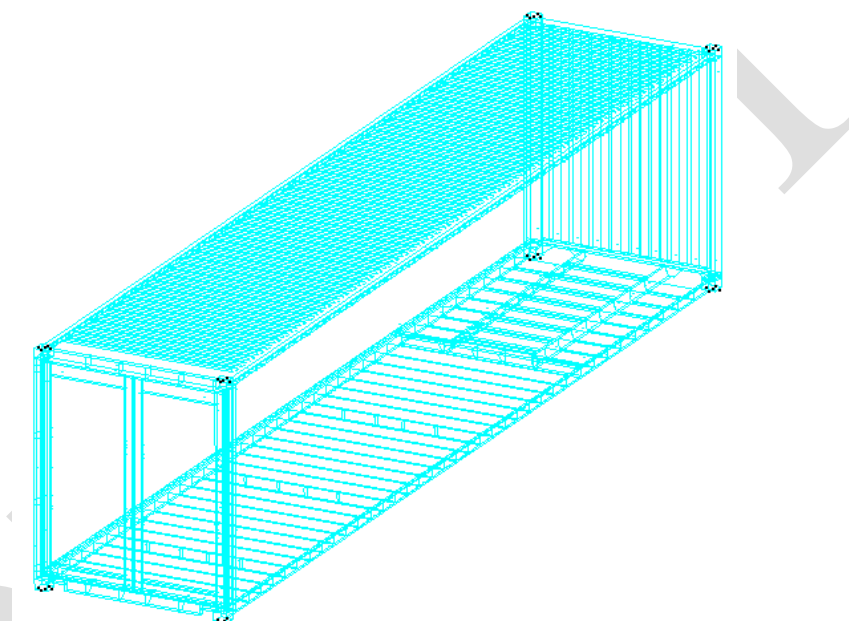


Figure 4.2 – Visual representation of the superelement of the 40-foot HQ container. At each corner casting, the 5 black dots represent the master nodes.

The superelements of the containers are stacked together connected by spring elements – *LINK180* from *ANSYS Mechanical* – which represent the twist locks. Each twist lock is modeled by link elements acting on the longitudinal, transversal and vertical direction. The distance between each tier corresponds to the mid-plate thickness of the twist lock. Additionally, a rigid surface was modeled between the corner castings and contact elements were added in order to represent the friction effects between containers. A friction coefficient (μ) of 0.25 was used.

The longitudinal, transversal and vertical values of twist lock stiffness were taken from previous studies performed at GL (Rathje, Darie and Schnorrer 2008), (Wolf and Rathje, Motion Simulation of Container Stacks on Deck 2009) and (Wolf, Darie and Rathje, Rule Development for Container Stowage on Deck 2011). The equivalent values were derived from detailed analysis using tri-dimensional solid elements, as it can be seen in Figure 4.3. Table 4.1 shows the stiffness values used on the study.

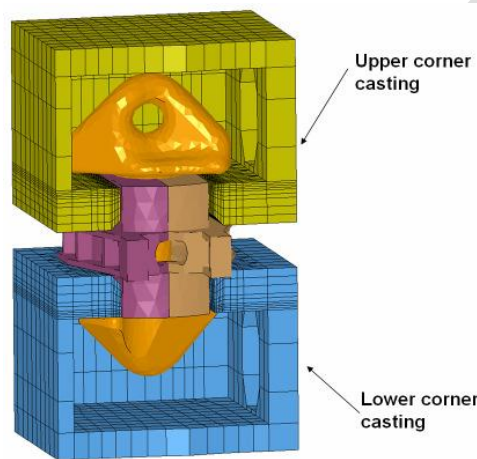


Figure 4.3 – Detailed solid model of a SAL placed between two corner castings (Rathje, Darie and Schnorrer 2008).

The stack model, composed by containers and locks, was previously validated using a 2-tier high stack of 20-foot standard empty containers. The experimental tests were performed at Monohakobi Technology Institute (MTI) in Yokohama, Japan (Wolf and Rathje, Motion Simulation of Container Stacks on Deck 2009).

Table 4.1 – Twist lock stiffness values.

<i>Direction</i>		<i>Value</i>	<i>Unit</i>
Longitudinal	(X)	140.0	kN/mm
Transversal	(Y)	250.0	kN/mm
Vertical	(Z)	750.0	kN/mm

Lashing assemblies were modelled using spring elements – *LINK180* from *ANSYS Mechanical* – only with tensile stiffness (working as a cable). The lashing assembly stiffness (k_{rod}) is defined by the overall length of the lashing assembly (L_{rod}), cross-sectional area of the rod (A_{rod}) and equivalent modulus of elasticity (E_{rod}). Lashing assembly stiffness definition is shown in Equation (4-1).

$$k_{rod} = \frac{A_{rod} \cdot E_{rod}}{L_{rod}} \quad (4-1)$$

According (GL 2012), L_{rod} is the distance between the lashing plate and the corner fitting; A_{rod} is the cross-sectional area of the lashing bar; and E_{rod} , for the case of 1st tier top lashing and 2nd tier bottom lashing, is 140 GPa. The diameter of the circular cross-section of the lashing rods was assumed as 26 mm.

As the hull and hatch cover were considered rigid, the lashing rod displacements are constrained at the lashing point on the hatch cover. In case of use of a lashing bridge, the whole structure is not modelled; only its stiffness in the load direction (k_{bridge}) is combined in series to the lashing rod stiffness (k_{rod}). The resultant stiffness is named equivalent lashing stiffness (k_{eq}). A better explanation about k_{eq} is given in section 5.2.3.

The lashing bridge stiffness values were taken from (GL 2012). According them, for the lashing bridge dimensioning a lashing force of 230 kN shall be considered. For this loading, the maximum allowed deformation of the lashing bridge in the load direction shall be 10 mm in case of 1-tier high lashing bridge and 25 mm for 2-tier high lashing bridge. It gives to the lashing assembly a foundation stiffness of 23 kN/mm, in case of 1-tier high, and 9.2 kN/mm in case of 2-tier high lashing bridge.

The base of the stack and the lashing point are connected to a pilot node, located at the rolling axis of the ship, by rigid elements – *MPC184* in *ANSYS Mechanical*. In this case, hull and hatch cover flexibility are not considered. Besides, the pilot node allows the application of a boundary condition representing the ship motion. Figure 4.4 shows the FEM model of a container stack used in the studies.

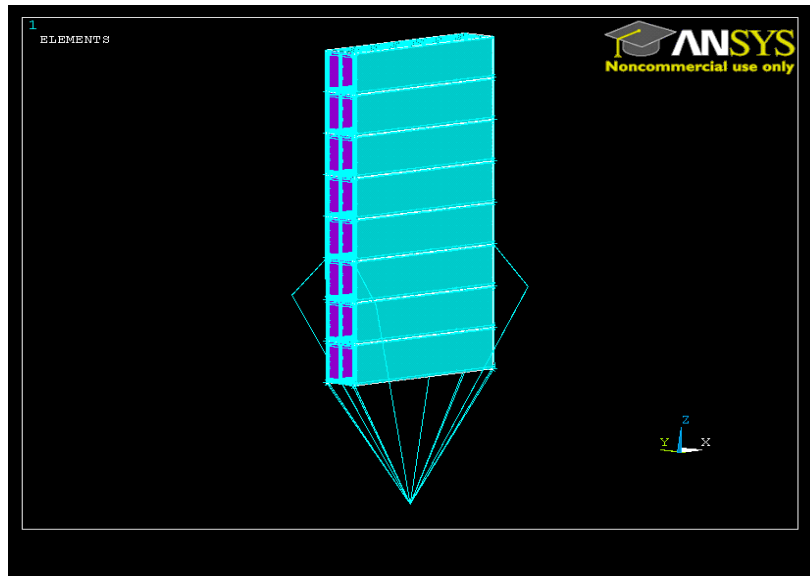


Figure 4.4 – FEM model of a 8-tier high container stack with 2-tier high lashing bridge used in the study. Containers are modelled with superelements; locks, lashing assemblies and lashing bridge are represented by linear springs; contact elements are modelled between containers to represent friction effects; and hull and hatch cover are considered rigid.

Static calculations were performed in order to evaluate the operational loads acting on containers and lashing elements of the stacks. The dynamic amplifications were not considered and the transversal component of the acceleration acting on the stack corresponds to the sum of the static and dynamic components presented on section 2.7. By applying a heeling angle (θ) on the stack, the gravity acceleration (g) is decomposed in two components: a vertical one (a_z) and a transversal one (a_y), according Figure 4.5.

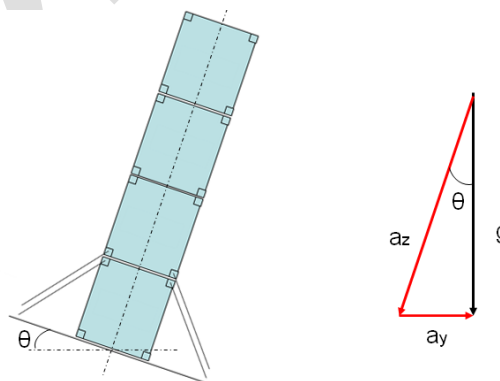


Figure 4.5 – Heeling angle and the transversal component of the acceleration.

The transversal component a_y can be obtained by equation (4-2) and the vertical component a_z by equation (4-3), both as a function of g and θ . In this case, instead of applying the stack motion by a prescribed displacement at the pilot node located in the rolling axis of the ship, the pilot node can be fixed (all translational and rotational DOF are constrained) and the components of the acceleration on the vertical and transversal directions are applied.

$$a_y = g \cdot \sin \theta \quad (4-2)$$

$$a_z = g \cdot \cos \theta \quad (4-3)$$

The static analyses are performed in 4 load steps. In the first one, the gravity acceleration g is applied in the vertical direction and the containers get in contact. It makes the model more stable before applying transverse loads and twist lock clearance.

In the second load step the lashing rod pre-tension is introduced. An axial contraction is applied on the spring elements representing the lashing assemblies. The value of the contraction is calibrated for each combination of stack parameters in order to give the axial force of interest. In operation, a lashing rod pre-tension is applied after the ship loading in order to keep the rod heads in contact with the corner casting during the transportation at sea. The tensioning on the lashing rod is given by adjusting the length of the turnbuckle. The value of the applied load is not controlled by the operators, but it is estimated to be up to 10 kN. In GL direct calculations the nominal value of the pre-tension is assumed as 5 kN (Wolf, Darie and Rathje, Rule Development for Container Stowage on Deck 2011).

The transversal component of the acceleration (a_y), which is given by the heeling angle (θ), is applied in the third load step. Due to the uplifting force on the lifted side of the stack, vertical force on the twist locks is observed at the end of this load step. At this time, there is no clearance on the twist locks.

The twist lock clearance, which is described in section 2.4.4, is applied on the fourth and last load step. As mentioned previously, the longitudinal, transversal and vertical stiffness of the twist locks are represented by spring elements. The length of these elements corresponds to the corner casting dimensions, in the case of longitudinal and transversal springs, and of the twist lock mid-plate thickness for the vertical springs. The stiffness values are given in Table 4.1. For the clearance application, the springs are expanded with the value of the gap on each

direction. Thus, the forces acting on the twist locks which are obtained on load step 3 tend to decrease and even disappear, if the clearance is bigger than the uplifting or the sliding. A summary of the analysis steps is presented in Table 4.2.

Table 4.2 – Load steps summary for the numerical analyses.

<i>Load Step</i>	<i>Constraints</i>	<i>Loading</i>
1	Pilot node – All DOF fixed	Gravity $\rightarrow 9.81 \text{ m/s}^2$ ($a_y = 0$)
2	Pilot node – All DOF fixed	Lashing pre-tension $\rightarrow 5 \text{ kN}$
3	Pilot node – All DOF fixed	Heeling angle (θ) $\rightarrow a_y$ and a_z
4	Pilot node – All DOF fixed	Gap release

Except the lashing rod pre-tension, which is taken at the end of the second load step, the operational loads acting on containers and lashing equipments are taken at the end of the fourth load step. For each tier of the stack, the forces were obtained at the corners or at the ends of the container, as shown in Figure 4.6. The door end is located in the positive direction of the longitudinal (X) axis – to the bow – while the front end is located in the negative direction – to the stern. The corner located at the door end and starboard side ($-Y$) was enumerated as 1; at door end and port side ($+Y$) as 2; at front end and starboard side as 3; and at front end and port side as 4.

The lashing forces (*FLASH*) are obtained at the top corners of the lowermost lashed tier and at the bottom of the uppermost lashed tier. Vertical forces on twist locks or uplifting forces (*FTLZ*) are obtained bottom of each tier – for tier 1 is the base twist lock and for tier 8 is the lock between the 7th and 8th tiers – and correspond to the axial forces acting on the vertical springs. Similarly the transverse forces on twist locks (*FTLY*) are also obtained at the bottom of each tier and correspond to the axial force on the transversal springs. They can be positive or negative, depending on the direction of the loading.

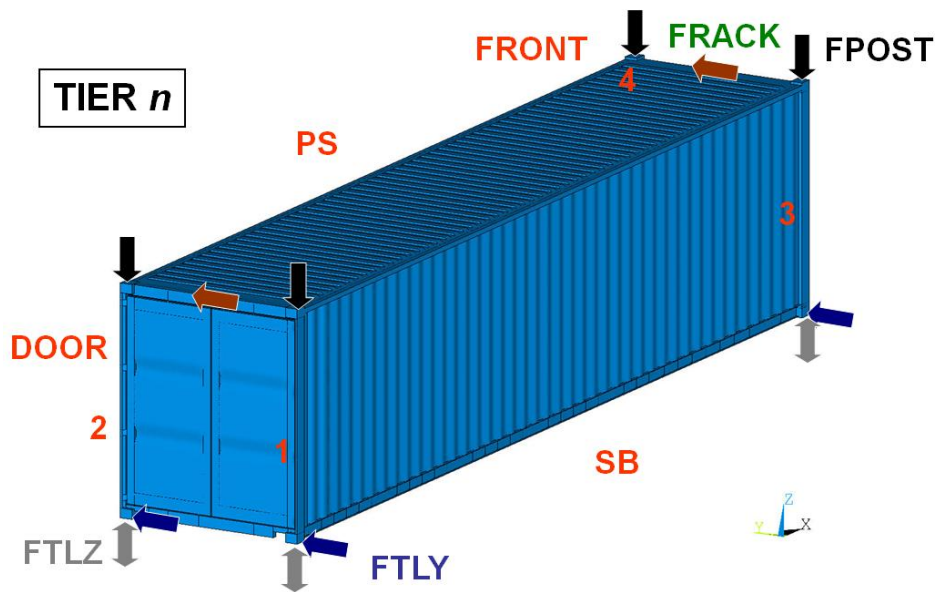


Figure 4.6 – Schematic description of the results obtained using the FE model.

The container post loads (*FPOST*) are taken at the top corners of each tier. They correspond to the compressive force acting on each post, which is the combination between the pressure force at the top corner and the vertical component of the lashing force, if it is present. This component is also relevant in case of internal lashing, where the loaded lashing rods are in the compressed side of the stack. In case of external lashing, the loaded lashing rods are in the lifted side of the stack (section 2.6).

Racking forces (*FRACK*) are taken at each end of the container (two results per tier). They correspond to the sum of the transversal forces acting on the top corners of each tier (friction forces, transverse forces on twist locks and transversal components of lashing forces) combined to the inertia forces of the cargo on each container.

Some examples of obtained results and correspondent position are shown below:

- *FPOST_TIER1_3* → Container post load at the corner in the front end and starboard side of the third tier;
- *FLASH_TIER2_4* → Lashing force at the corner in the front end and port side of the second tier (it can be in the top or bottom of the container, depending on the lashing configuration adopted);
- *FRACK_TIER7_DOOR* → Racking force at the door end of the seventh tier.

5. PARAMETRIC STUDIES

In order to investigate the behavior of the external lashing system, a real case was chosen. Two stacks were modeled using the data from a CSM and the forces acting on containers, locks and lashing elements were measured.

According (Wolf, Darie and Rathje, Rule Development for Container Stowage on Deck 2011), the sea and wind induced dynamic response of container stacks depends on various system characteristics, such as container flexibility, container cargo weights, lashing bridge type, clearances in lashing elements, lashing pretension, etc. The physics of the resulting vertical and lateral forces on containers and lashing equipment are fairly complex, e.g., due to sliding, uplifting and bouncing of stacked containers which may occur even in moderate sea conditions.

5.1. Ship Dimensions

A container ship classified by GL and with a CSM approved by the same classification society was used for this study. The ship is 347 m long, 45 m wide and its capacity is 10,730 TEU. The ship dimensions can be seen on Table 5.1.

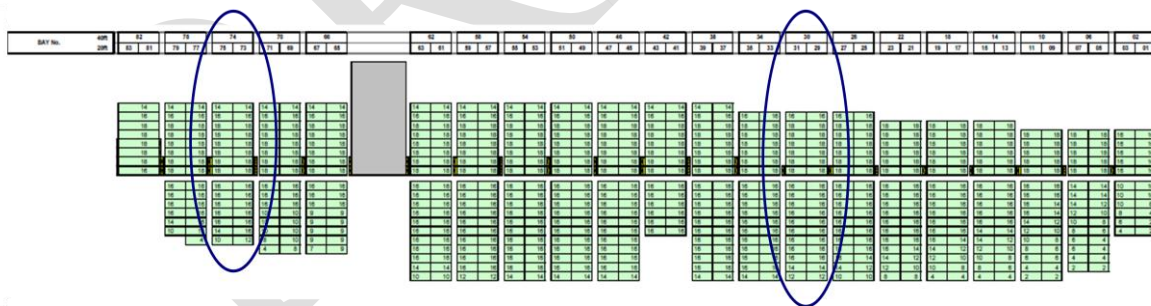


Figure 5.1 – Container stowage plan.

The ship has 21 40-foot bays, 18 rows and up to 8 tiers high stacks of high-cube containers on deck. In the fore part of the ship, containers are stacked up to 6 tiers high and in the aft part up to 8 tiers high. Lashing bridges are placed between each 40-foot bay, being 1-tier high in the fore part and 2-tier high in the aft part. Internal lashing system is used from bay 2 to bay 14

and external lashing system from bay 20 to bay 78. The last bay (Bay nr. 82) is secured by cell guides (Figure 5.1).

Table 5.1 – Ship dimensions for the parametric studies.

<i>Dimension</i>	<i>Value</i>	<i>Unit</i>
Length Overall (LOA)	347.0	m
Length Between Perpendiculars (Lpp)	331.0	m
Breadth (B)	45.2	m
Depth (D)	29.7	m
Draught (T)	13.5	m
Maximum Speed (Vmax)	25.6	kn
Cargo Capacity	10,730	TEU

For the parametric study, two bays of 40-foot containers were chosen: Bay 30, with 18 rows of 6 tiers high stacks of HQ containers and located in the fore part of the ship; and Bay 74, with 18 rows of 8 tiers high stacks of HQ containers and located in the aft part of the ship (Figure 5.1). For each of these bays, the stack at row number 2, which is beside the centerline of the ship, was chosen for the calculations. Figure 5.2 shows the weight distribution along the chosen stacks and the individual weights of each container.

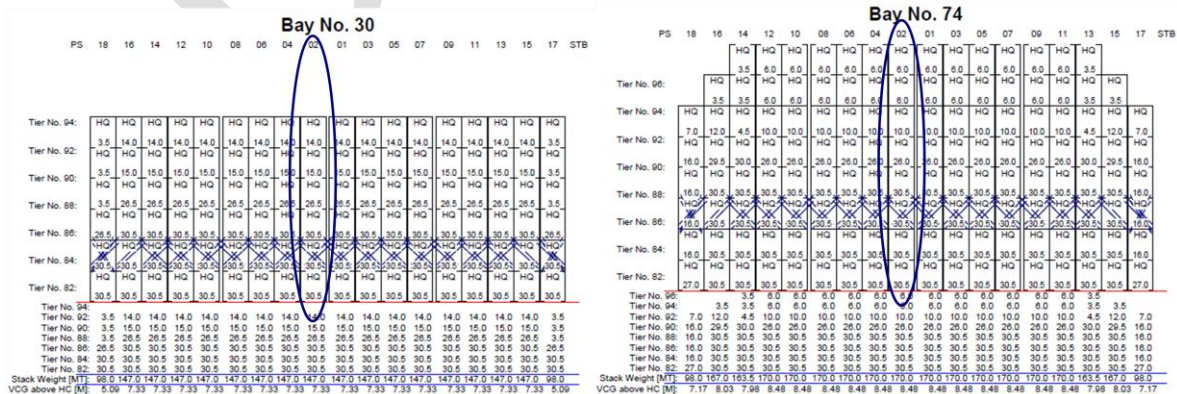


Figure 5.2 – Container stacks taken from the stowage plan.

Additionally, a 6 tiers high stack with no lashing bridge (lashing bar connected directly to the hatch cover) was modeled and analyzed. The stack configuration can be seen on Figure 5.3.

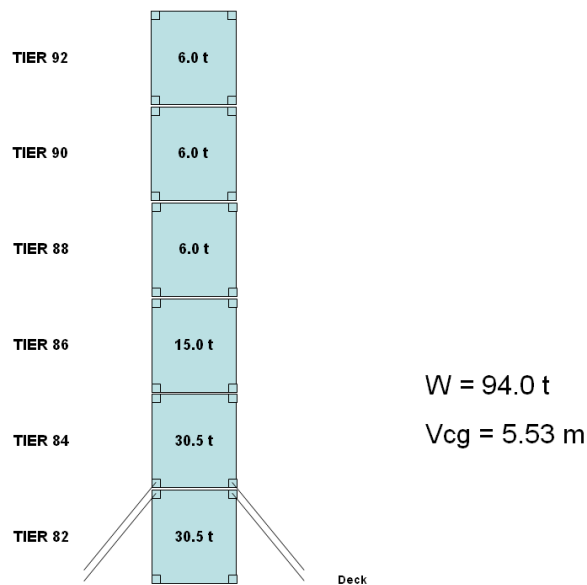


Figure 5.3 – Additional stack used for the parametric studies.

The results obtained with the nominal values for each parameter were used as baseline results.

5.2. Studied Parameters

Later, parametric studies were performed varying the parameter values and evaluating their influence on the operational loads acting on container frames and lashing components. The most relevant parameters were identified after the studies and their sensitivity on the operational loads were evaluated. The studied parameters are described in the sequence.

5.2.1. Lashing assembly pre-tension

During operation, the force applied on the tensioning element (lashing rod) by the tensioning device (turnbuckle) to remove the slack is not very controlled. Besides, stack movements due to ship motion can make the lashing assembly slack, varying the pre-tension force. The studies will investigate if this variation can have influence on the loads distributed between lashing components and containers.

5.2.2. Twist lock vertical stiffness

Twist lock designs can be different as explained in section 2.4.4. However, these devices are generally much stiffer than containers and lashing assemblies, acting almost like rigid bodies on a stack. The variation of the twist lock stiffness was evaluated to check its influence on the operational loads acting on container frames and lashing equipments.

5.2.3. Lashing stiffness (lashing assembly and lashing bridge)

The lashing assembly and the lashing bridge were described in section 2.4.3 and section 2.5, respectively. In the numerical model used for the calculations, the stiffness of both were combined in the same element, with an equivalent stiffness correspondent to the association of springs in series (Figure 5.4).

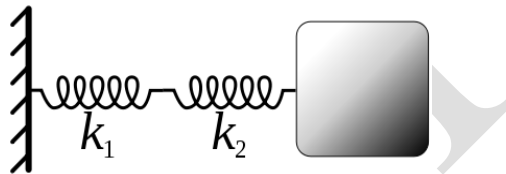


Figure 5.4 – Association of springs in series.

The lashing assembly stiffness (k_{rod}), which is obtained from equation (4-1), combined to the lashing bridge stiffness (k_{bridge}), results on the lashing equivalent stiffness (k_{eq}), according equation (5-1).

$$\frac{1}{k_{eq}} = \frac{1}{k_{rod}} + \frac{1}{k_{bridge}} \quad (5-1)$$

The equivalent lashing stiffness can be modified by the design of the lashing bridge, modifying its stiffness (k_{bridge}) and by the parameters which define the lashing assembly stiffness (k_{rod}), which are: equivalent modulus of elasticity (E_{rod}), cross-sectional area (A_{rod}) and overall length (L_{rod}).

It is known that the lashing stiffness can change the load sharing between containers and lashing components, and its influence must be checked and quantified by means of this parametric study.

5.2.4. Vertical clearance of locks

As explained in section 2.4.4, there are gaps on the twist lock fitting on corner casting. These gaps, both in the horizontal and vertical direction, are called twist lock clearance. Due to the fact of the external lashing arrangement secures the lifted side of the stack, the uplifting forces are shared by lashing assemblies and twist locks. Depending on the twist lock clearance, twist locks or lashing assemblies can be overloaded.

5.3. Nominal Values

Assuming the nominal values for each input parameter, the baseline results were obtained for each stack configuration. In order to have the baseline results below the force limits established by GL (GL 2012), the transverse acceleration, which is a function of θ , was calibrated for each stack. It was necessary because results obtained from direct calculation can be considerably different from rule based results, and a design configuration approved by the classification society using a simplified approach can be over the limits when evaluated by FEM, for example.

5.3.1. Bay 74 – Row 02

The stack configuration for the bay 74 and row 2 with the approved condition on the CSM of the studied ship can be seen on Figure 5.5. It is an 8-tier high stack of HQ containers with a 2-tier high lashing bridge. Lashing rods are connected to the top corners of the 3rd tier as well as the bottom corners of the 4th tier. The stack weight is 170 tons and the vertical position of the stack's gravity center above the hatch cover is 8.52 m. The dimensions of the semi-automatic locks used between every container are shown in Table 5.2.

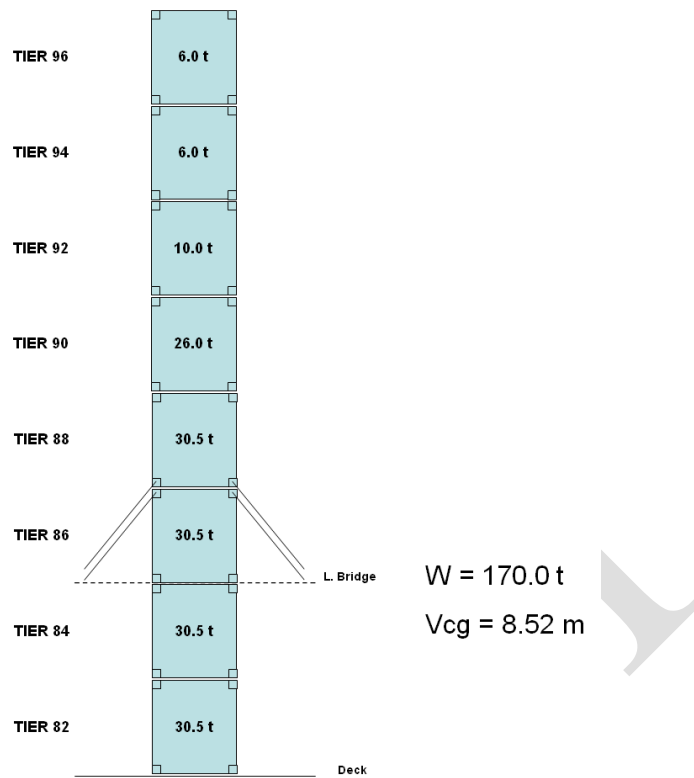


Figure 5.5 – Container stack from bay 74 and row 2.

Table 5.2 – Semi-automatic lock dimensions.

<i>Dimension</i>	<i>Value</i>	<i>Unit</i>
Mid-plate thickness	30.0	mm
Longitudinal clearance	8.0	mm
Transverse clearance	3.5	mm
Vertical clearance	15.0	mm

Using a heeling angle of 25° to the starboard, which gives a vertical acceleration (a_z) of $0.91g$ and a transverse acceleration (a_y) of $0.42g$, the forces acting on the stack were obtained. The total displacement of the topmost point of the stack was 533 mm (Figure 5.6).

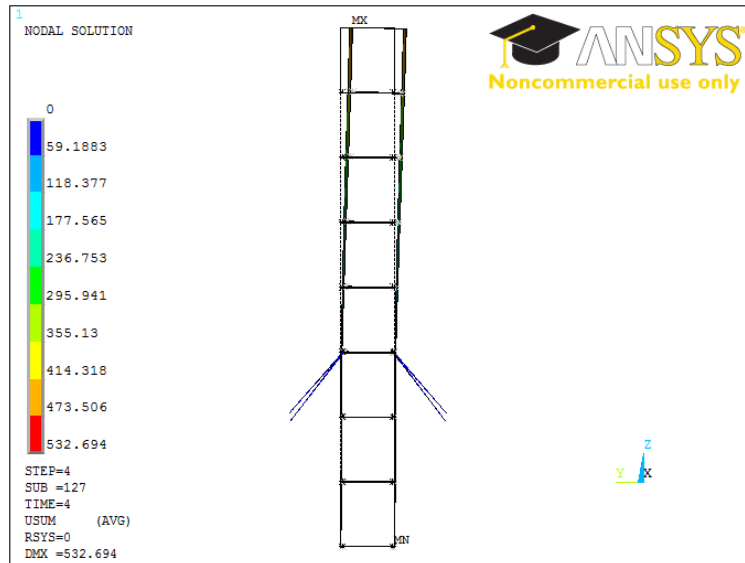


Figure 5.6 – Stack deformation using the nominal values for the stack from bay 74 and row 2.

Table 5.3 presents the forces obtained. As one can see, the lashing rods connected to the starboard side of the containers (corners 1 and 3) have no forces because this is the compressed side of the stack. In the lifted side (corners 2 and 4) the maximum force is obtained in the front end of the 4th tier container, as explained on section 2.6.2. This force is the closest to the limits established by GL, while racking forces, container post loads and uplifting forces have a higher safety margin.

Table 5.3 – Operational loads for the nominal case with the stack from bay 74 and row 2.

RESULT (kN)								LIMIT (kN)
FLASH_TIER3_1	FLASH_TIER3_2	FLASH_TIER3_3	FLASH_TIER3_4	FLASH_TIER4_1	FLASH_TIER4_2	FLASH_TIER4_3	FLASH_TIER4_4	230
0,0	185,5	0,0	139,0	0,0	203,5	0,0	226,4	
FRACK_TIER1_DOOR	FRACK_TIER1_FRONT	FRACK_TIER2_DOOR	FRACK_TIER2_FRONT	FRACK_TIER3_DOOR	FRACK_TIER3_FRONT	FRACK_TIER4_DOOR	FRACK_TIER4_FRONT	150
-74,2	-95,9	-23,0	-20,3	54,0	26,7	-133,8	-133,7	
FRACK_TIER5_DOOR	FRACK_TIER5_FRONT	FRACK_TIER6_DOOR	FRACK_TIER6_FRONT	FRACK_TIER7_DOOR	FRACK_TIER7_FRONT	FRACK_TIER8_DOOR	FRACK_TIER8_FRONT	848
-74,8	-71,9	-36,9	-33,0	-19,8	-13,7	-6,2	-6,2	
FPOST_TIER1_1	FPOST_TIER1_2	FPOST_TIER1_3	FPOST_TIER1_4	FPOST_TIER2_1	FPOST_TIER2_2	FPOST_TIER2_3	FPOST_TIER2_4	250
570,4	344,9	698,5	189,4	492,6	286,4	581,1	172,7	
FPOST_TIER3_1	FPOST_TIER3_2	FPOST_TIER3_3	FPOST_TIER3_4	FPOST_TIER4_1	FPOST_TIER4_2	FPOST_TIER4_3	FPOST_TIER4_4	160,1
372,3	127,7	672,2	0,0	274,3	0,0	289,3	0,0	
FPOST_TIER5_1	FPOST_TIER5_2	FPOST_TIER5_3	FPOST_TIER5_4	FPOST_TIER6_1	FPOST_TIER6_2	FPOST_TIER6_3	FPOST_TIER6_4	1,6
157,9	0,0	96,9	0,0	64,8	0,0	51,7	0,0	
FPOST_TIER7_1	FPOST_TIER7_2	FPOST_TIER7_3	FPOST_TIER7_4	FPOST_TIER8_1	FPOST_TIER8_2	FPOST_TIER8_3	FPOST_TIER8_4	0,0
26,7	0,0	14,5	11,4	0,0	0,0	0,0	0,0	
FTLZ_TIER1_1	FTLZ_TIER1_2	FTLZ_TIER1_3	FTLZ_TIER1_4	FTLZ_TIER2_1	FTLZ_TIER2_2	FTLZ_TIER2_3	FTLZ_TIER2_4	0,0
0,0	0,0	0,0	0,0	0,0	0,0	0,0	0,0	
FTLZ_TIER3_1	FTLZ_TIER3_2	FTLZ_TIER3_3	FTLZ_TIER3_4	FTLZ_TIER4_1	FTLZ_TIER4_2	FTLZ_TIER4_3	FTLZ_TIER4_4	0,0
0,0	0,0	0,0	0,0	0,0	0,0	0,0	160,1	
FTLZ_TIER5_1	FTLZ_TIER5_2	FTLZ_TIER5_3	FTLZ_TIER5_4	FTLZ_TIER6_1	FTLZ_TIER6_2	FTLZ_TIER6_3	FTLZ_TIER6_4	0,0
0,0	59,7	0,0	79,6	0,0	59,4	0,0	1,6	
FTLZ_TIER7_1	FTLZ_TIER7_2	FTLZ_TIER7_3	FTLZ_TIER7_4	FTLZ_TIER8_1	FTLZ_TIER8_2	FTLZ_TIER8_3	FTLZ_TIER8_4	0,0
0,0	11,2	0,0	0,0	0,0	0,0	0,0	0,0	

5.3.2. Bay 30 – Row 02

The stack configuration for the bay 30 and row 2 with the approved condition on the CSM of the studied ship can be seen on Figure 5.7. It is a 6-tiers high stack of HQ containers with a 1-tier high lashing bridge. Lashing rods are connected to the top corners of the 2nd tier as well as the bottom corners of the 3rd tier. The stack weight is 147 tons and the vertical position of the stack’s gravity center above the hatch cover is 7.38 m. The dimensions of the semi-automatic locks used between every container are shown in Table 5.2.

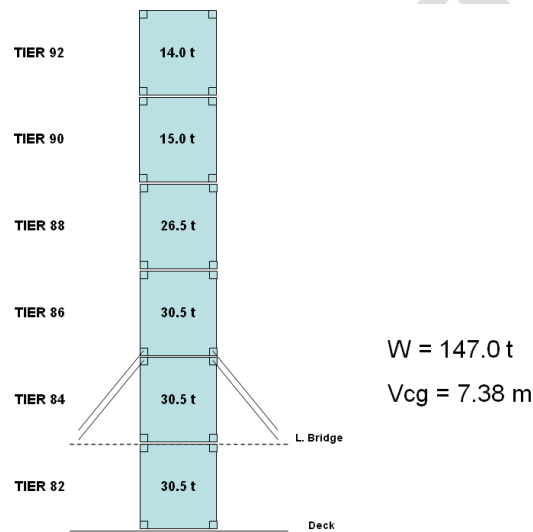


Figure 5.7 – Container stack from bay 30 and row 2.

Using a heeling angle of 20° to the starboard, which gives a vertical acceleration (a_z) of 0.94g and a transverse acceleration (a_y) of 0.34g, the forces acting on the stack were obtained. The total displacement of the topmost point of the stack was 331 mm (Figure 5.8).

Table 5.4 – Operational loads for the nominal case with the stack from bay 30 and row 2.

RESULT (kN)								LIMIT (kN)
FLASH_TIER2_1	FLASH_TIER2_2	FLASH_TIER2_3	FLASH_TIER2_4	FLASH_TIER3_1	FLASH_TIER3_2	FLASH_TIER3_3	FLASH_TIER3_4	230
0,0	134,5	0,0	94,4	0,0	148,8	0,0	225,4	
FRACK_TIER1_DOOR	FRACK_TIER1_FRONT	FRACK_TIER2_DOOR	FRACK_TIER2_FRONT	FRACK_TIER3_DOOR	FRACK_TIER3_FRONT	FRACK_TIER4_DOOR	FRACK_TIER4_FRONT	150
-39,5	-16,1	18,8	26,9	-121,3	-121,6	-73,5	-73,2	
FRACK_TIER5_DOOR	FRACK_TIER5_FRONT	FRACK_TIER6_DOOR	FRACK_TIER6_FRONT					848
-37,6	-31,0	-11,7	-11,7					
FPOST_TIER1_1	FPOST_TIER1_2	FPOST_TIER1_3	FPOST_TIER1_4	FPOST_TIER2_1	FPOST_TIER2_2	FPOST_TIER2_3	FPOST_TIER2_4	250
447,2	298,0	660,3	110,5	356,4	148,4	669,7	0,0	
FPOST_TIER3_1	FPOST_TIER3_2	FPOST_TIER3_3	FPOST_TIER3_4	FPOST_TIER4_1	FPOST_TIER4_2	FPOST_TIER4_3	FPOST_TIER4_4	250
256,7	0,0	315,0	0,0	133,9	0,0	124,9	6,8	
FPOST_TIER5_1	FPOST_TIER5_2	FPOST_TIER5_3	FPOST_TIER5_4	FPOST_TIER6_1	FPOST_TIER6_2	FPOST_TIER6_3	FPOST_TIER6_4	250
64,6	0,0	29,5	34,1	0,0	0,0	0,0	0,0	
FTLZ_TIER1_1	FTLZ_TIER1_2	FTLZ_TIER1_3	FTLZ_TIER1_4	FTLZ_TIER2_1	FTLZ_TIER2_2	FTLZ_TIER2_3	FTLZ_TIER2_4	250
0,0	0,0	0,0	0,0	0,0	0,0	0,0	0,0	
FTLZ_TIER3_1	FTLZ_TIER3_2	FTLZ_TIER3_3	FTLZ_TIER3_4	FTLZ_TIER4_1	FTLZ_TIER4_2	FTLZ_TIER4_3	FTLZ_TIER4_4	250
0,0	0,0	0,0	112,8	0,0	0,0	0,0	62,1	
FTLZ_TIER5_1	FTLZ_TIER5_2	FTLZ_TIER5_3	FTLZ_TIER5_4	FTLZ_TIER6_1	FTLZ_TIER6_2	FTLZ_TIER6_3	FTLZ_TIER6_4	250
0,0	0,0	0,0	0,0	0,0	0,0	0,0	0,0	

Table 5.4 presents the forces obtained. As one can see, the lashing rods connected to the starboard side of the containers (corners 1 and 3) have no forces because this is the compressed side of the stack. In the lifted side (corners 2 and 4) the maximum force is obtained in the front end of the 3rd tier container, as explained on section 2.6.2. This force is the closest to the limits established by GL, while racking forces, container post loads and uplifting forces have a higher safety margin.

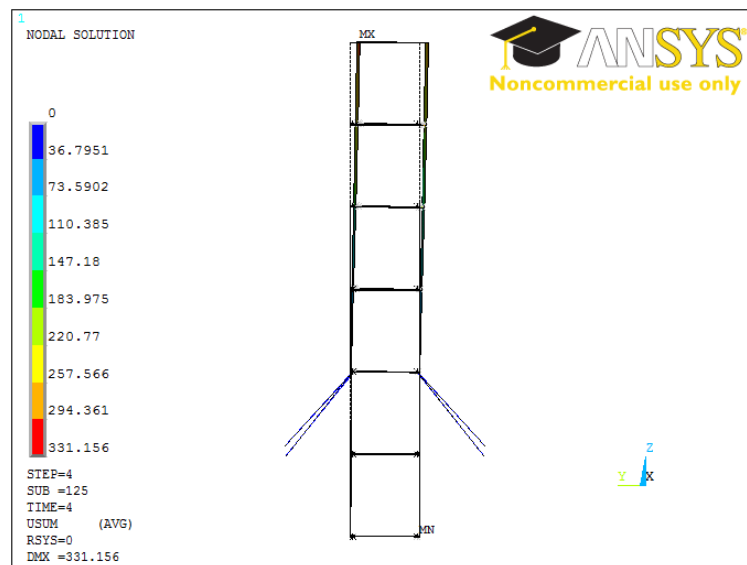


Figure 5.8 – Stack deformation using the nominal values for the stack from bay 30 and row 2.

5.3.3. Additional Stack

The additional stack configuration can be seen on Figure 5.3. It is a 6-tiers high stack of HQ containers with no lashing bridge. Lashing rods are connected to the top corners of the 1st tier as well as the bottom corners of the 2nd tier. The stack weight is 94 tons and the vertical position of the stack's gravity center above the hatch cover is 5.53 m. The dimensions of the semi-automatic locks used between every container are shown in Table 5.2.

Using a heeling angle of 20° to the starboard, which gives a vertical acceleration (a_z) of 0.94g and a transverse acceleration (a_y) of 0.34g, the forces acting on the stack were obtained. The total displacement of the topmost point of the stack was 354 mm.

Table 5.5 presents the forces obtained. As one can see, the lashing rods connected to the starboard side of the containers (corners 1 and 3) have no forces because this is the compressed side of the stack. In the lifted side (corners 2 and 4) the maximum force is obtained in the front end of the 2nd tier container, as explained on section 2.6.2. This force is the closest to the limits established by GL, while racking forces, container post loads and uplifting forces have a higher safety margin.

Table 5.5 – Operational loads for the nominal case with the additional stack.

RESULT (kN)								LIMIT (kN)
FLASH_TIER2_1	FLASH_TIER2_2	FLASH_TIER2_3	FLASH_TIER2_4	FLASH_TIER3_1	FLASH_TIER3_2	FLASH_TIER3_3	FLASH_TIER3_4	230
0,0	81,9	0,0	36,1	0,0	94,7	0,0	224,1	
FRACK_TIER1_DOOR	FRACK_TIER1_FRONT	FRACK_TIER2_DOOR	FRACK_TIER2_FRONT	FRACK_TIER3_DOOR	FRACK_TIER3_FRONT	FRACK_TIER4_DOOR	FRACK_TIER4_FRONT	150
-12,1	29,6	-82,3	-81,8	-44,3	-43,6	-26,6	-26,1	
FRACK_TIER5_DOOR	FRACK_TIER5_FRONT	FRACK_TIER6_DOOR	FRACK_TIER6_FRONT					848
-16,0	-11,7	-5,0	-5,0					
FPOST_TIER1_1	FPOST_TIER1_2	FPOST_TIER1_3	FPOST_TIER1_4	FPOST_TIER2_1	FPOST_TIER2_2	FPOST_TIER2_3	FPOST_TIER2_4	250
281,6	80,8	452,7	0,0	190,7	0,0	192,7	0,0	
FPOST_TIER3_1	FPOST_TIER3_2	FPOST_TIER3_3	FPOST_TIER3_4	FPOST_TIER4_1	FPOST_TIER4_2	FPOST_TIER4_3	FPOST_TIER4_4	250
115,3	0,0	85,7	0,0	55,8	0,0	50,6	3,4	
FPOST_TIER5_1	FPOST_TIER5_2	FPOST_TIER5_3	FPOST_TIER5_4	FPOST_TIER6_1	FPOST_TIER6_2	FPOST_TIER6_3	FPOST_TIER6_4	250
27,9	0,0	11,6	15,4	0,0	0,0	0,0	0,0	
FTLZ_TIER1_1	FTLZ_TIER1_2	FTLZ_TIER1_3	FTLZ_TIER1_4	FTLZ_TIER2_1	FTLZ_TIER2_2	FTLZ_TIER2_3	FTLZ_TIER2_4	250
0,0	0,0	0,0	0,0	0,0	0,0	0,0	0,0	
FTLZ_TIER3_1	FTLZ_TIER3_2	FTLZ_TIER3_3	FTLZ_TIER3_4	FTLZ_TIER4_1	FTLZ_TIER4_2	FTLZ_TIER4_3	FTLZ_TIER4_4	250
0,0	37,0	0,0	42,9	0,0	31,4	0,0	4,6	
FTLZ_TIER5_1	FTLZ_TIER5_2	FTLZ_TIER5_3	FTLZ_TIER5_4	FTLZ_TIER6_1	FTLZ_TIER6_2	FTLZ_TIER6_3	FTLZ_TIER6_4	250
0,0	0,0	0,0	0,0	0,0	0,0	0,0	0,0	

5.4. Lashing Rod Pre-Tension Variation

The lashing rod pre-tension was described on section 5.2.1. Initially, the parametric study was performed only with the 8-tier high stack from bay 74 and row 2. If the parameter would be considered of interest, the study should be performed with the other stacks.

The nominal value of the parameter is 5 kN, the lower bound is 0 kN (no pre-tension) and the upper bound is 20 kN (very high pre-tension). The results were plotted against the parameter variation and can be seen from Figure 5.9 to Figure 5.12.

There is no considerable variation on the results when the lashing rod pre-tension is varied. It shows this is not a parameter of interest, and basically there are no variations on the forces acting on the containers and lashing elements if the pre-tension is null, lower or higher.

The calculations were not performed with other stacks, assuming the same behaviour for the case with 1-tier high lashing bridge and with no lashing bridge.

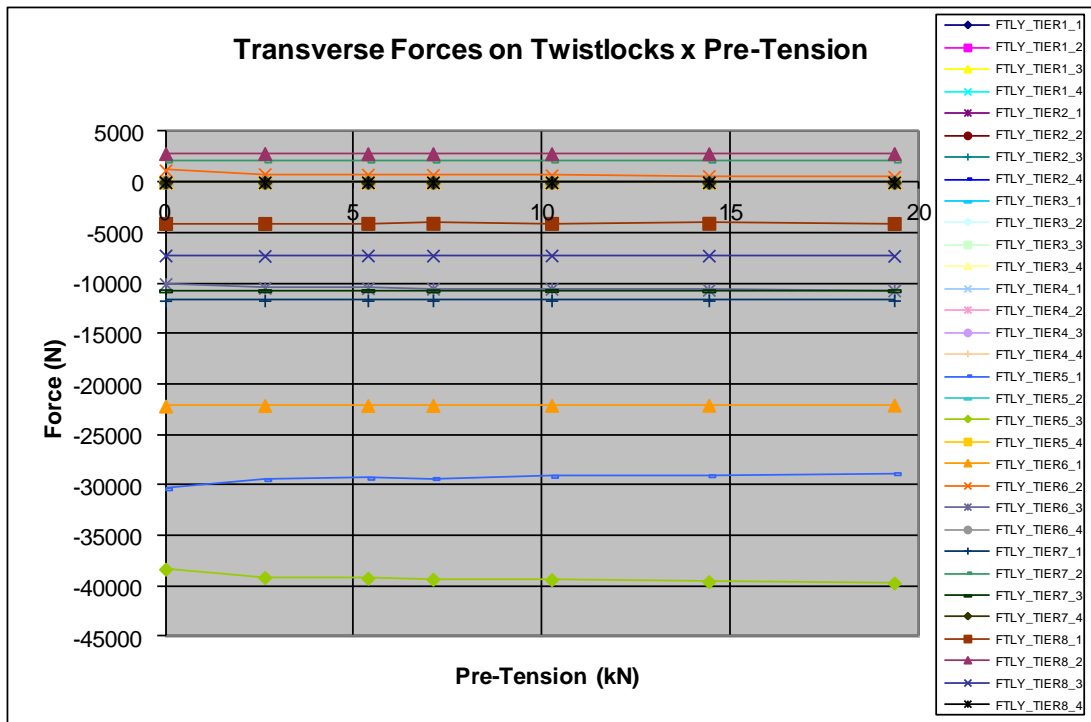


Figure 5.11 – Transverse Forces on Twistlocks x Pre-Tension for bay 74 and row 2.

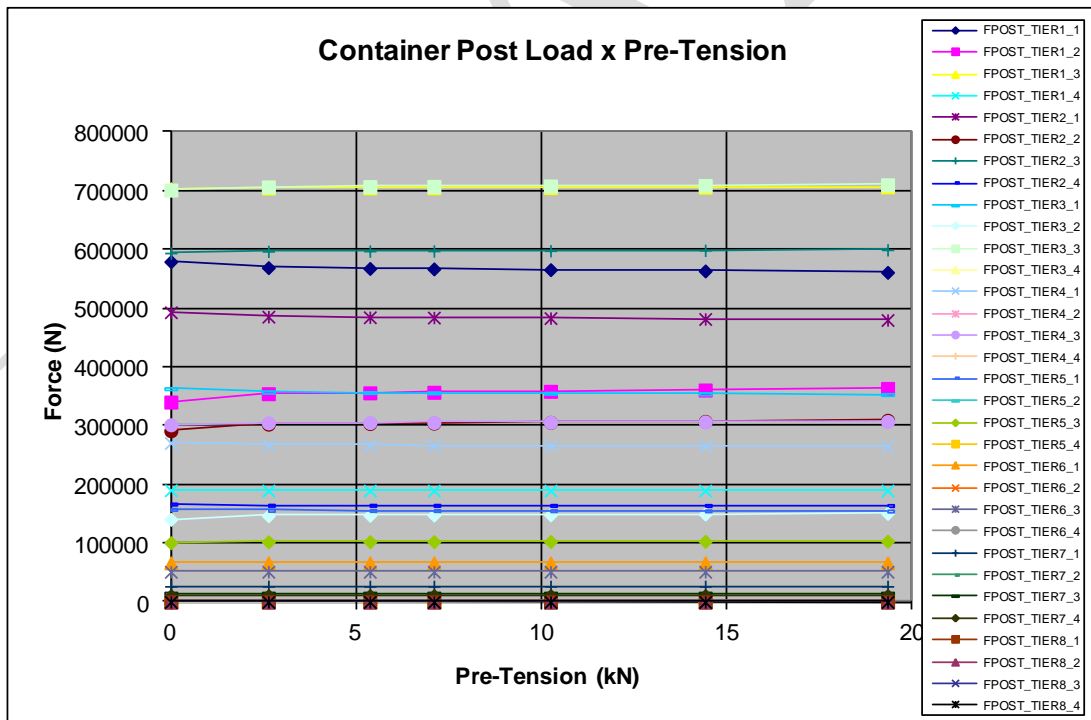


Figure 5.12 – Container Post Load x Pre-Tension for bay 74 and row 2.

5.5. Twist Lock Vertical Stiffness

The variation of the vertical stiffness of the twist locks, which was described on section 2.4.4, was also analyzed. As in the previous section, the parametric study was initially performed only with the 8-tier high stack from bay 74 and row 2. If the parameter would be considered of interest, the study should be performed with the other stacks.

The nominal value of the parameter is 750 kN/mm, the lower bound is 375 kN/mm and the upper bound is 1,125 kN/mm ($K_0 \pm 50\%$). The results were plotted against the parameter variation and can be seen from Figure 5.13 to Figure 5.16.

There is no considerable variation on the results when the twist lock stiffness is varied. It shows this is not a parameter of interest, and basically there are no variations on the forces acting on the containers and lashing elements if the stiffness is much lower or higher. It can be understood due to the fact the twist locks are much stiffer than the containers and lashing rods, with behaviour similar to rigid body.

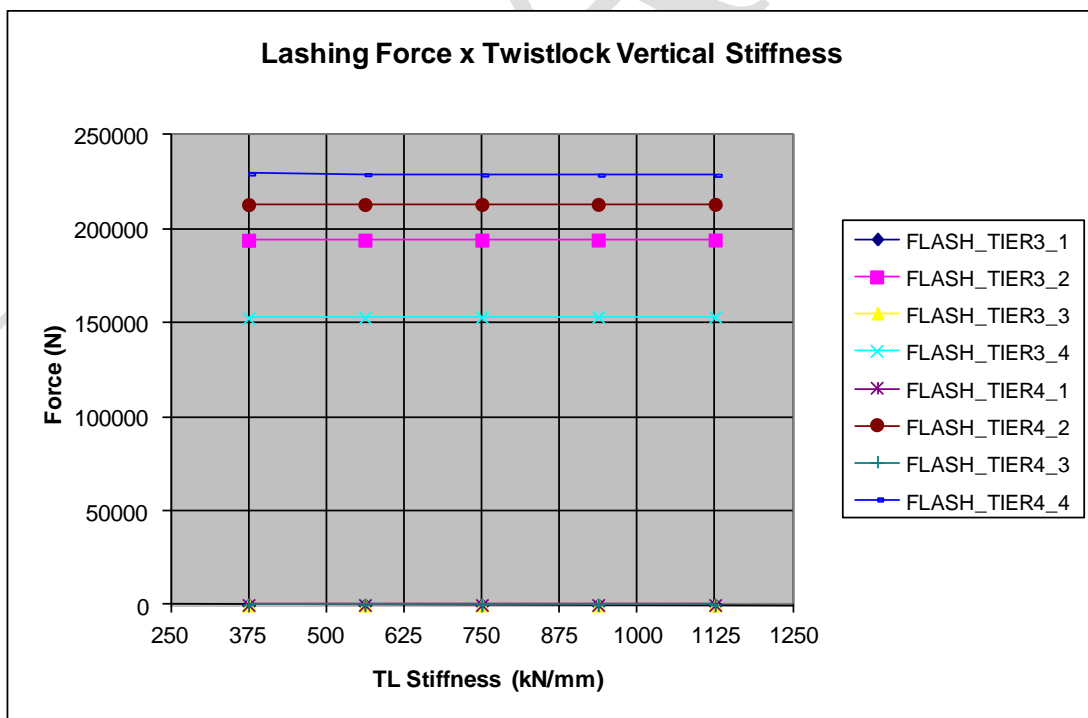


Figure 5.13 – Lashing Force x Twist Lock Stiffness for bay 74 and row 2.

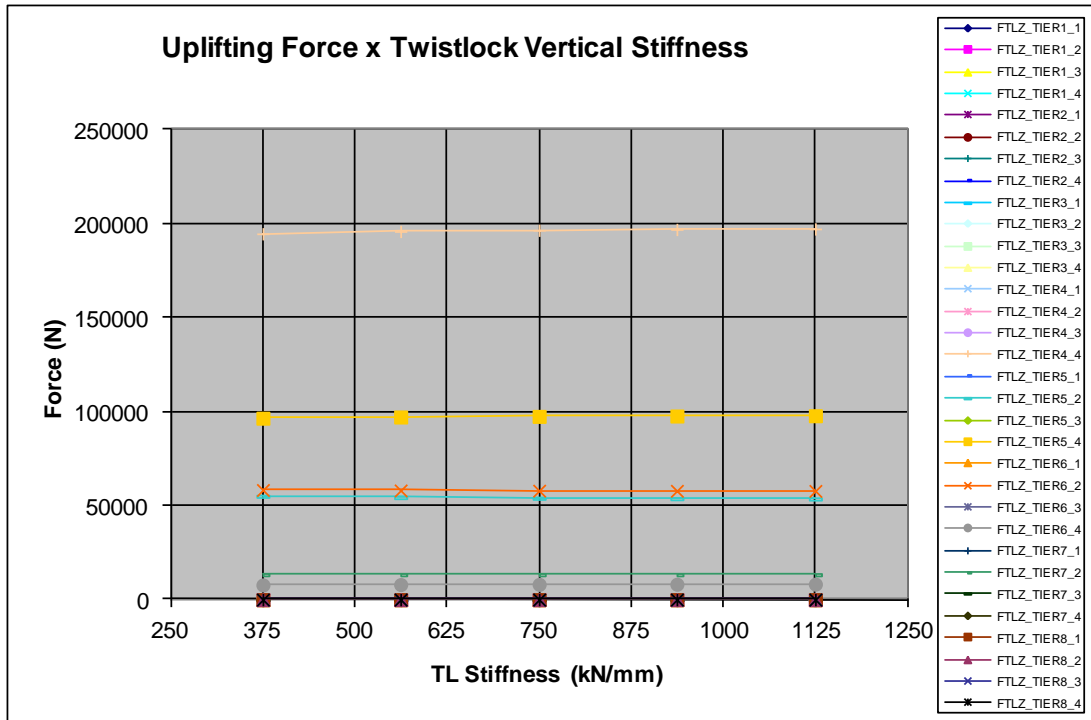


Figure 5.14 – Uplifting Force x Twist Lock Stiffness for bay 74 and row 2.

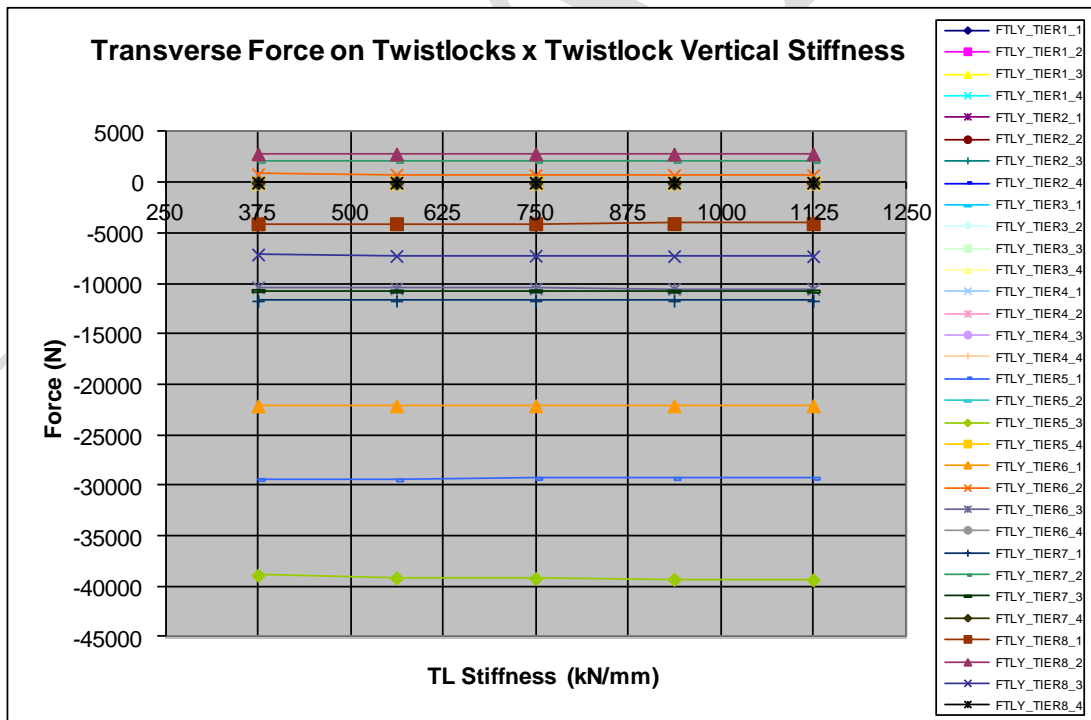


Figure 5.15 – Transverse Forces on Twistlocks x Twist Lock Stiffness for bay 74 and row 2.

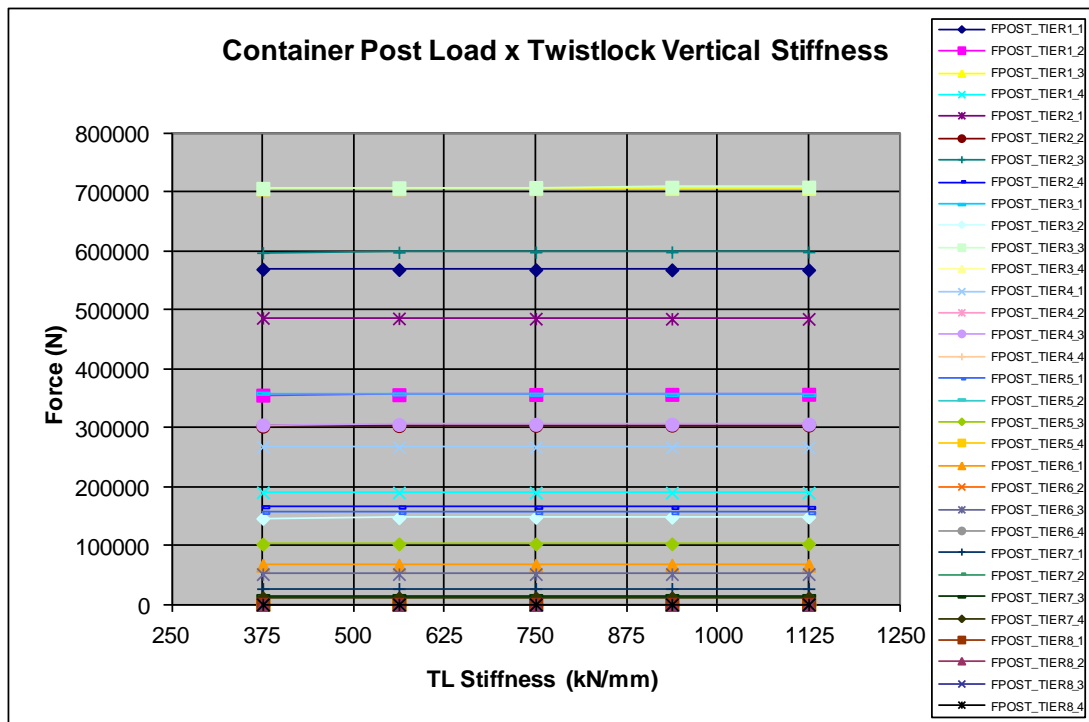


Figure 5.16 – Container Post Load x Twist Lock Stiffness for bay 74 and row 2.

The stack response to the twist lock stiffness variation was also observed as insensitive in the parametric studies performed in (Wolf and Rathje, Motion Simulation of Container Stacks on Deck 2009). The calculations were not performed with other stacks, assuming the same behaviour for the case with 1-tier high lashing bridge and with no lashing bridge.

5.6. Lashing Stiffness Variation

As described in section 5.2.3, the equivalent stiffness of the series association of lashing bridge stiffness and lashing rod stiffness was named lashing stiffness. In this case, any variation both in the lashing rod and in the lashing bridge stiffness would change the equivalent lashing stiffness. This parameter is expected to have influence on the results, and the parametric study was performed with the 8-tier high stack from bay 74 and row 2 as well as with the 6-tier high stack from bay 30 and row 2. The stiffness of the lashing assembly is an important factor in the load sharing between the lashings and containers.

5.6.1. Bay 74 – Row 02

With the nominal values of 140 GPa for the equivalent elastic modulus of the lashing rod (E_{rod}) and 9.2 kN/mm for the lashing bridge stiffness (K_b), an equivalent lashing stiffness (K_{eq}) of 6.2 kN/mm was obtained. The range of E_{rod} is between 70 GPa and 210 GPa ($\pm 50\%$) and the range of K_b is between 4.6 kN/mm and 18.5 kN/mm (- 50%; + 100%). It gives a lower bound of 3.7 kN/mm and an upper bound of 10.4 kN/mm for K_{eq} (Table 5.6).

Table 5.6 – Lashing stiffness values for the container stack from bay 74 and row 2.

k_{eq} (N/mm)	k_{bridge} (N/mm)	k_{rod} (N/mm)	E_{rod} (N/mm ²)	A_{rod} (mm ²)	l_{rod} (mm)
3713,8	4600,0	19277,1	140000,0	531,0	3856,4
4707,1	9200,0	9638,5	70000,0	531,0	3856,4
5081,2	6900,0	19277,1	140000,0	531,0	3856,4
5622,3	9200,0	14457,8	105000,0	531,0	3856,4
6227,8	9200,0	19277,1	140000,0	531,0	3856,4
6658,0	9200,0	24096,4	175000,0	531,0	3856,4
6979,4	9200,0	28915,6	210000,0	531,0	3856,4
7203,0	11500,0	19277,1	140000,0	531,0	3856,4
8042,5	13800,0	19277,1	140000,0	531,0	3856,4
8772,9	16100,0	19277,1	140000,0	531,0	3856,4
9414,2	18400,0	19277,1	140000,0	531,0	3856,4
10433,2	18400,0	24096,4	175000,0	531,0	3856,4

The influence of the lashing stiffness on the forces acting on containers and lashing elements was observed in the obtained results. The lashing force on the bottom corner of the door end and port side of the 4th tier container (FLASH_TIER4_4), where the uplifting occurs, is directly proportional to the lashing stiffness, while the vertical force acting on the twist lock at the same corner (FTLZ_TIER4_4) is inversely proportional. The obtained results can be seen from Figure 5.17 to Figure 5.20.

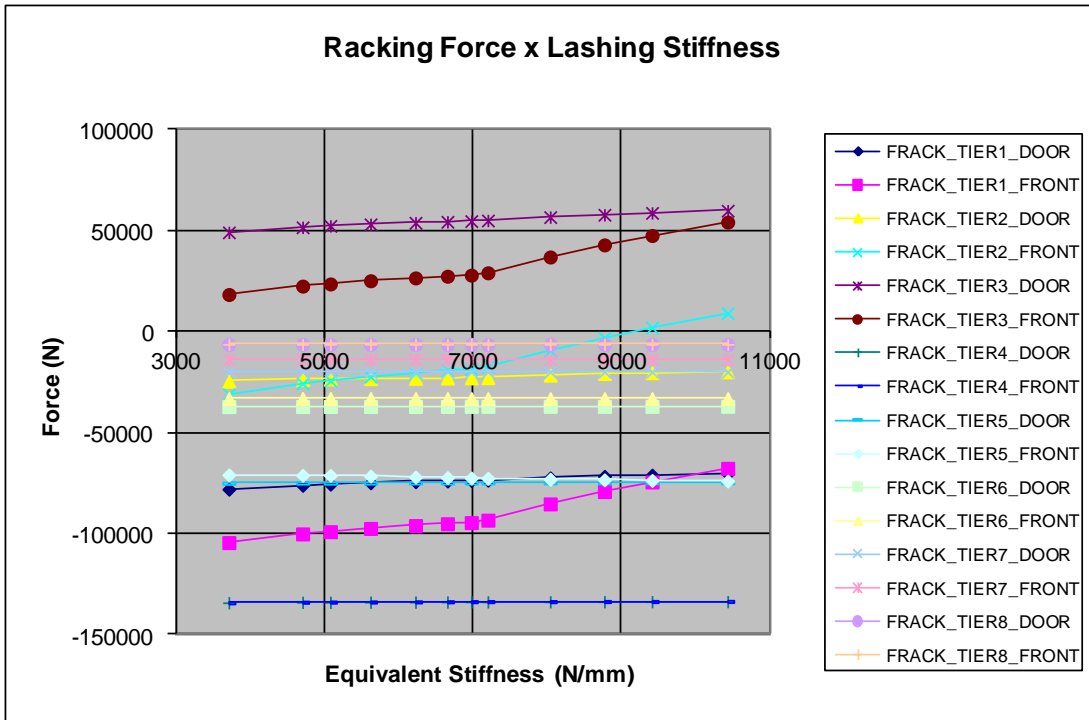


Figure 5.19 – Racking Force x Lashing Stiffness for bay 74 and row 2.

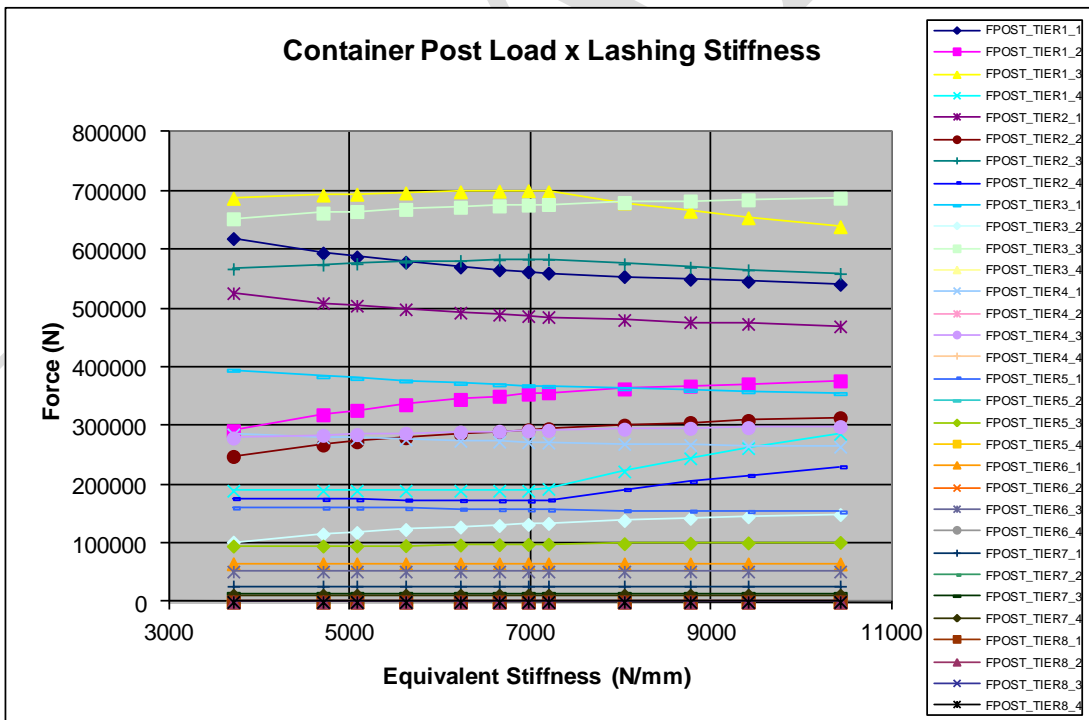


Figure 5.20 – Container Post Load x Lashing Stiffness for bay 74 and row 2.

5.6.2. Bay 30 – Row 02

With the nominal values of 140 GPa for the equivalent elastic modulus of the lashing rod (E_{rod}) and 23.0 kN/mm for the lashing bridge stiffness (k_{bridge}), an equivalent lashing stiffness (K_{eq}) of 10.6 kN/mm was obtained. The range of E_{rod} is between 70 GPa and 210 GPa ($\pm 50\%$) and the range of k_{bridge} is between 11.5 kN/mm and 34.5 kN/mm ($\pm 50\%$). It gives a lower bound of 6.9 kN/mm and an upper bound of 13.0 kN/mm for k_{eq} (Table 5.7).

Table 5.7 – Lashing stiffness values for the container stack from bay 30 and row 2.

k_{eq} (N/mm)	k_{bridge} (N/mm)	k_{rod} (N/mm)	E_{rod} (N/mm ²)	A_{rod} (mm ²)	l_{rod} (mm)
6917,3	23000,0	9892,4	70000,0	531,0	3757,4
7272,7	11500,0	19784,8	140000,0	531,0	3757,4
9019,6	23000,0	14838,6	105000,0	531,0	3757,4
9215,3	17250,0	19784,8	140000,0	531,0	3757,4
10635,8	23000,0	19784,8	140000,0	531,0	3757,4
11719,7	28750,0	19784,8	140000,0	531,0	3757,4
11917,1	23000,0	24731,0	175000,0	531,0	3757,4
12574,0	34500,0	19784,8	140000,0	531,0	3757,4
12957,7	23000,0	29677,2	210000,0	531,0	3757,4

The influence of the lashing stiffness on the forces acting on containers and lashing elements was observed in the obtained results. The lashing force on the bottom corner of the door end and port side of the 3rd tier container (FLASH_TIER3_4), where the uplifting occurs, is directly proportional to the lashing stiffness, while the vertical force acting on the twist lock at the same corner (FTLZ_TIER3_4) is inversely proportional. The obtained results can be seen from Figure 5.21 to Figure 5.24.

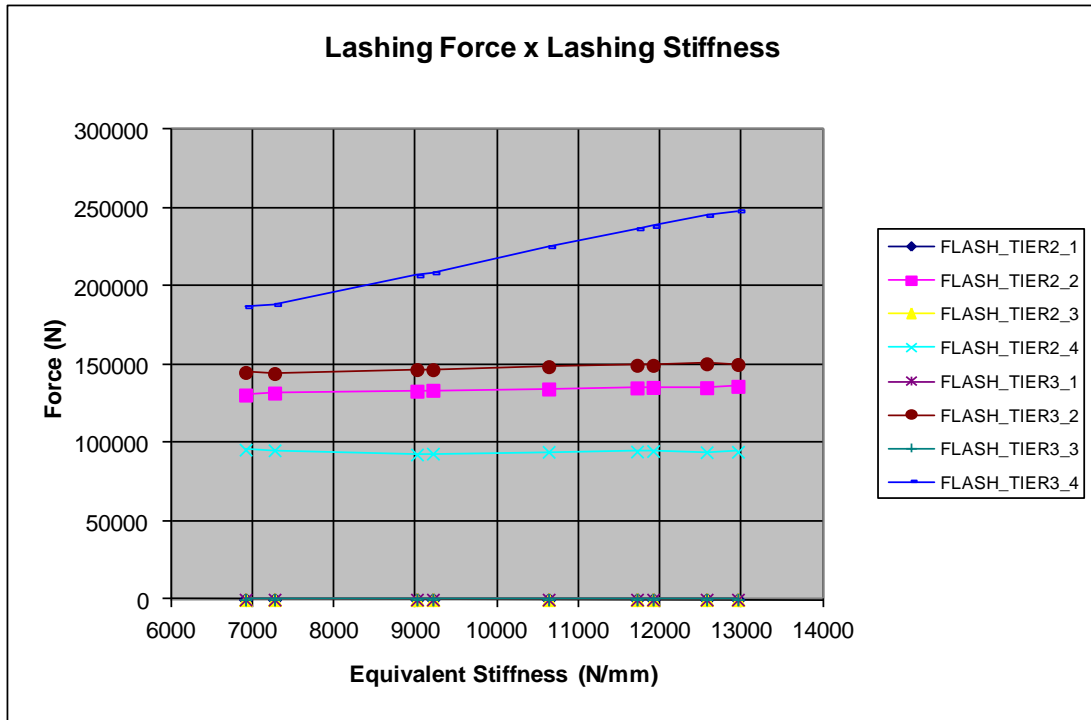


Figure 5.21 – Lashing Force x Lashing Stiffness for bay 30 and row 2.

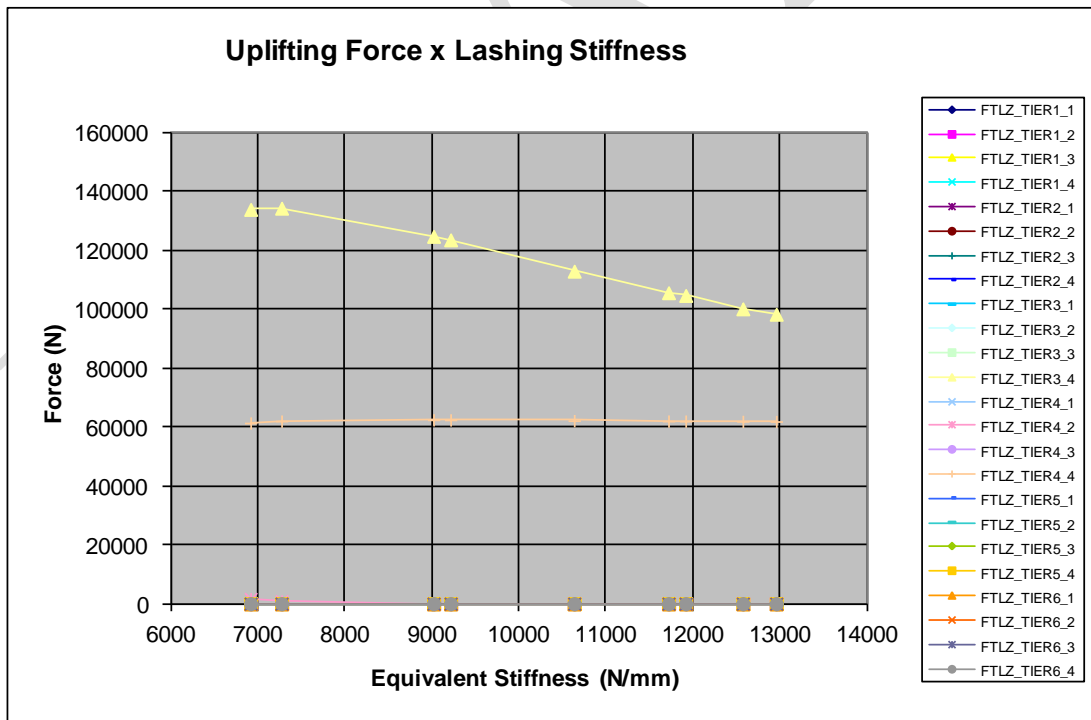


Figure 5.22 – Uplifting Force x Lashing Stiffness for bay 30 and row 2.

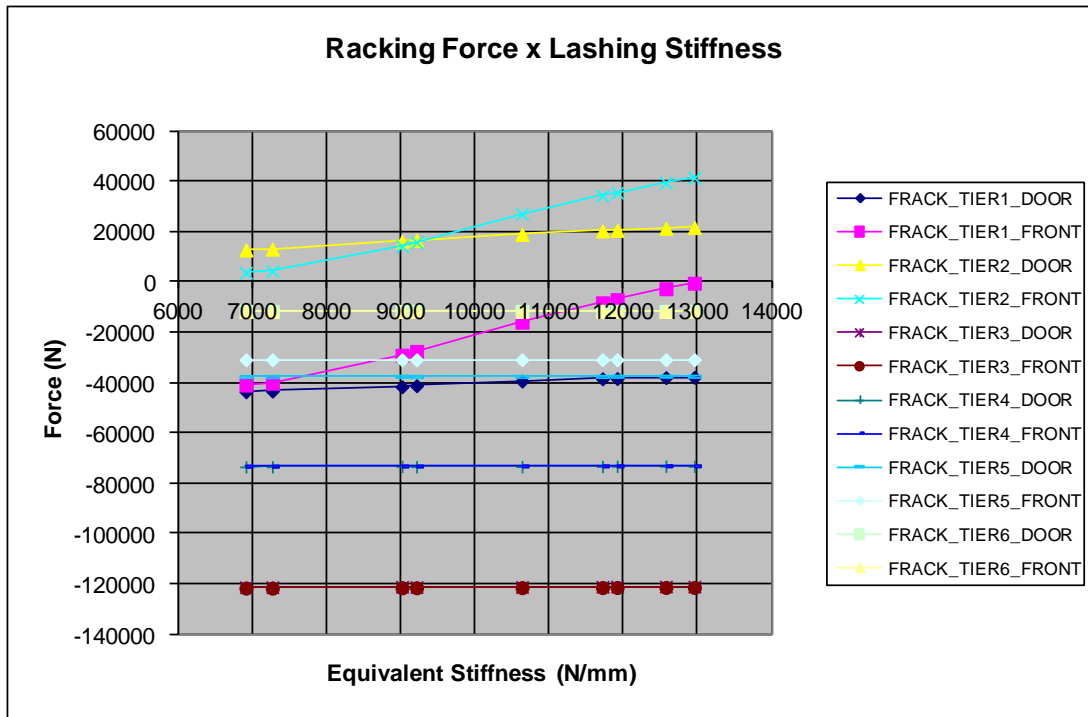


Figure 5.23 – Racking Force x Lashing Stiffness for bay 30 and row 2.

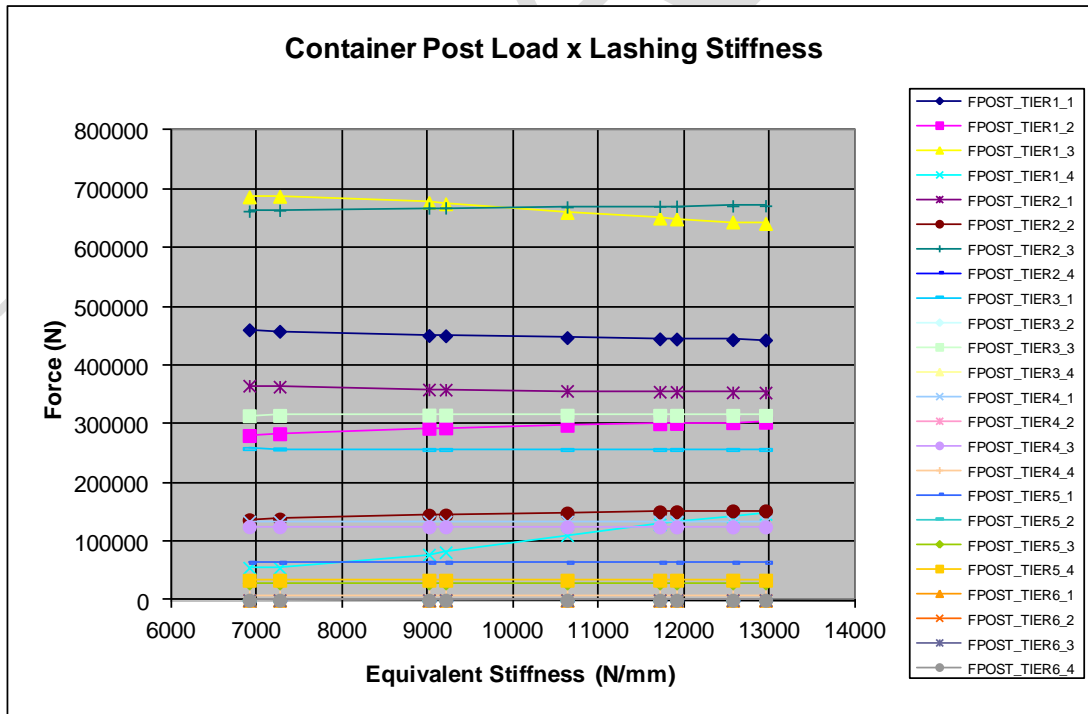


Figure 5.24 – Container Post Load x Lashing Stiffness for bay 30 and row 2.

5.7. Variation of the Vertical Clearance of Locks

The variation of the vertical clearance of the twist locks, which was minutely described on section 2.4.4, was also analyzed. This parameter was expected to be the most important one, due to the overloading on the lashing rod connected to the uplifted corner, as explained in section 2.6.2. Thus, the parametric study was performed with the 8-tier high stack from bay 74 and row 2, as well as with the 6-tier high stack from bay 30 and row 2 and the 6-tier high additional stack. To analyze its dependence on the lashing stiffness, the parametric studies were performed with 3 different values for E_{rod} : 70 GPa, 140 GPa and 210 GPa.

5.7.1. Bay 74 – Row 02

The vertical clearance of the SAL, which has a nominal value of 15 mm, was varied on a range from 5 mm to 35 mm. For each value of E_{rod} , the operational loads acting on containers and lashing elements were evaluated. The results can be seen in the following sections.

- $E_{rod} = 70$ GPa

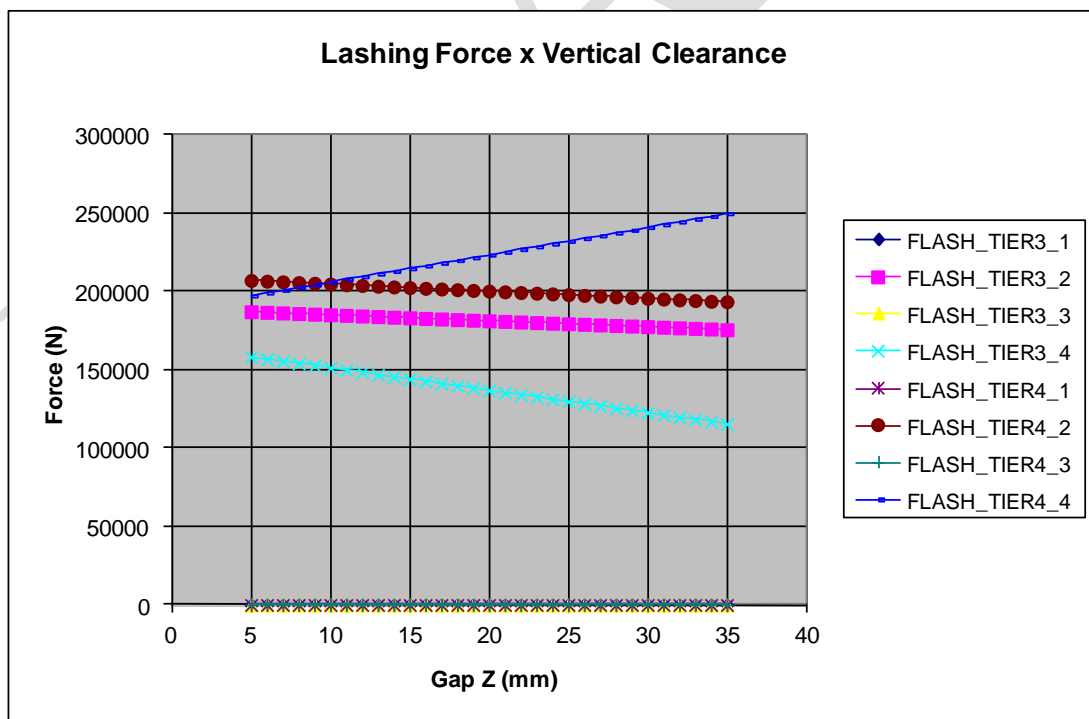


Figure 5.25 – Lashing Force x Vertical Clearance for bay 74 and row 2 ($E_{rod} = 70$ GPa).

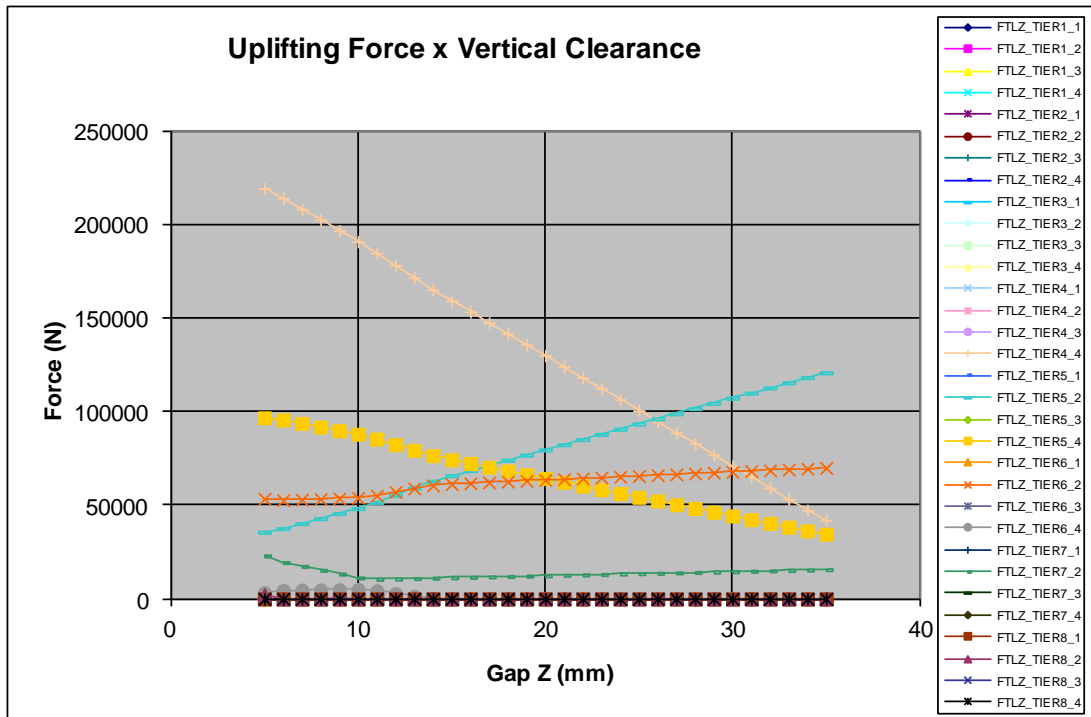


Figure 5.26 – Uplifting Force x Vertical Clearance for bay 74 and row 2 ($E_{rod} = 70$ GPa).

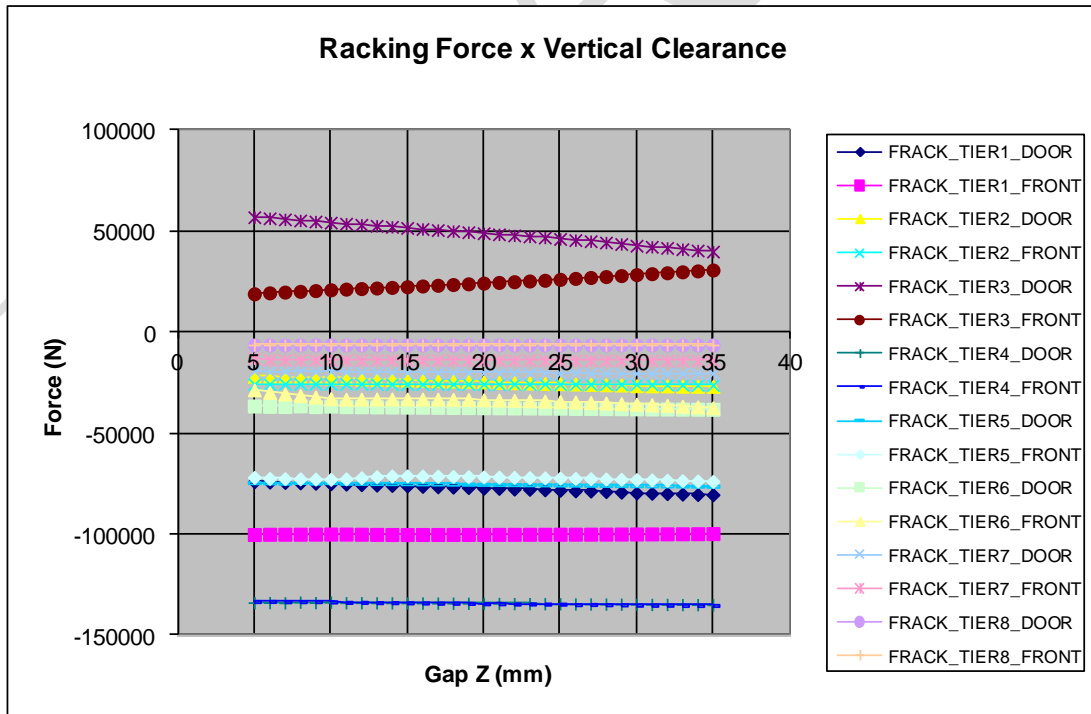


Figure 5.27 – Racking Force x Vertical Clearance for bay 74 and row 2 ($E_{rod} = 70$ GPa).

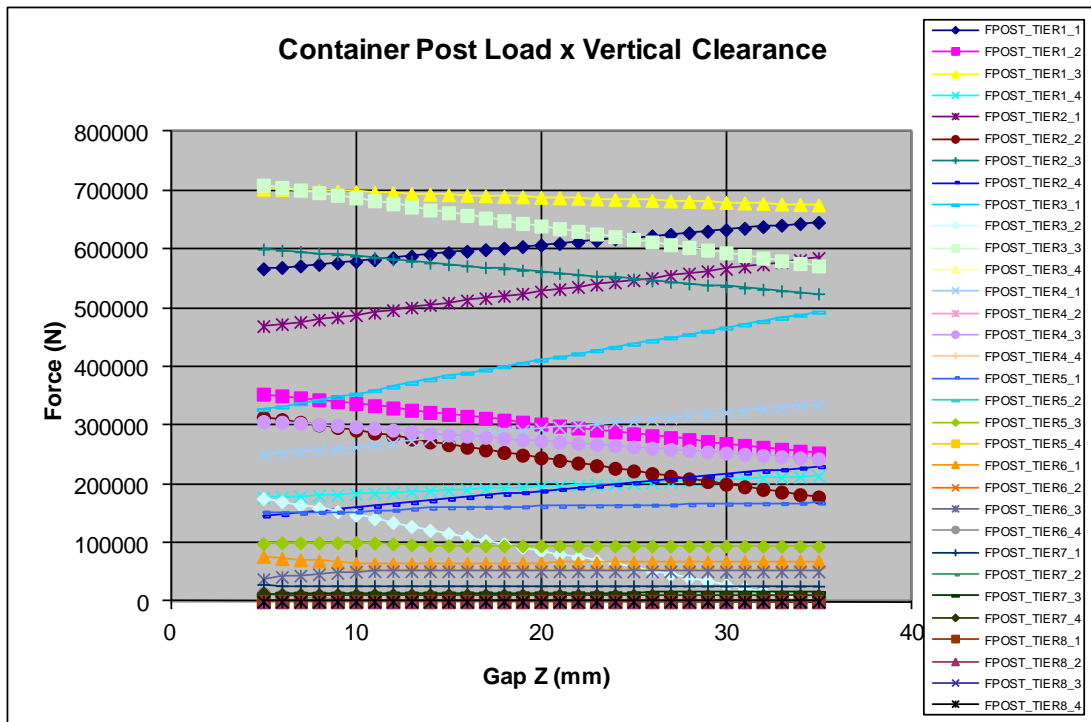


Figure 5.28 – Container Post Load x Vertical Clearance for bay 74 and row 2 ($E_{rod} = 70$ GPa).

- $E_{rod} = 140$ GPa

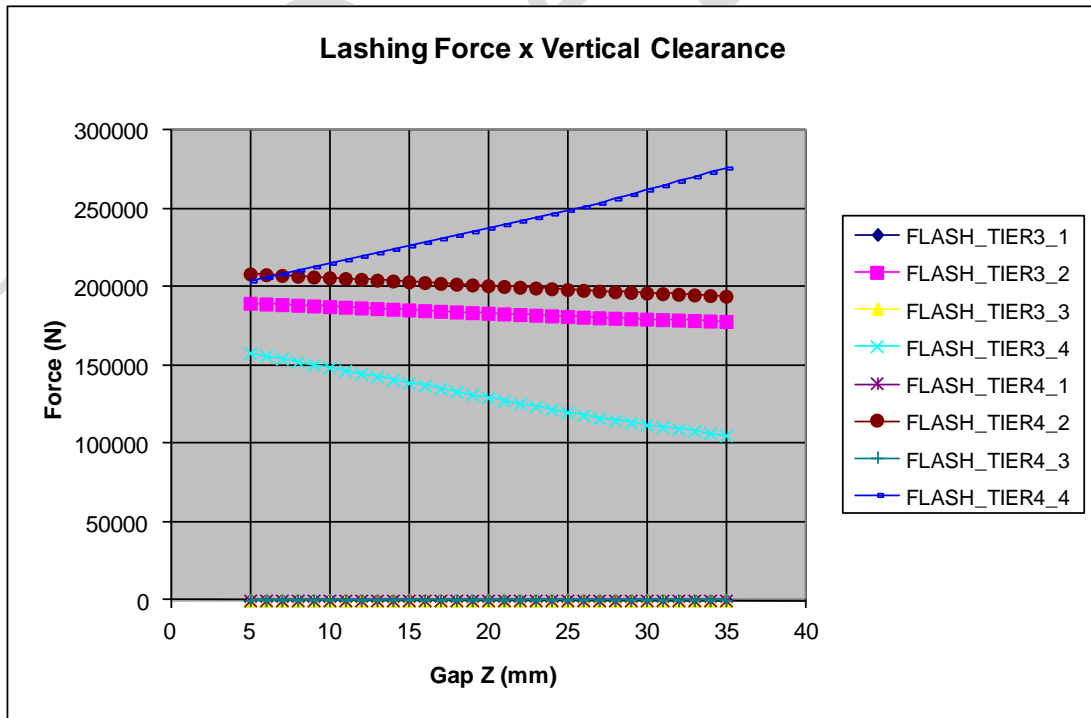


Figure 5.29 – Lashing Force x Vertical Clearance for bay 74 and row 2 ($E_{rod} = 140$ GPa).

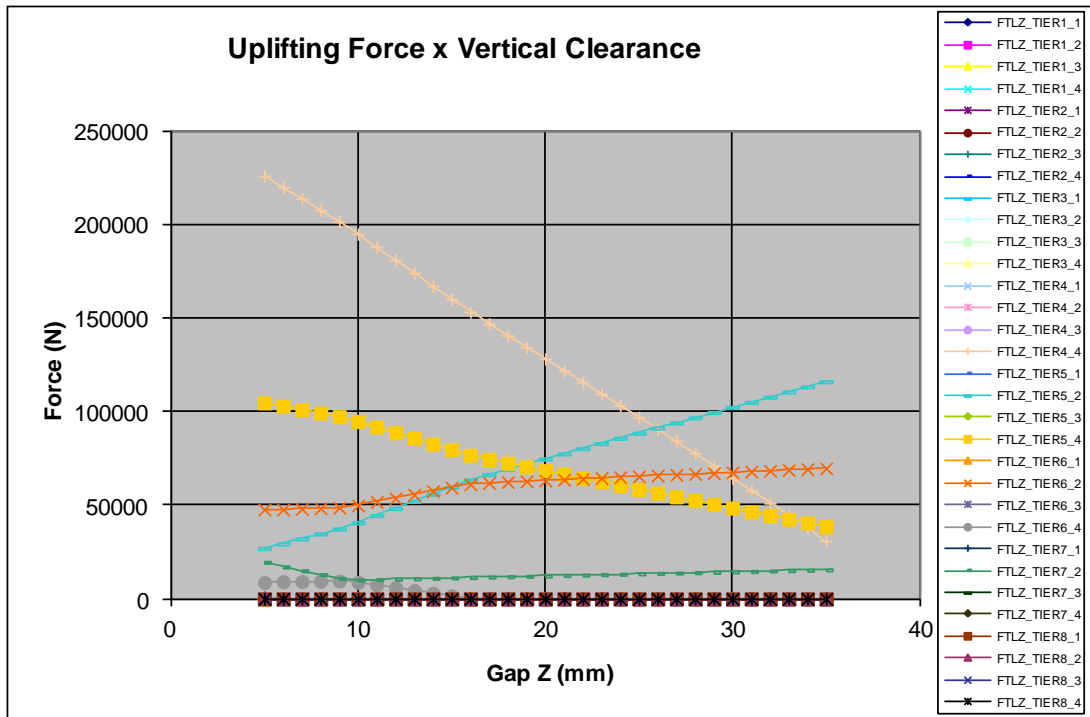


Figure 5.30 – Uplifting Force x Vertical Clearance for bay 74 and row 2 ($E_{rod} = 140$ GPa).

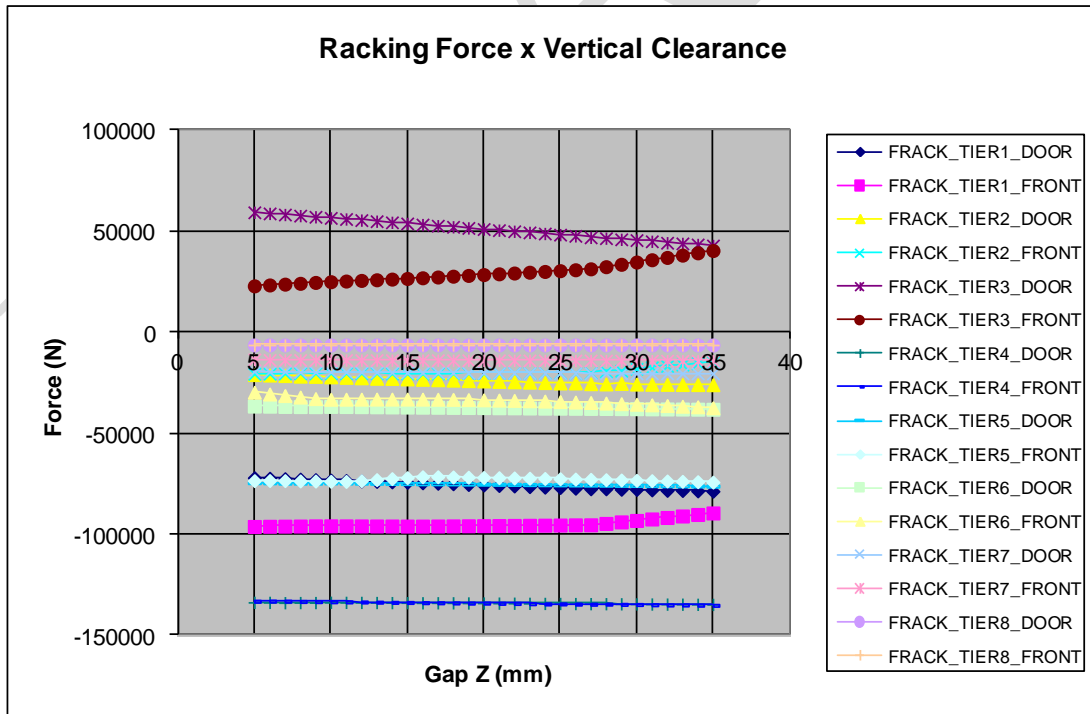


Figure 5.31 – Racking Force x Vertical Clearance for bay 74 and row 2 ($E_{rod} = 140$ GPa).

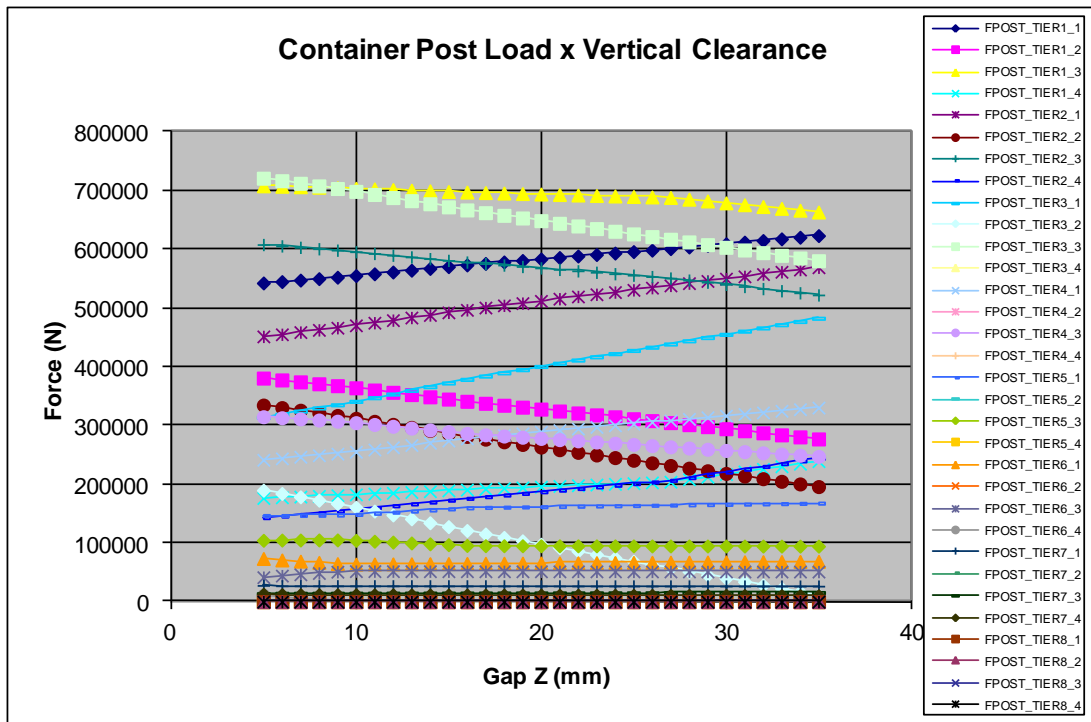


Figure 5.32 – Container Post Load x Vertical Clearance for bay 74 and row 2 ($E_{rod} = 140$ GPa).

- $E_{rod} = 210$ GPa

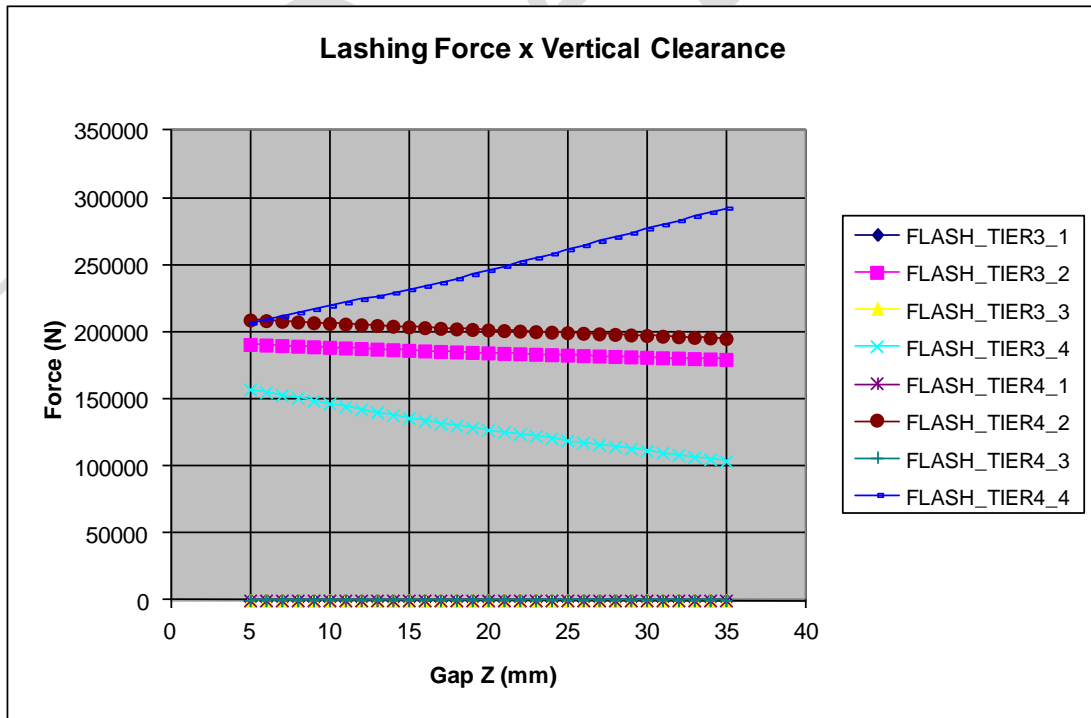


Figure 5.33 – Lashing Force x Vertical Clearance for bay 74 and row 2 ($E_{rod} = 210$ GPa).

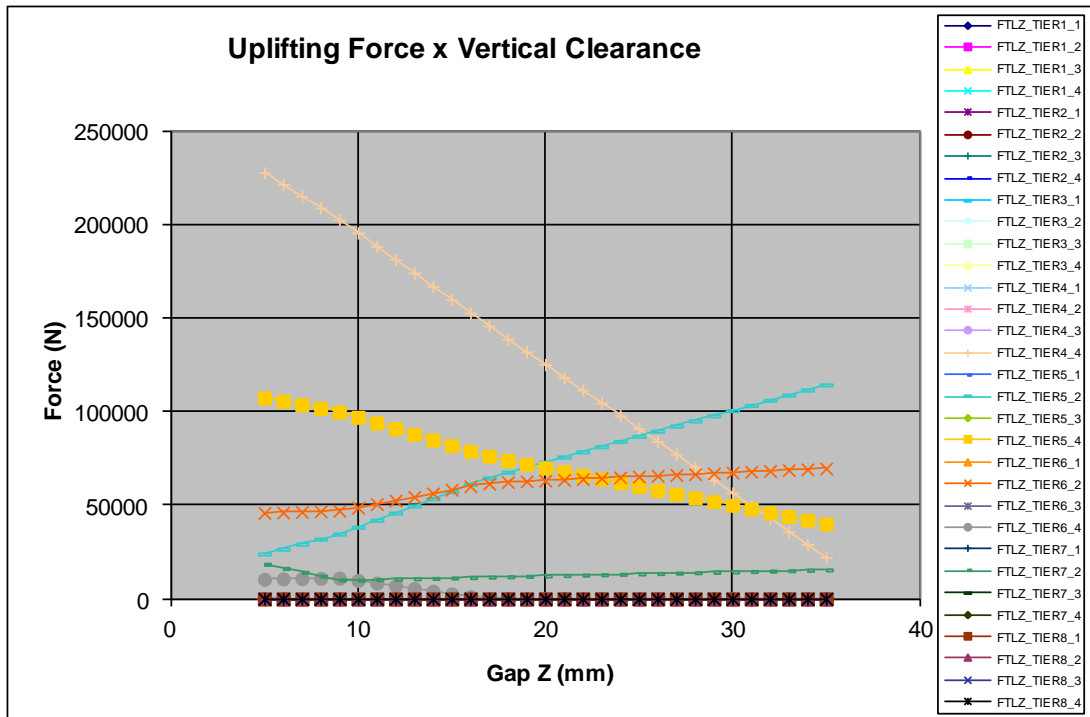


Figure 5.34 – Uplifting Force x Vertical Clearance for bay 74 and row 2 ($E_{rod} = 210$ GPa).

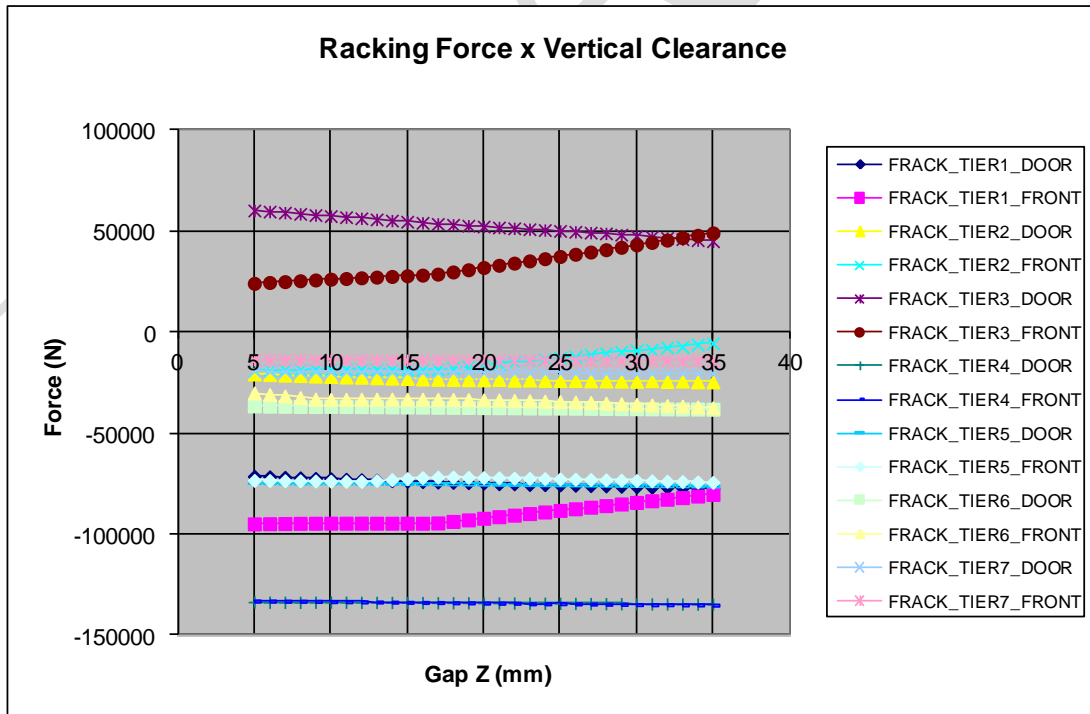


Figure 5.35 – Racking Force x Vertical Clearance for bay 74 and row 2 ($E_{rod} = 210$ GPa).

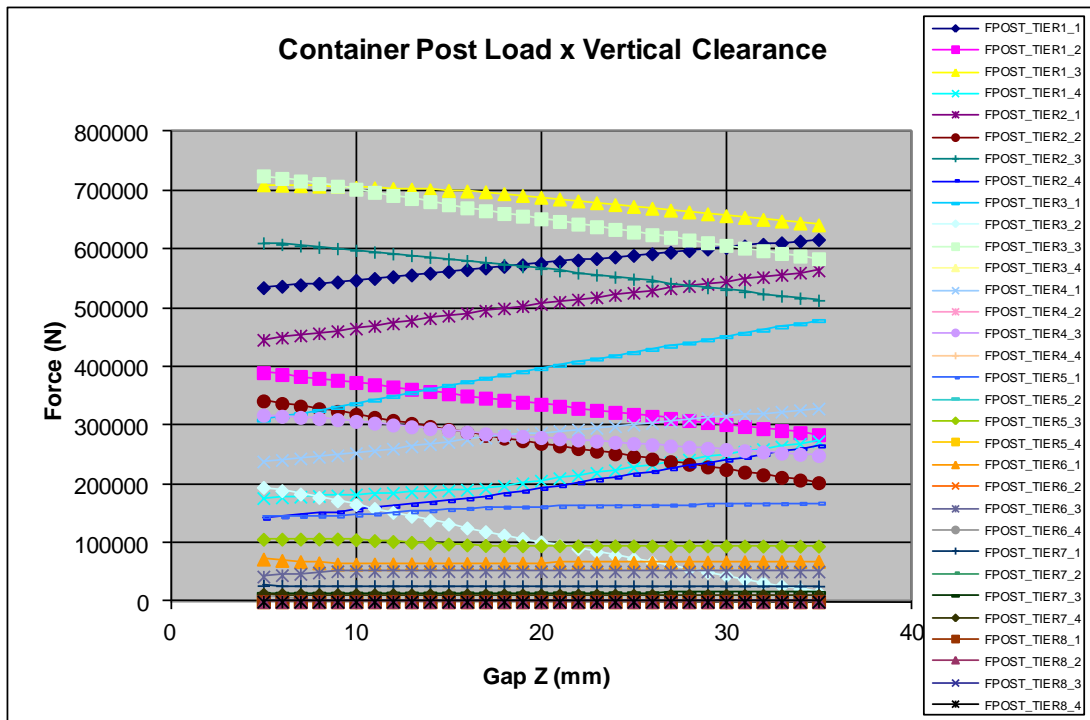


Figure 5.36 – Container Post Load x Vertical Clearance for bay 74 and row 2 ($E_{rod} = 210$ GPa).

It is possible to see in the obtained results the strong dependence of the lashing force (FLASH_TIER4_4) and vertical force on the lock (FTLZ_TIER4_4) of the bottom corner in the port side of the front end of the 4th tier container of the stack. While the lashing force is directly proportional to the vertical clearance of the twist lock, the vertical force acting on the twist lock is inversely proportional. The same behaviour was noted on the three cases (different values of lashing stiffness), but the difference between them is the rate of variation of those results: the higher the stiffness, the higher the rate.

5.7.2. Bay 30 – Row 02

The vertical clearance of the SAL, which has a nominal value of 15 mm, was varied on a range from 5 mm to 30 mm. For each value of E_{rod} , the operational loads acting on containers and lashing elements were evaluated. The results can be seen in the following sections.

- $E_{rod} = 70 \text{ GPa}$

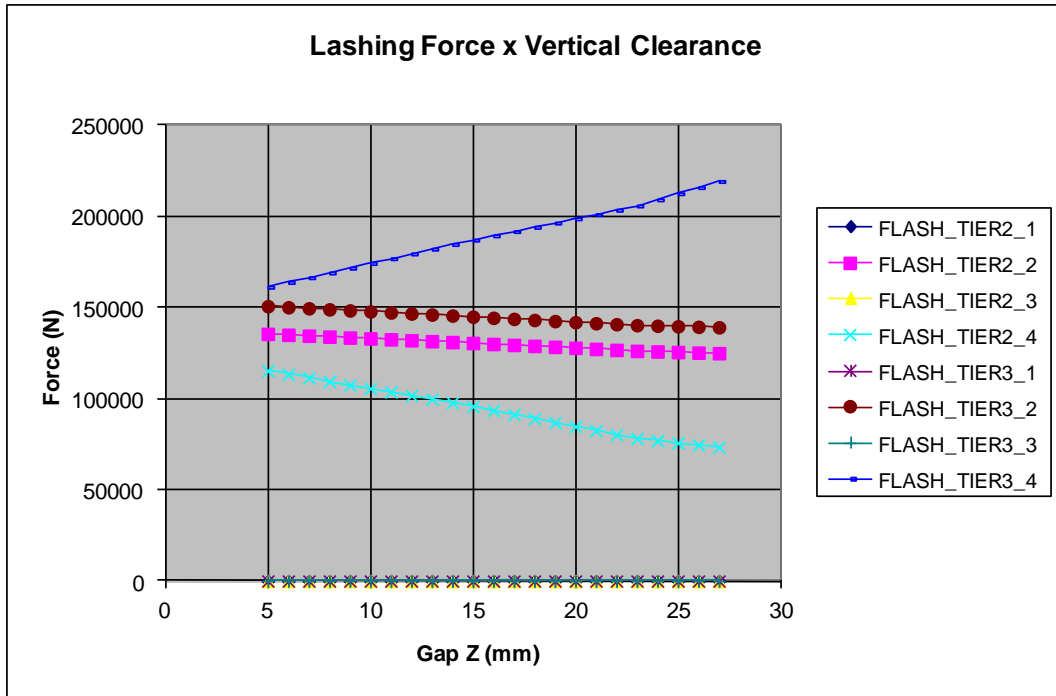


Figure 5.37 – Lashing Force x Vertical Clearance for bay 30 and row 2 ($E_{rod} = 70 \text{ GPa}$).

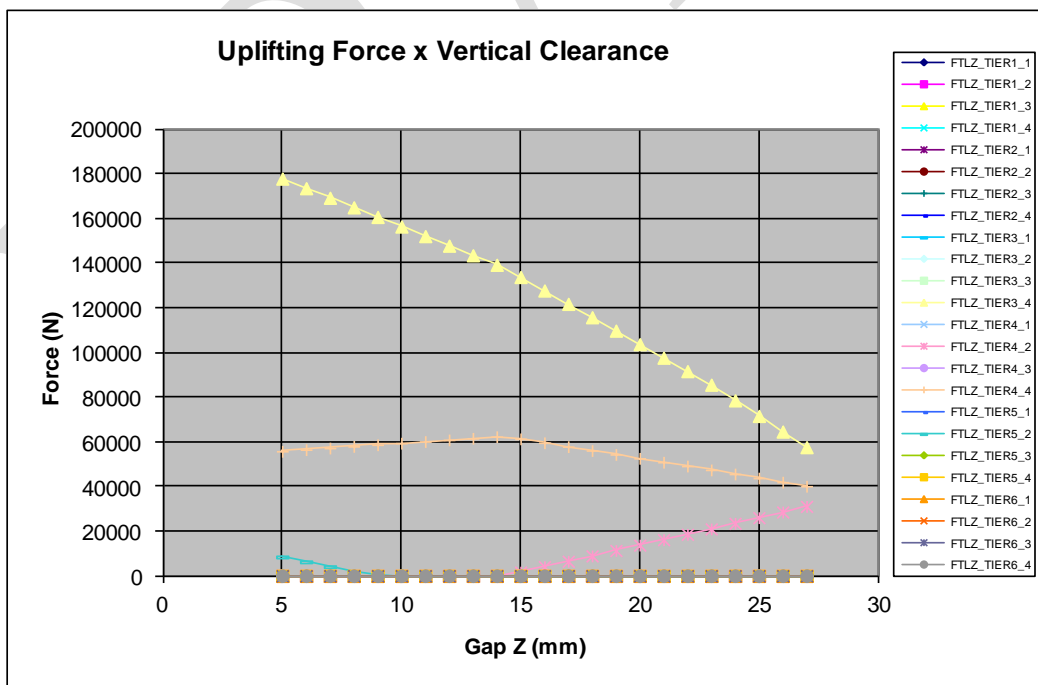


Figure 5.38 – Uplifting Force x Vertical Clearance for bay 30 and row 2 ($E_{rod} = 70 \text{ GPa}$).

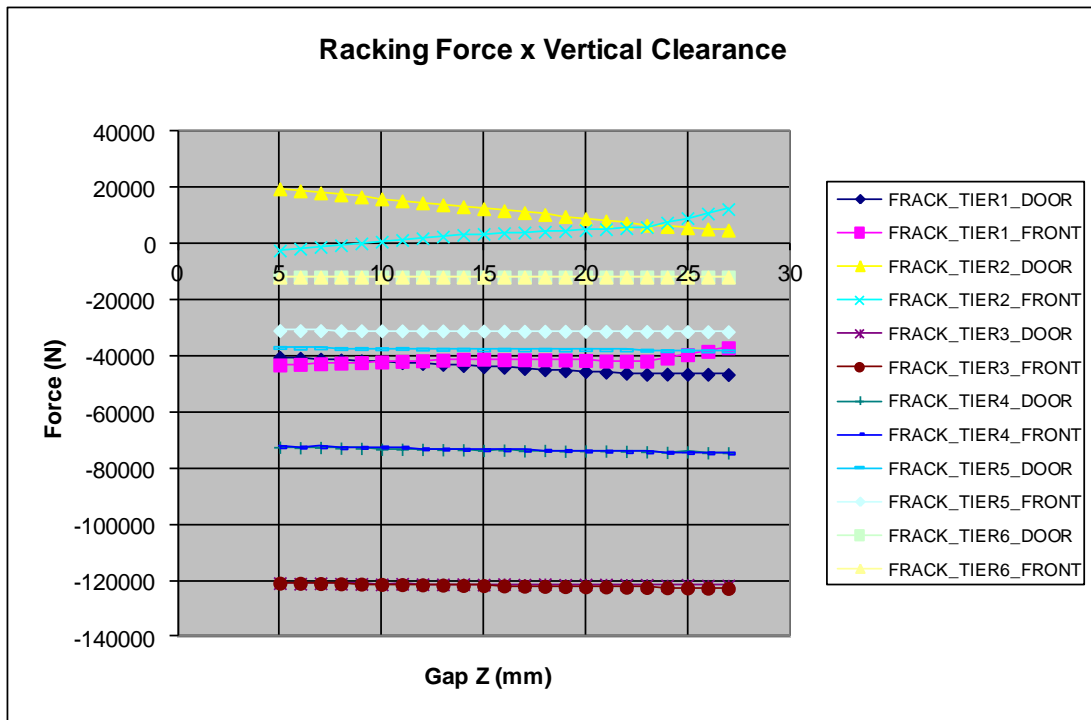


Figure 5.39 – Racking Force x Vertical Clearance for bay 30 and row 2 ($E_{rod} = 70$ GPa).

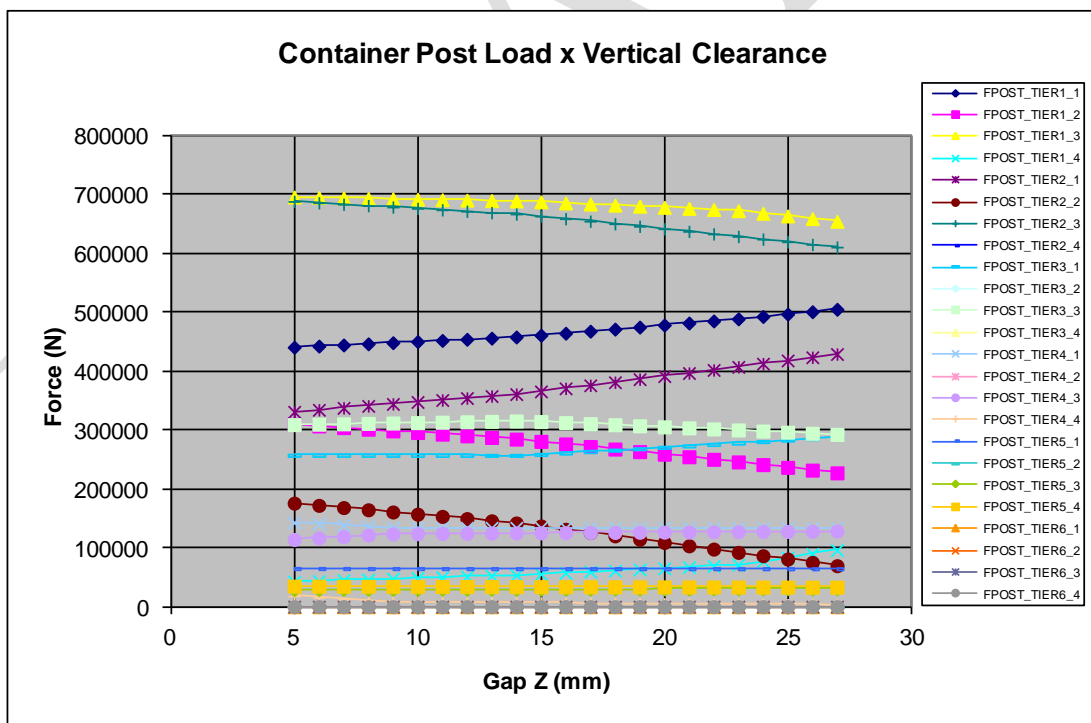


Figure 5.40 – Container Post Load x Vertical Clearance for bay 30 and row 2 ($E_{rod} = 70$ GPa).

- $E_{rod} = 140 \text{ GPa}$

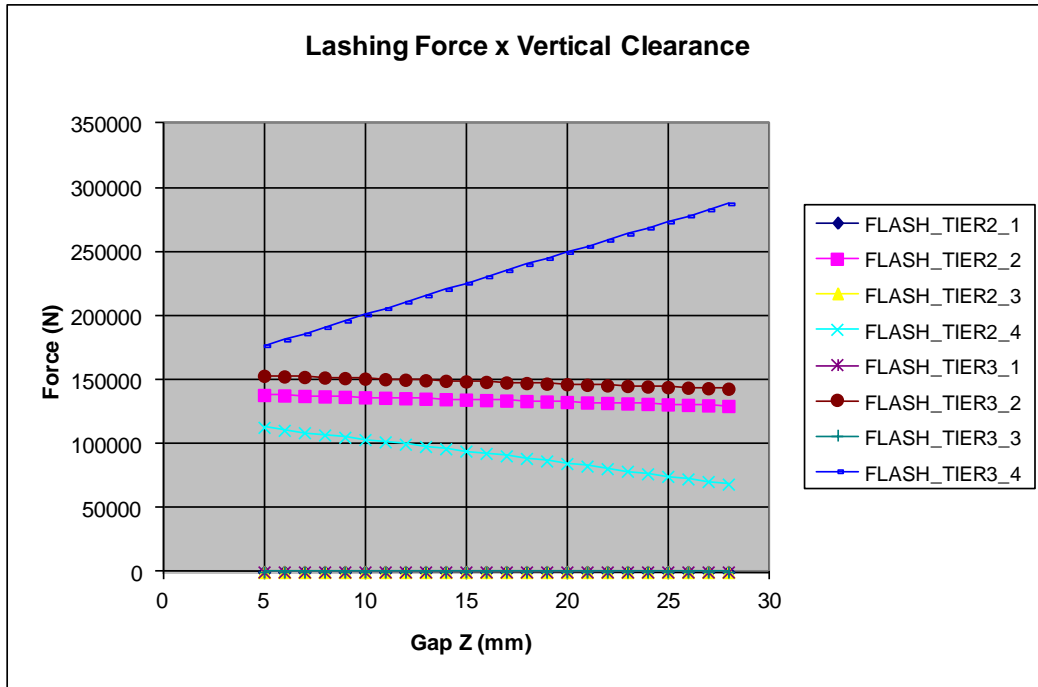


Figure 5.41 – Lashing Force x Vertical Clearance for bay 30 and row 2 ($E_{rod} = 140 \text{ GPa}$).

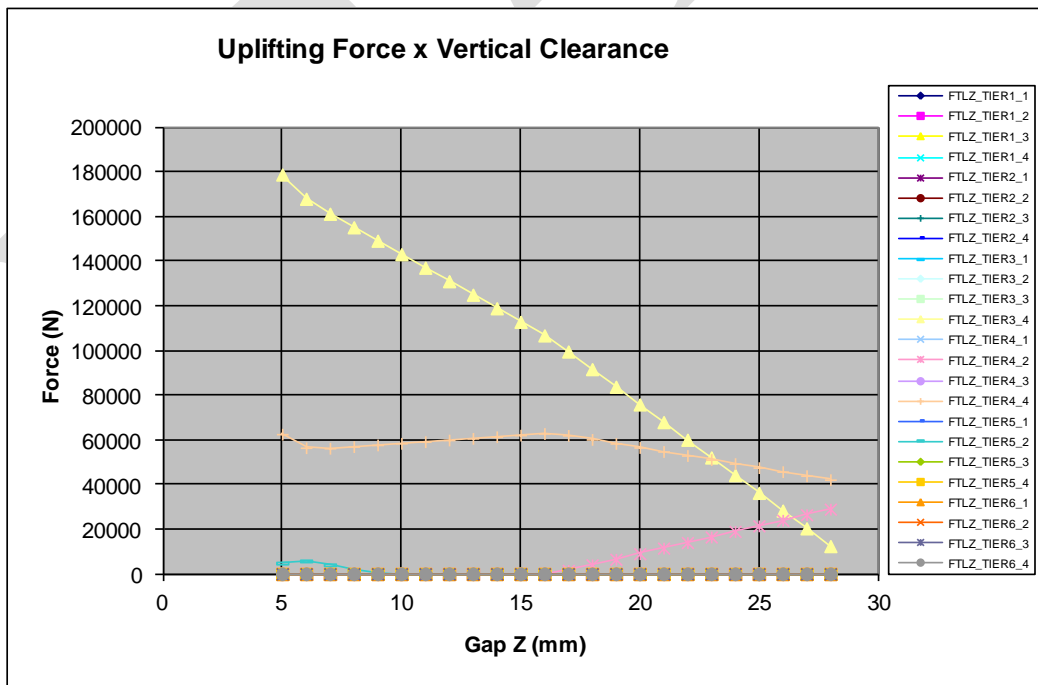


Figure 5.42 – Uplifting Force x Vertical Clearance for bay 30 and row 2 ($E_{rod} = 140 \text{ GPa}$).

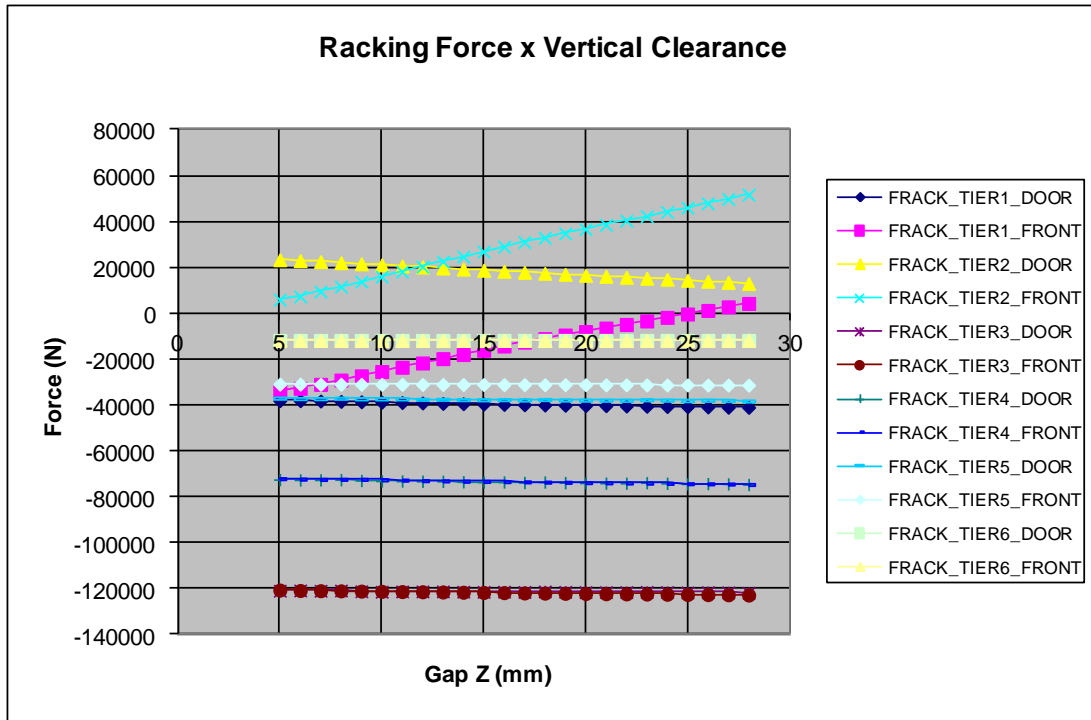


Figure 5.43 – Racking Force x Vertical Clearance for bay 30 and row 2 ($E_{rod} = 140$ GPa).

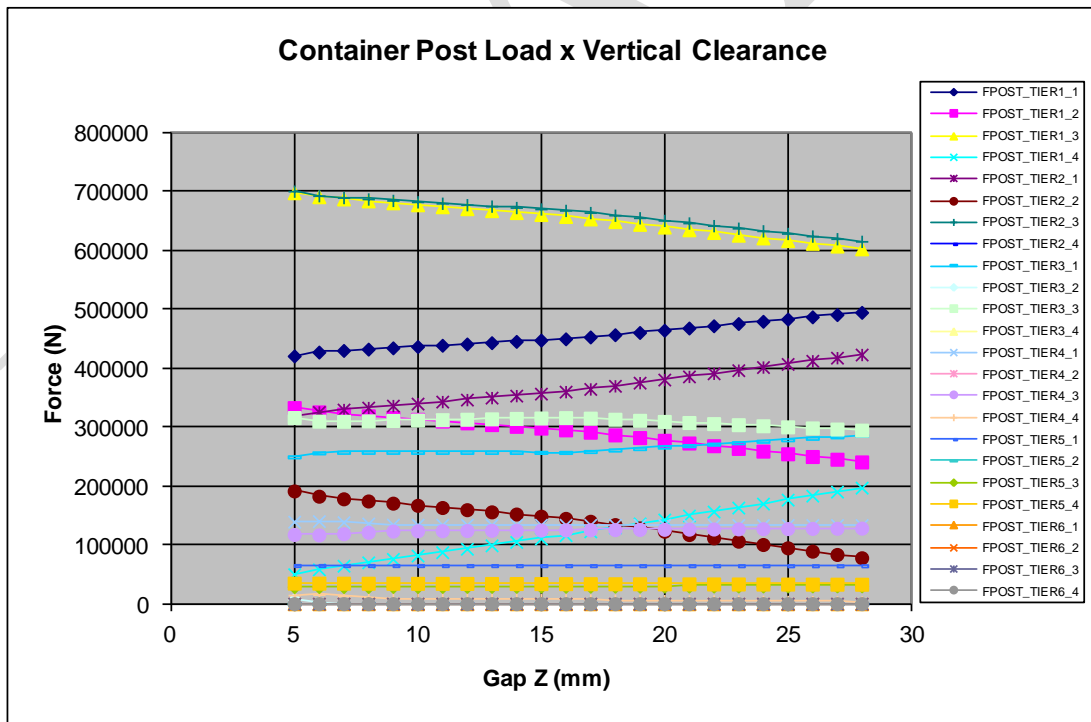


Figure 5.44 – Container Post Load x Vertical Clearance for bay 30 and row 2 ($E_{rod} = 140$ GPa).

- $E_{rod} = 210 \text{ GPa}$

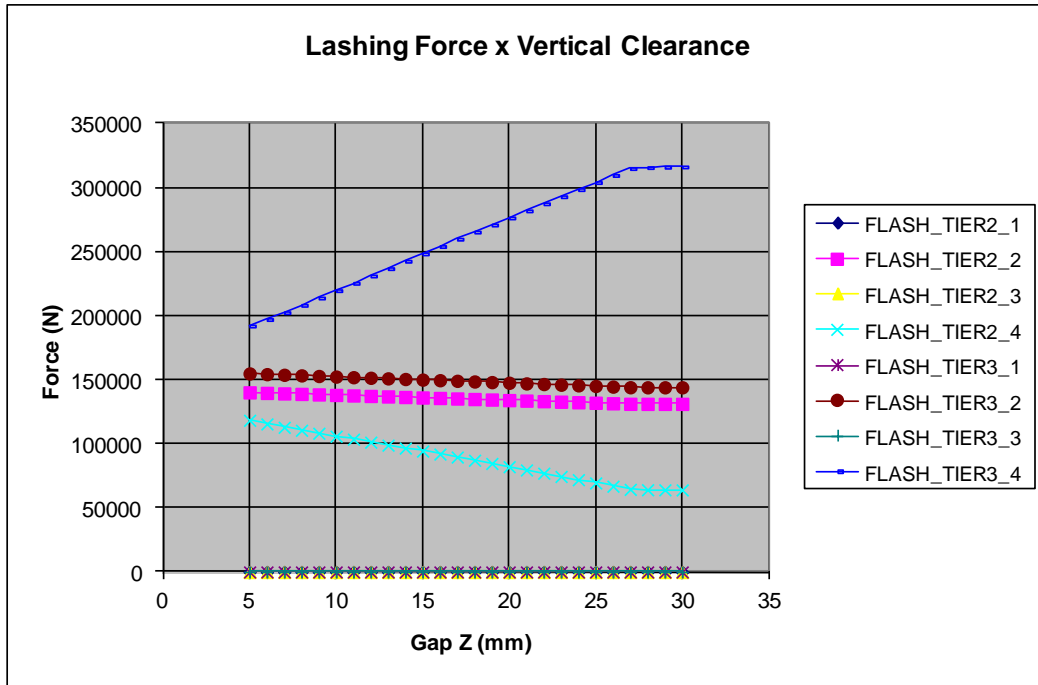


Figure 5.45 – Lashing Force x Vertical Clearance for bay 30 and row 2 ($E_{rod} = 210 \text{ GPa}$).

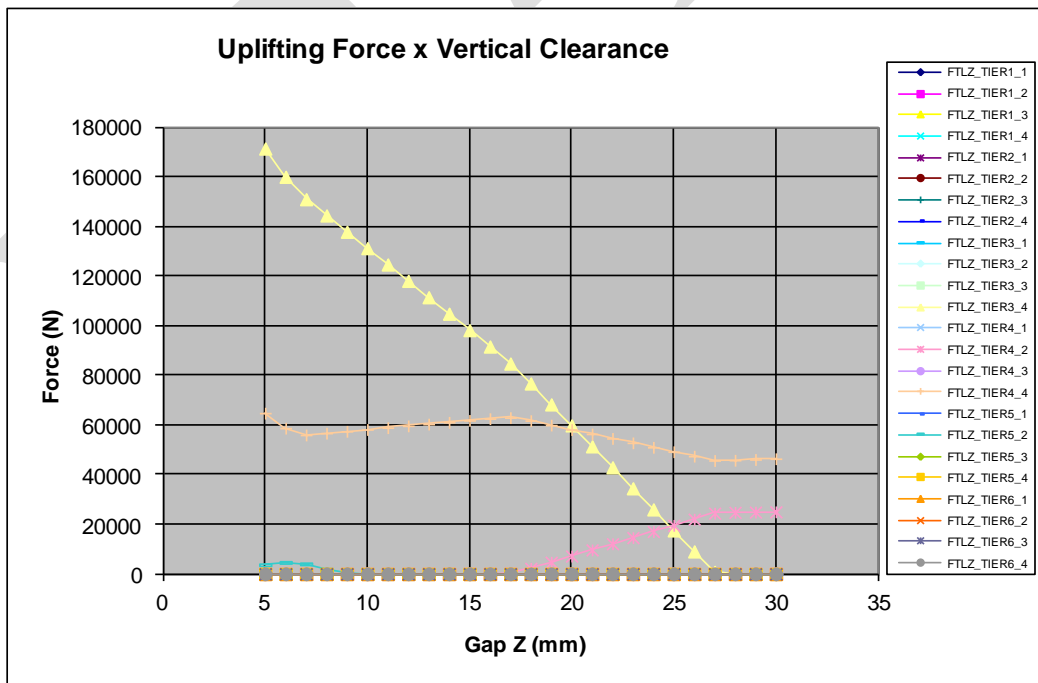


Figure 5.46 – Uplifting Force x Vertical Clearance for bay 30 and row 2 ($E_{rod} = 210 \text{ GPa}$).

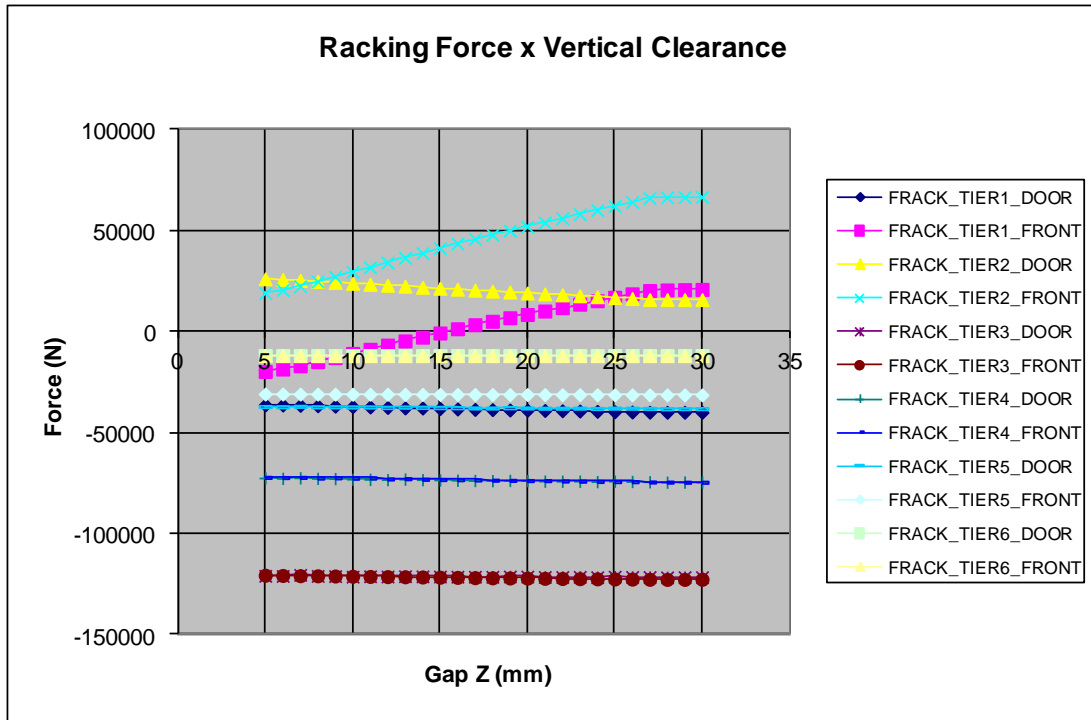


Figure 5.47 – Racking Force x Vertical Clearance for bay 30 and row 2 ($E_{rod} = 210$ GPa).

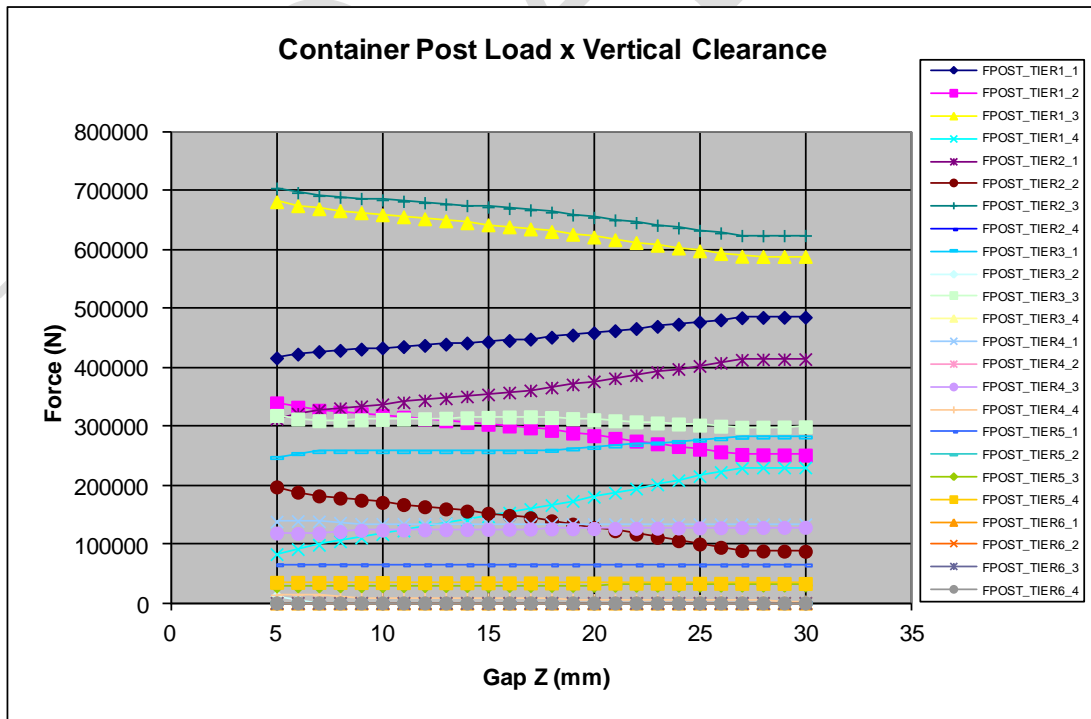


Figure 5.48 – Container Post Load x Vertical Clearance for bay 30 and row 2 ($E_{rod} = 210$ GPa).

It is possible to see in the obtained results the strong dependence of the lashing force (FLASH_TIER3_4) and vertical force on twist lock (FTLZ_TIER3_4) of the bottom corner in the port side of the front end of the 3rd tier container of the stack. While the lashing force is directly proportional to the vertical clearance of the twist lock, the vertical force acting on the twist lock is inversely proportional. As in the previous case, the same behaviour was noted with the three different values of lashing stiffness, with different rate of force variation against clearance increasing. In Figure 5.46, one can see the uplifting force is null when the vertical clearance is equal to 27 mm. When the clearance is higher than that, the twist lock is not working anymore and the lashing force at the same corner remains constant (Figure 5.45).

5.7.3. Additional Stack

The vertical clearance of the SAL, which has a nominal value of 15 mm, was varied on a range from 5 mm to 25 mm. For each value of E_{rod} , the operational loads acting on containers and lashing elements were evaluated. The results can be seen in the following sections.

- $E_{rod} = 70 \text{ GPa}$

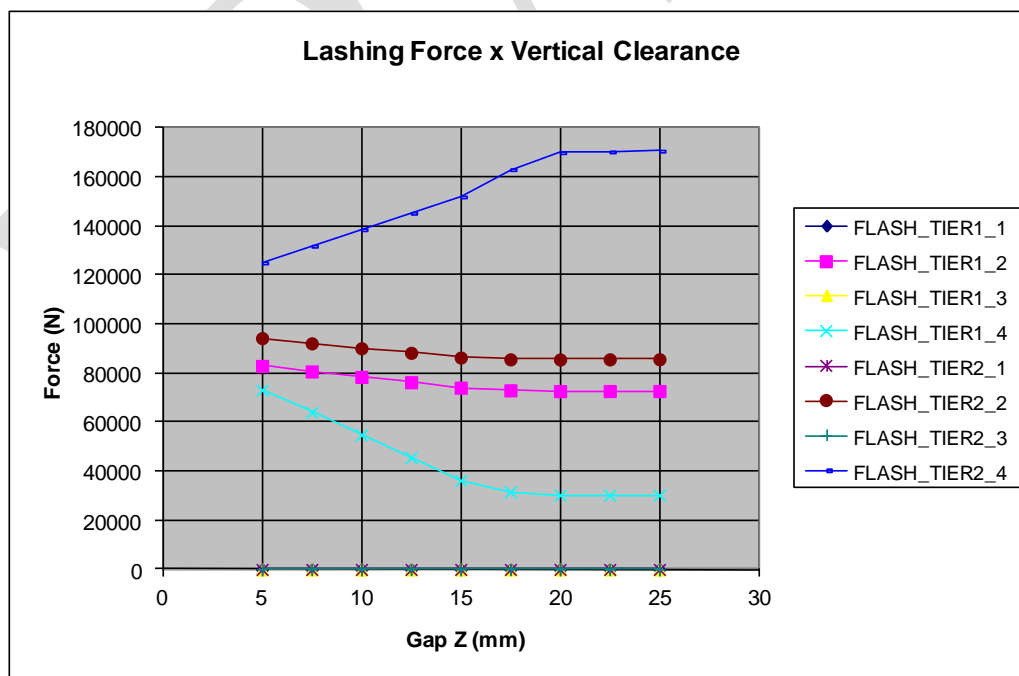


Figure 5.49 – Lashing Force x Vertical Clearance for the additional stack ($E_{rod} = 70 \text{ GPa}$).

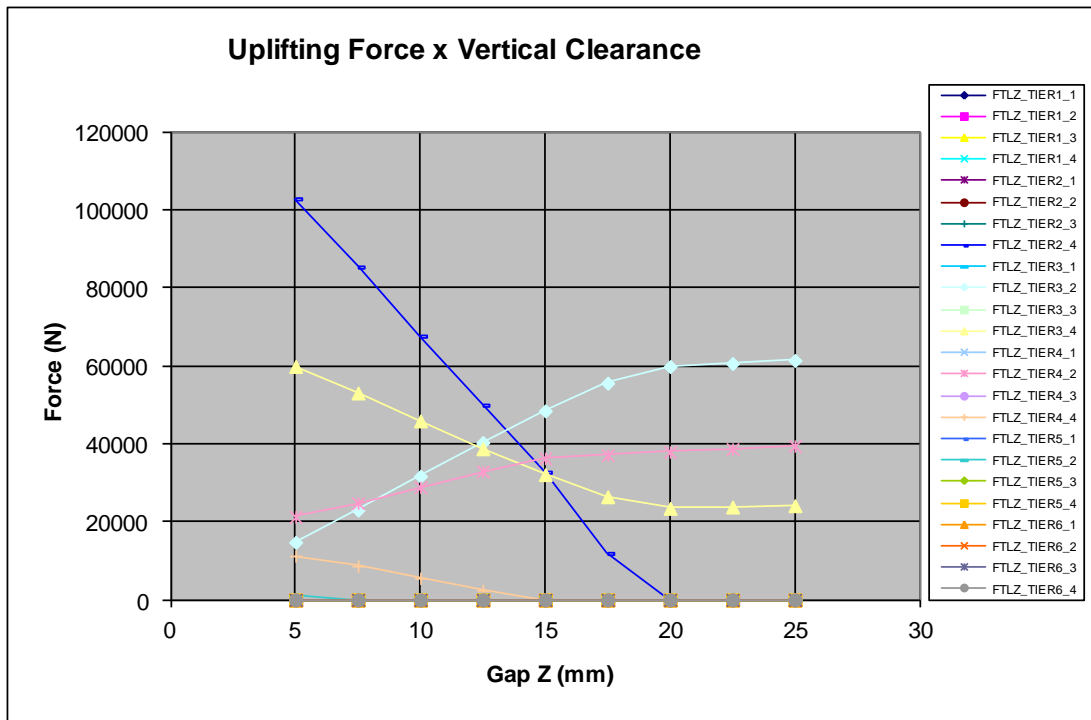


Figure 5.50 – Uplifting Force x Vertical Clearance for the additional stack ($E_{rod} = 70$ GPa).

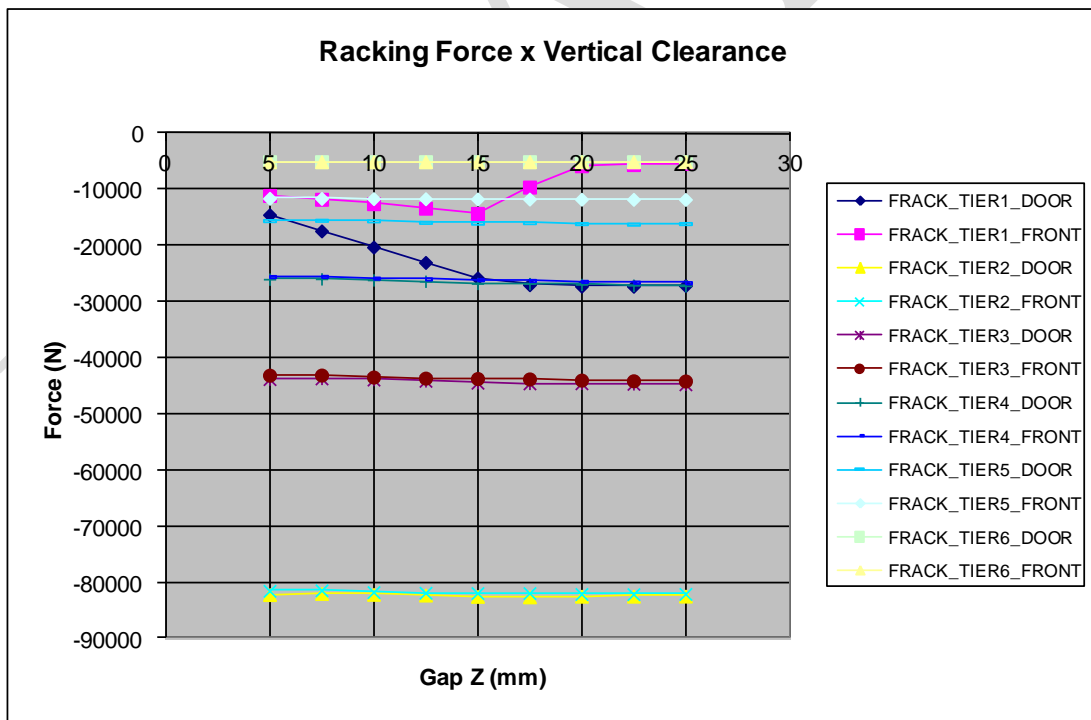


Figure 5.51 – Racking Force x Vertical Clearance for the additional stack ($E_{rod} = 70$ GPa).

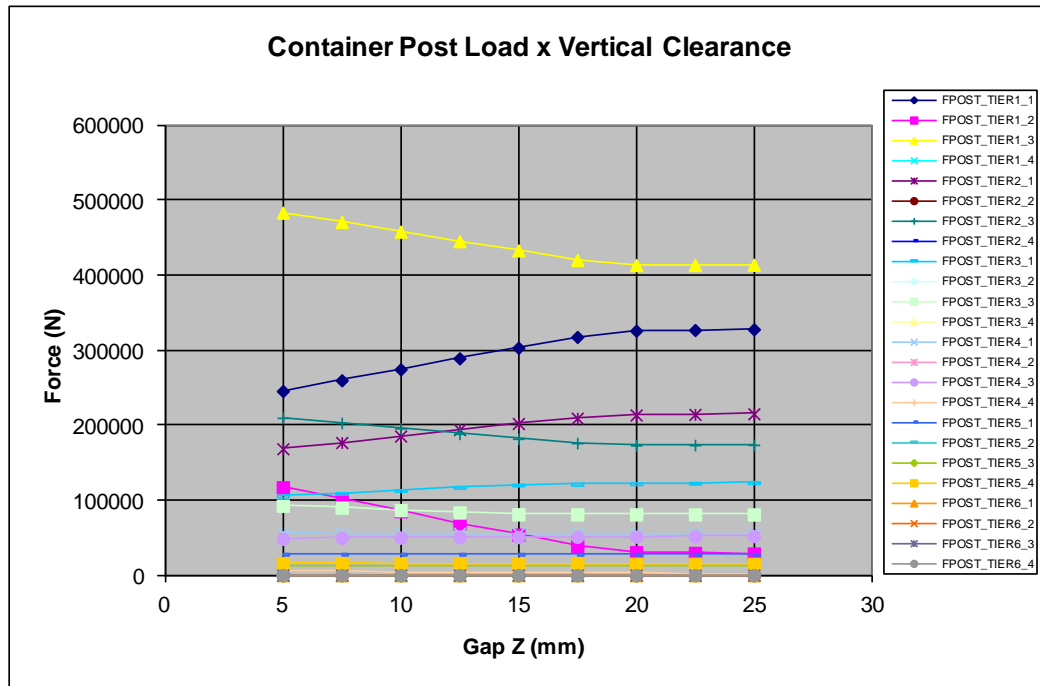


Figure 5.52 – Container Post Load x Vertical Clearance for the additional stack ($E_{rod} = 70$ GPa).

- $E_{rod} = 140$ GPa

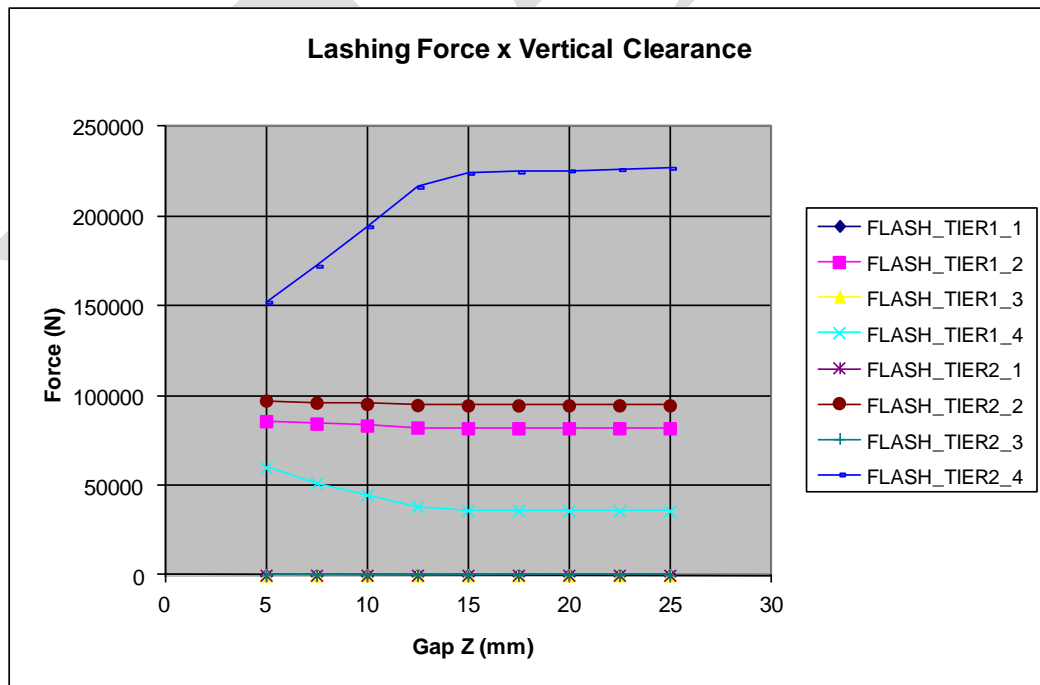


Figure 5.53 – Lashing Force x Vertical Clearance for the additional stack ($E_{rod} = 140$ GPa).

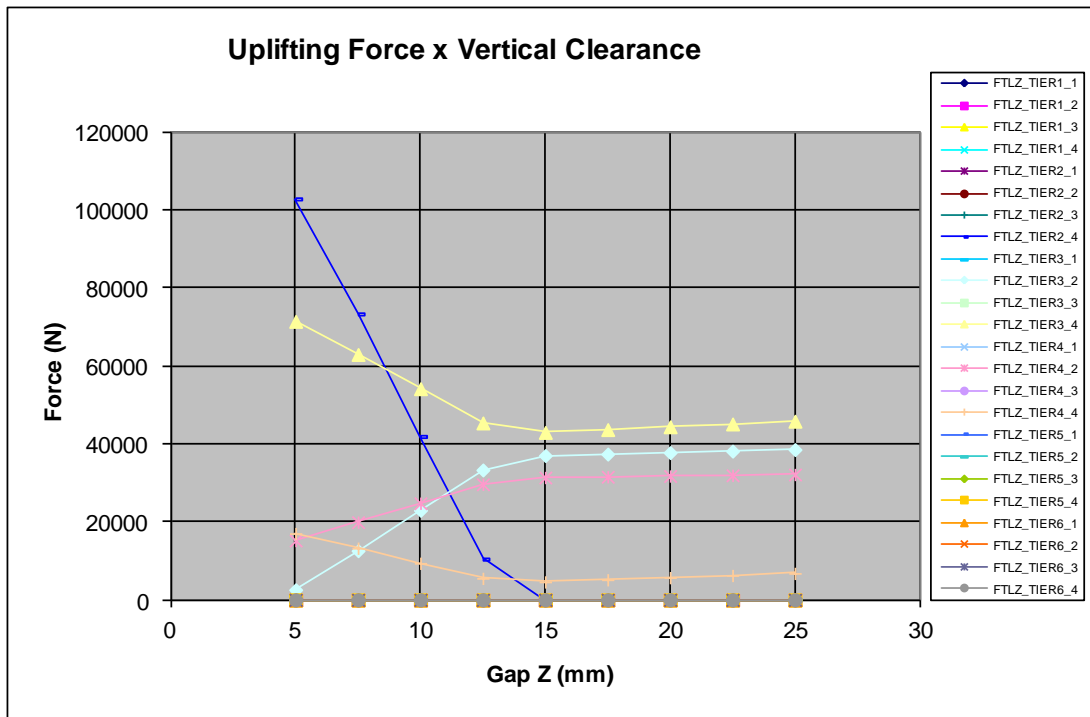


Figure 5.54 – Uplifting Force x Vertical Clearance for the additional stack ($E_{rod} = 140$ GPa).

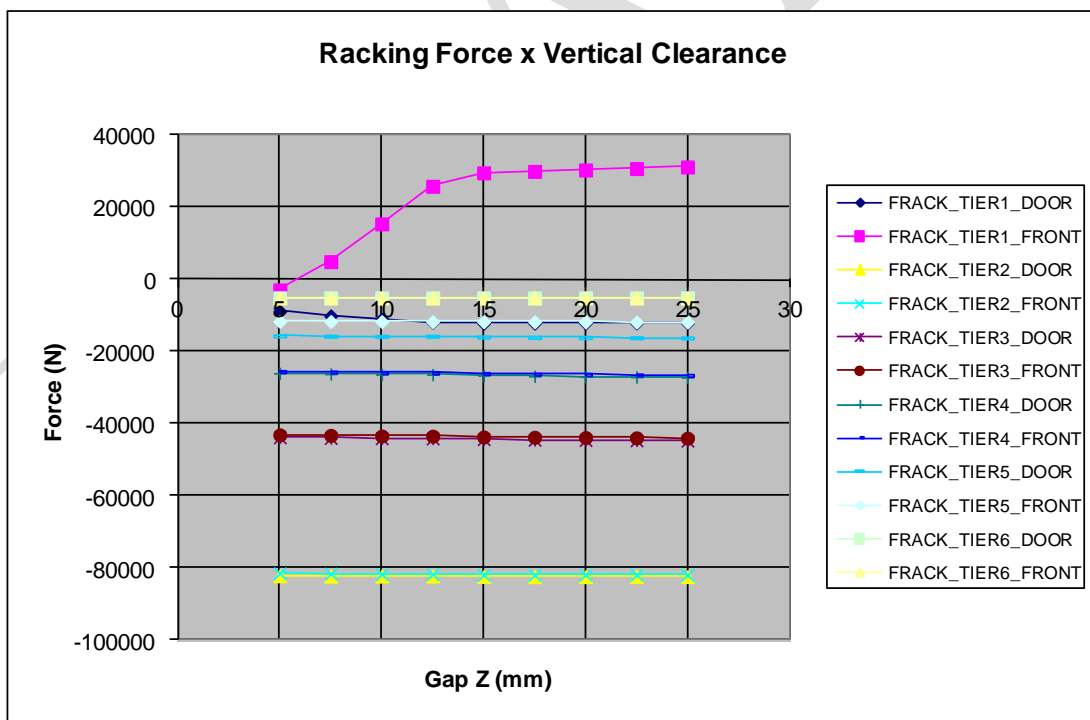


Figure 5.55 – Racking Force x Vertical Clearance for the additional stack ($E_{rod} = 140$ GPa).

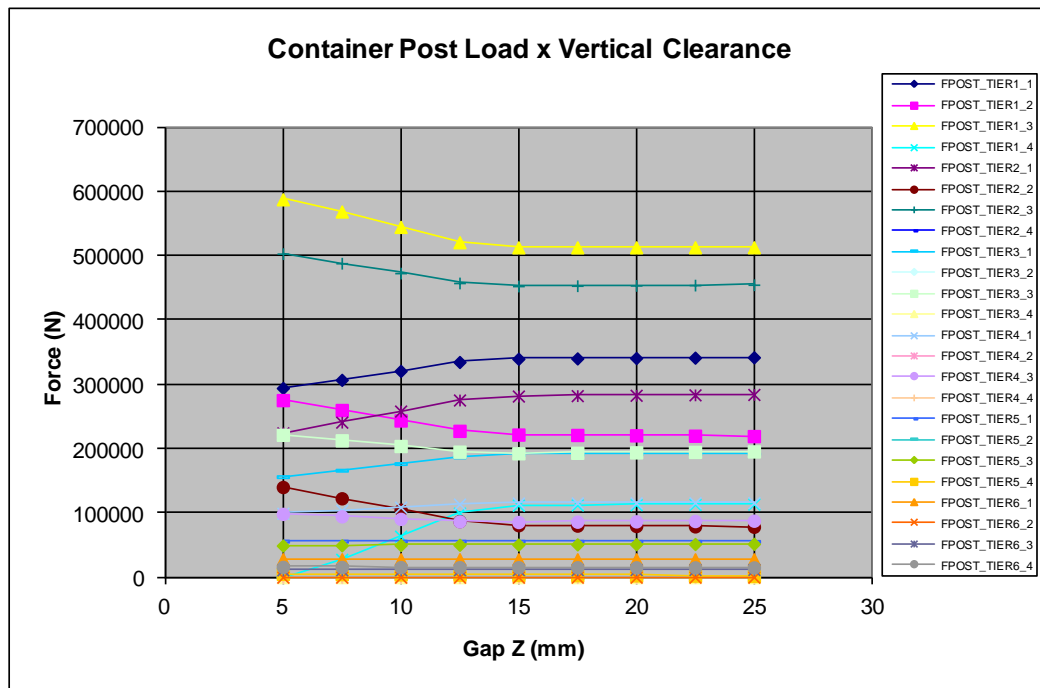


Figure 5.56 – Container Post Load x Vertical Clearance for the additional stack ($E_{rod} = 140$ GPa).

- $E_{rod} = 210$ GPa

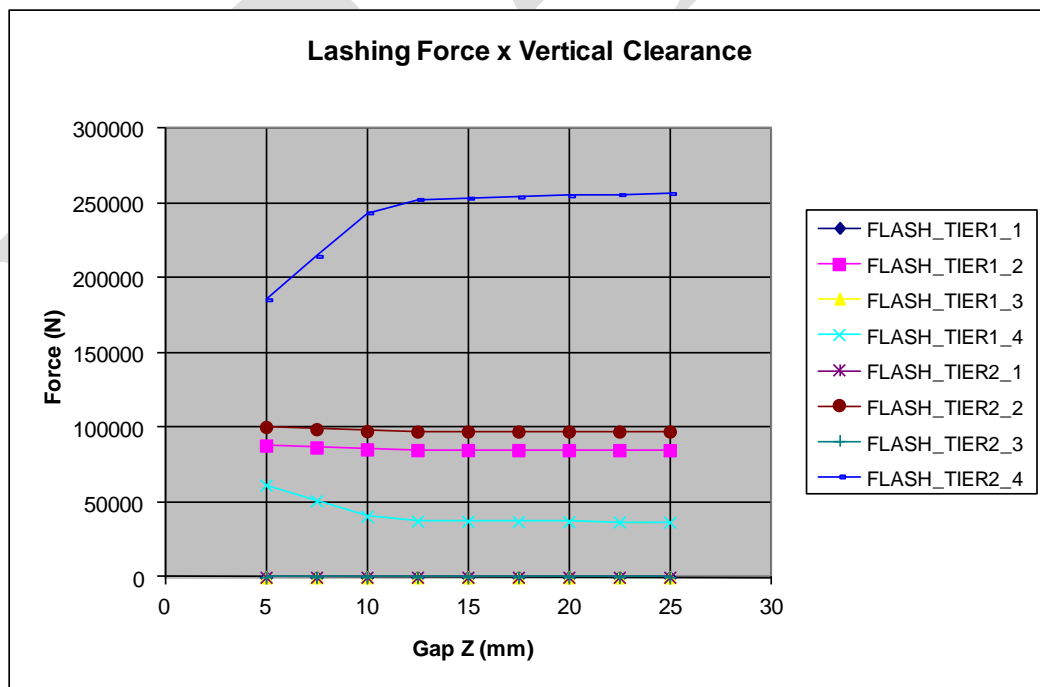


Figure 5.57 – Lashing Force x Vertical Clearance for the additional stack ($E_{rod} = 210$ GPa).

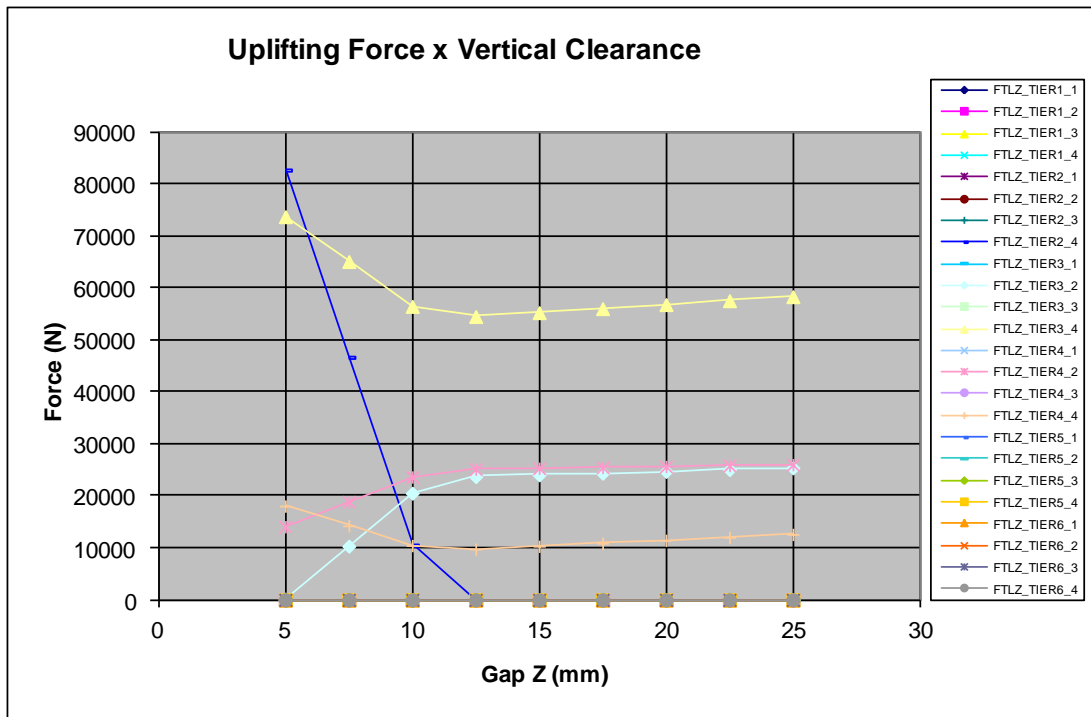


Figure 5.58 – Uplifting Force x Vertical Clearance for the additional stack ($E_{rod} = 210$ GPa).

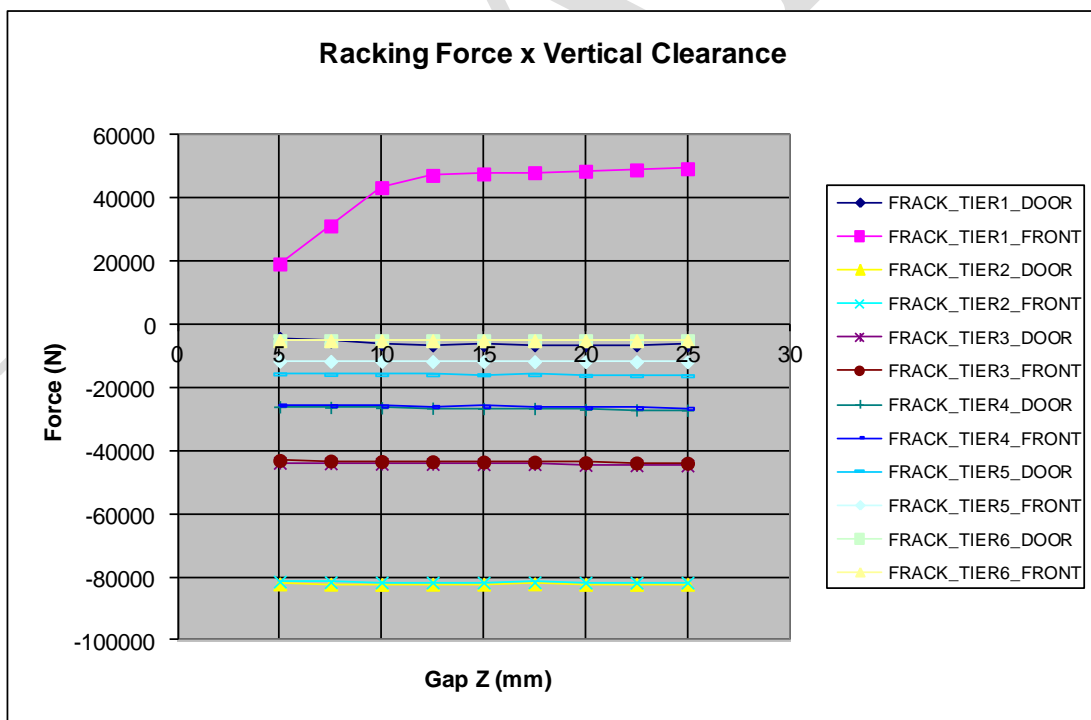


Figure 5.59 – Racking Force x Vertical Clearance for the additional stack ($E_{rod} = 210$ GPa).

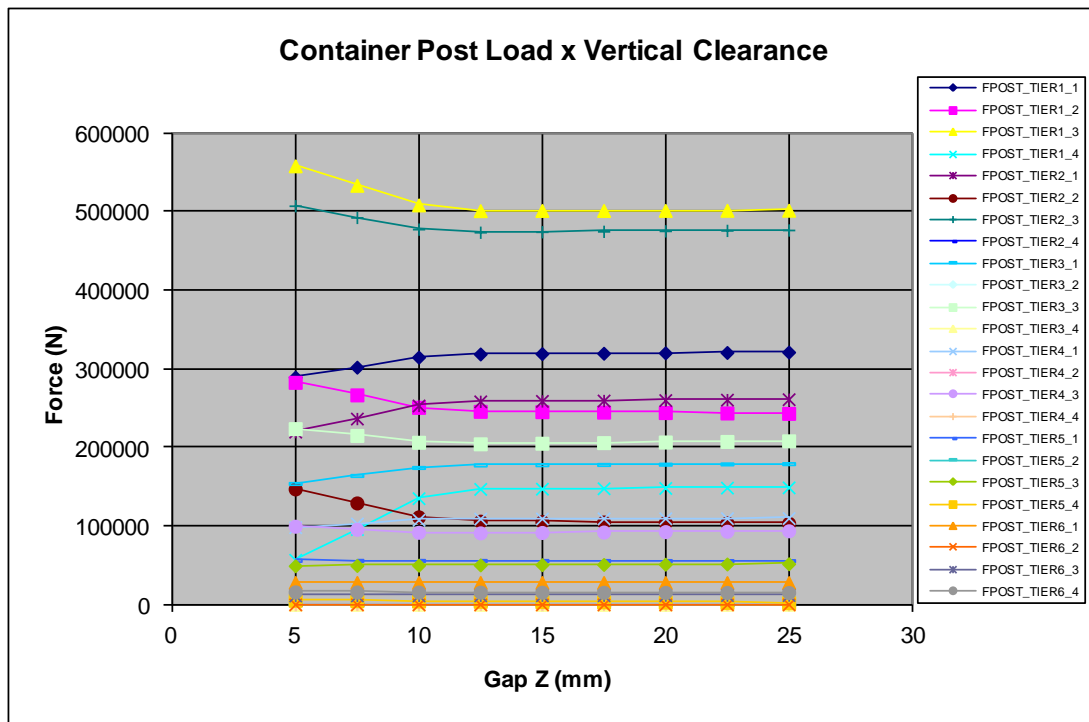


Figure 5.60 – Container Post Load x Vertical Clearance for the additional stack ($E_{rod} = 210$ GPa).

It is possible to see in the obtained results the strong dependence of the lashing force (FLASH_TIER2_4) and vertical force on twist lock (FTLZ_TIER2_4) of the bottom corner in the port side of the front end of the 2nd tier container of the stack. While the lashing force is directly proportional to the vertical clearance of the twist lock, the vertical force acting on the twist lock is inversely proportional. As in the previous cases, the same behaviour was noted with the three different values of lashing stiffness, with different rate of force variation against clearance increasing. In Figure 5.50, Figure 5.54 and Figure 5.58 it is possible to see the vertical force acting on the lock at the uplifted corner (FTLZ_TIER2_4) is null at 20 mm of clearance for E_{rod} equal to 70 GPa, 13 mm for E_{rod} equal to 140 GPa and 11 mm for E_{rod} equal to 210 GPa. When the clearance is higher than those values, for each case, the twist lock is not working anymore and the lashing force at the same corner remains constant (Figure 5.49, Figure 5.53 and Figure 5.57).

DRAFT

6. DESIGN CRITERIA

After the parametric studies, the influence of the stack parameters on the operational loads was evaluated. The lashing force and the vertical clearance of the locks were identified as the most significant parameters and the lashing force and vertical force on locks (or uplifting force) as the most influenced results. The lashing force was identified as the critical point when external lashing system is used and it can be very high depending on the lock design adopted, due to the vertical clearance it allows.

The rule based approach used by (GL 2012) to determine the operational loads acting on a stack but does not take into account the clearance of the locks. It gives suitable results when internal lashing system is used, because the uplifting does not overload the lashing rod.

In the case of external lashing system, if the rule based approach is intended to be used, it is necessary to somehow add the clearance dependant portion of the lashing force. Using the parametric results obtained by FEM, a simplified method was developed to determine the overloading on the lashing force.

The results of 18 cases, where the height of lashing bridge, cargo distribution, stack weight, heeling angle and lashing rod stiffness were modified, were used on the procedure. For each case, the curve of the lashing rod force on the lifted corner (bottom corner on the port side of the front end of the top lashed container) against the clearance variation was plotted. In order to compare the slopes of the curves, which means the rate of variation of the lashing force, the curves were shifted to have all the same origin (Figure 6.1).

The value of the parameters can be read on the name of each case. For example, the case 1Tier.Zg7378.W147.020.E140 means:

- 1-tier high lashing bridge ($k_{bridge} = 23$ kN/mm)
- Vertical height of the stack gravity center equal to 7378 mm
- Stack weight equal to 147 tons
- Heeling angle equal to 20 degrees
- Lashing rod equivalent modulus of elasticity equal to 140 GPa

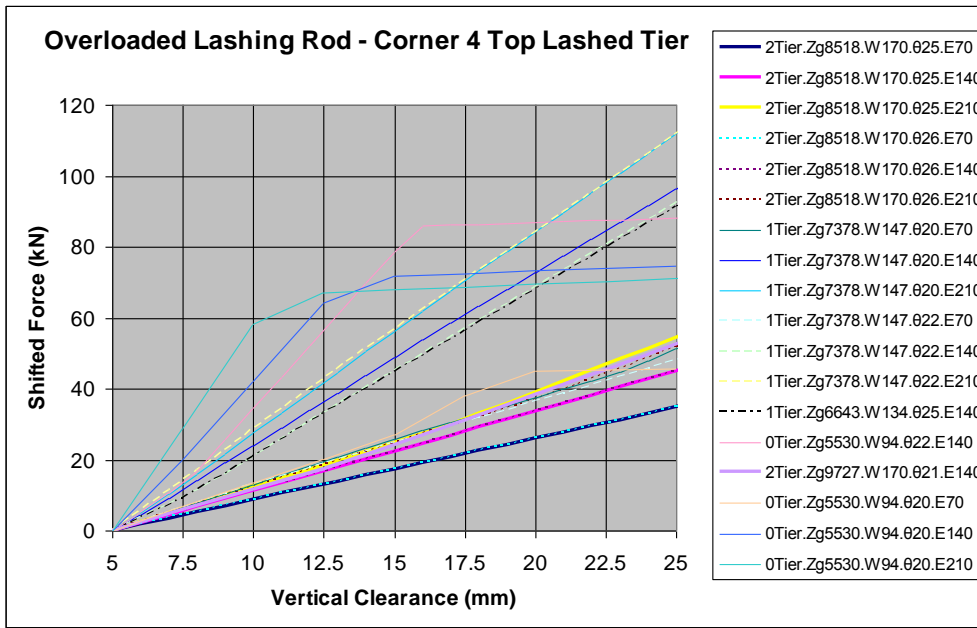


Figure 6.1 – Lashing force variation versus vertical clearance for several stack configurations.

From the shifted lashing rod forces plotted on Figure 6.1, it is possible to see the dependence of the slope of the curve on the lashing stiffness (lashing bridge height and equivalent modulus of elasticity of the lashing rod). The slope of each curve (sensitivity) was taken and plotted against the equivalent lashing bridge stiffness, showing the rate of variation of the lashing force as a function of the lashing stiffness (Figure 6.2).

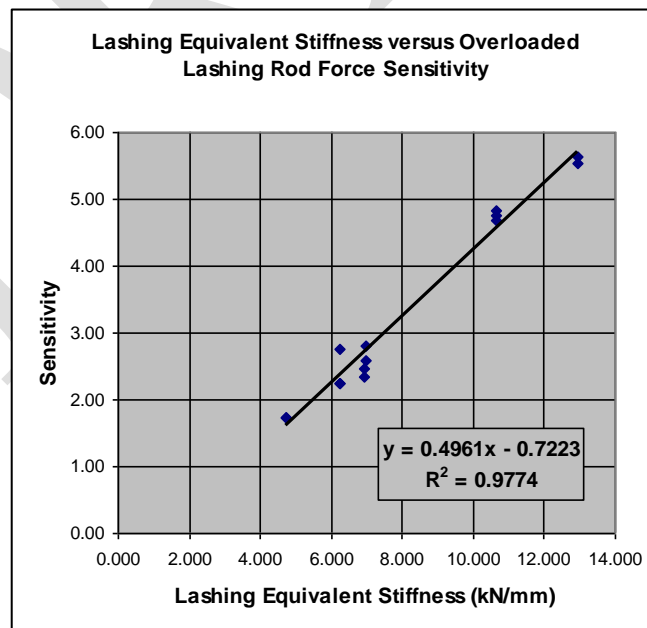


Figure 6.2 – Sensitivity of the lashing force variation as a function of the lashing stiffness.

The results obtained in Figure 6.2 were adjusted into a curve and a linear equation correlating the parameters was obtained (Equation (6-1)), where x is the equivalent lashing stiffness value, in kN/mm, and y is the sensitivity of the lashing force increasing.

$$y = 0.4961x - 0.7223 \quad (6-1)$$

Using the sensitivity, which is a function of the lashing stiffness, it is possible to correct the value of the lashing rod force acting on the corner 4 (port side and front end) of the top lashed container which was evaluated by the rule based approach, using Equation (6-2).

$$Sensitivity = f(k_{eq}) = \frac{(FLASH_a - FLASH_b)}{(GAP_a - GAP_b)} \quad (6-2)$$

As the value of $FLASH_b$ is evaluated by the rule based method (nominal value), GAP_b is equal to 0 (no clearance). Thus, GAP_a will be the vertical clearance of the lock and $FLASH_a$ will be the corrected value of the lashing rod force. By the equality of Equation (6-1) and Equation (6-2) and rearranging the equation members, Equation (6-3) is obtained.

$$FLASH' = FLASH_0 + GAP_z(0.4961 * k_{eq} - 0.7223) \quad (6-3)$$

Where $FLASH'$ and $FLASH_0$ are respectively the corrected and the nominal values of the lashing force in kN, GAP_z is the vertical clearance of the lock in mm and k_{eq} is the equivalent lashing stiffness in kN/mm.

As observed in section 5.7, while the lashing force on the uplifted corner increases with the vertical clearance, the uplifting force at the same corner decreases and tends to zero. When it occurs, the lock at this corner is not working anymore and the lashing force will remain constant even with higher clearance values. To evaluate this clearance value, which will be called GAP^* , the curve of the uplifting force on the corner 4 of the top lashed tier against the vertical clearance can be used. The curves of the 18 cases analyzed are shown in Figure 6.3.

As with the lashing force, the slopes (sensitivities) of the curves were measured and plotted as a function of the equivalent lashing stiffness (Figure 6.4). The results were adjusted into a

curve and a linear equation to correlate the sensitivity (y) and the equivalent lashing stiffness (x), in kN/mm, was obtained (Equation (6-4)).

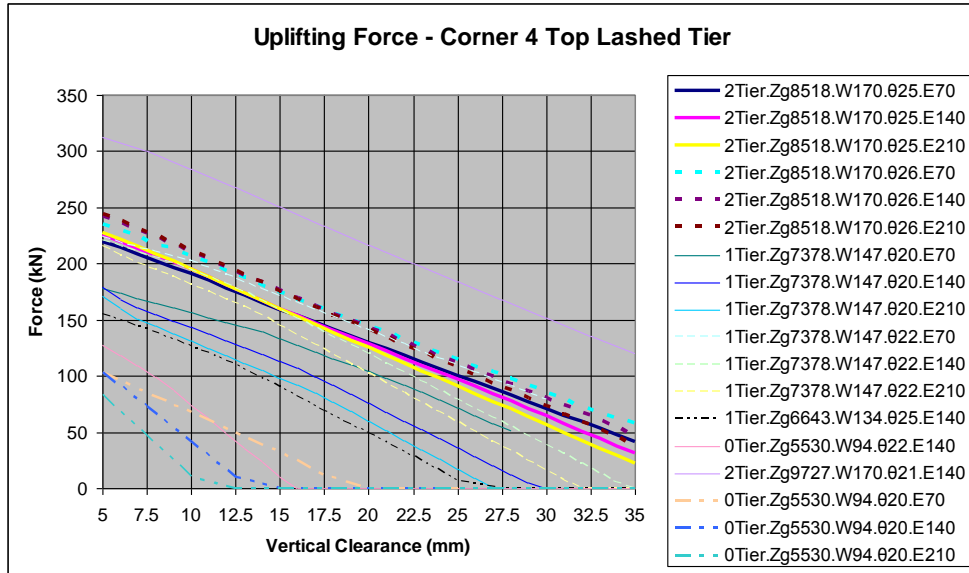


Figure 6.3 – Uplifting force variation versus vertical clearance for several stack configurations.

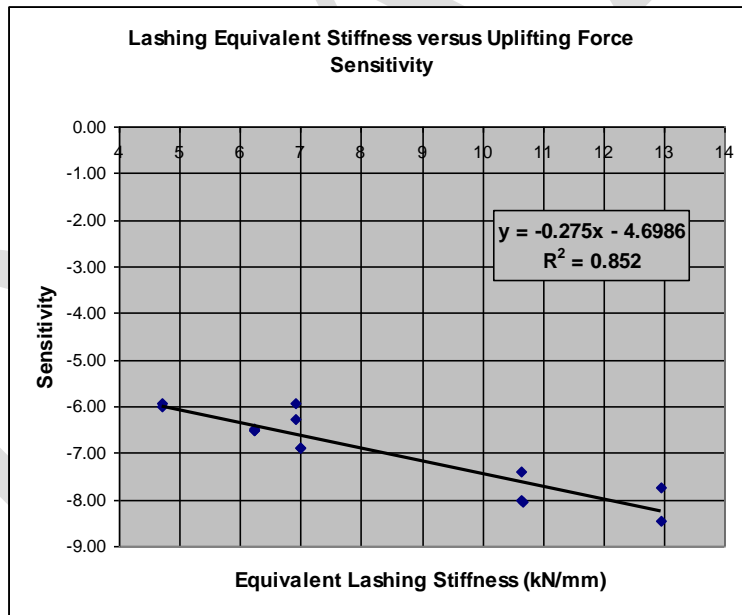


Figure 6.4 – Sensitivity of the uplifting force variation as a function of the lashing stiffness.

$$y = -0.275x - 4.6986 \tag{6-4}$$

The equation to correct the uplifting force is obtained in the sequence. Equation (6-5) shows the relation between the corrected ($FTLZ'$) and the nominal ($FTLZ_0$) values of the uplifting force, the vertical clearance of the lock (GAP_Z), in mm, and the equivalent lashing stiffness (k_{eq}) in kN/mm.

$$FTLZ' = FTLZ_0 - GAP_Z(0.275 * k_{eq} + 4.6986) \quad (6-5)$$

Thus, if the clearance of the lock (GAP_Z) is bigger than GAP^* , the uplifting force will be equal to zero and the lashing force will be equal to the value at GAP^* . A brief summary of the design correction procedure is shown below. A workflow of the procedure is presented in section 15.

1. The nominal values of the lashing force and uplifting force at the uplifted corner (corner 4, in case of heeling to the starboard) of the top lashed container are obtained by the rule based approach;
2. The equivalent lashing stiffness (k_{eq}) is evaluated and the sensitivity for the uplifting force is evaluated;
3. Using Equation (6-5), $FTLZ'$ is assumed as zero and GAP^* is obtained. If GAP_Z is bigger than GAP^* , the uplifting force at this corner will be null. If it is smaller, the uplifted force is corrected using Equation (6-5) and $FTLZ'$ is obtained;
4. The sensitivity for the lashing force is evaluated using k_{eq} ;
5. The correction of the lashing force is done using Equation (6-3) and $FLASH'$ is obtained. If GAP_Z is bigger than GAP^* , the corrected lashing force is evaluated at this point. If it is smaller, the actual clearance value is used;
6. The corrected values are compared to the limit values defined by GL. If these limits are extrapolated, the stack weight and cargo distribution must be modified.

DRAFT

7. COMPARISON BETWEEN LASHING ARRANGEMENTS

One of the main goals of this study is the comparison between the often used internal lashing arrangement and the more recent external lashing. This system, as described in section 1.1 and section 2.6.2, is an alternative method of cargo securing and is expected to allow higher stack weights and better cargo distribution on deck.

The comparison was made in two steps:

- The maximum cargo capacity for each lashing arrangement was obtained for three different stack heights;
- The cargo capacity was made using linear weight distribution from the bottom to the top of the stack, simulating weight distributions more close to the reality.

The stiffness of the lashing rods (k_{rod}) was obtained based on GL rules ($E_{rod} = 140 \text{ GPa}$) and the cross-sectional area (A_{rod}) was based on a 26 mm diameter. The lashing bridge stiffness was based on GL rules as well, with 9.2 kN/mm for 2-tier high and 23.0 kN/mm for 1-tier high lashing bridge (GL 2012). The lashing positioning was based on the container ship from section 5.1. The stiffness values of the twist locks were taken from Table 4.1 and the clearance values were based on the SAL from section 5 (see Table 5.2). Stacks using internal lashing were also analyzed with vertical clearance value of 25 mm, simulating a FAL, and the dependence of the results on the vertical clearance of the locks was checked for this lashing configuration.

The loading applied on the stacks corresponds to the procedure described in section 4 with a heeling angle (θ) of 25° to the starboard, which gives a transverse acceleration (a_y) of 0.42g.

7.1. Maximum Cargo Capacity

To compare the maximum cargo capacity for each stack and lashing configuration, all the containers were fully loaded ($m_{max} = 30.5 \text{ tons}$). If the load limits were exceeded, cargo was removed from the topmost container to the container in the base. Then, when all the operational loads were below the limits, the maximum cargo capacity of the stack was

obtained for the adopted lashing configuration. With this methodology, the vertical position of the stack gravity center (V_{cg}) is always the lowest for the correspondent stack weight (W_{stack}).

7.1.1. 8-Tier High Stack with 2-Tier High Lashing Bridge

Using external lashing arrangement, the maximum cargo capacity for an 8-tier high stack with 2-tier high lashing bridge was 173.0 tons (W_{stack}), with a vertical height of the stack gravity center (V_{cg}) of 8.47 meters. The obtained stack has 5 fully loaded containers at the base, 1 intermediate container of 12.5 tons at the 6th tier and 2 empty boxes at the top (Figure 7.1).

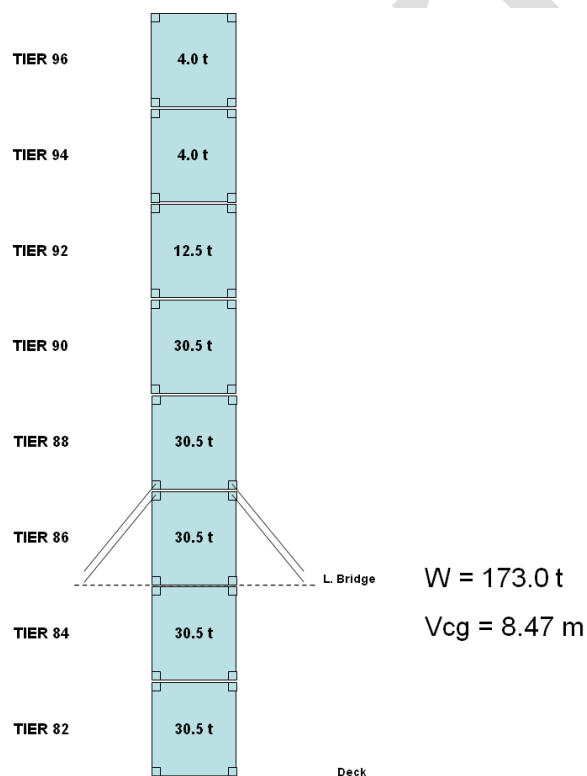


Figure 7.1 - Maximum cargo capacity for 8-tier high stack with 2-tier high lashing bridge, using external lashing arrangement.

The cargo capacity was limited by the lashing force at the uplifted corner (FLASH_TIER4_4) – bottom corner at the port side of the front end of the 4th tier container (Table 7.1).

Table 7.1 – Numerical results of the maximum cargo capacity for 8-tier high stack with 2-tier high lashing bridge, using external lashing arrangement.

RESULT (kN)								LIMIT (kN)
FLASH_TIER3_1	FLASH_TIER3_2	FLASH_TIER3_3	FLASH_TIER3_4	FLASH_TIER4_1	FLASH_TIER4_2	FLASH_TIER4_3	FLASH_TIER4_4	230
0,0	189,5	0,0	141,5	0,0	208,1	0,0	229,4	
FRACK_TIER1_DOOR	FRACK_TIER1_FRONT	FRACK_TIER2_DOOR	FRACK_TIER2_FRONT	FRACK_TIER3_DOOR	FRACK_TIER3_FRONT	FRACK_TIER4_DOOR	FRACK_TIER4_FRONT	150
-75,8	-98,4	-25,1	-22,4	53,0	23,6	-140,2	-140,1	
FRACK_TIER5_DOOR	FRACK_TIER5_FRONT	FRACK_TIER6_DOOR	FRACK_TIER6_FRONT	FRACK_TIER7_DOOR	FRACK_TIER7_FRONT	FRACK_TIER8_DOOR	FRACK_TIER8_FRONT	
-76,2	-73,3	-30,7	-28,3	-13,2	-8,4	-4,1	-4,1	
FPOST_TIER1_1	FPOST_TIER1_2	FPOST_TIER1_3	FPOST_TIER1_4	FPOST_TIER2_1	FPOST_TIER2_2	FPOST_TIER2_3	FPOST_TIER2_4	848
561,3	373,8	712,1	193,0	480,4	318,2	593,2	178,0	
FPOST_TIER3_1	FPOST_TIER3_2	FPOST_TIER3_3	FPOST_TIER3_4	FPOST_TIER4_1	FPOST_TIER4_2	FPOST_TIER4_3	FPOST_TIER4_4	
355,3	308,5	684,8	110,0	254,0	0,0	288,0	0,0	
FPOST_TIER5_1	FPOST_TIER5_2	FPOST_TIER5_3	FPOST_TIER5_4	FPOST_TIER6_1	FPOST_TIER6_2	FPOST_TIER6_3	FPOST_TIER6_4	
120,5	0,0	88,8	0,0	41,9	0,0	34,3	0,0	
FPOST_TIER7_1	FPOST_TIER7_2	FPOST_TIER7_3	FPOST_TIER7_4	FPOST_TIER8_1	FPOST_TIER8_2	FPOST_TIER8_3	FPOST_TIER8_4	250
18,0	0,0	8,8	8,3	0,0	0,0	0,0	0,0	
FTLZ_TIER1_1	FTLZ_TIER1_2	FTLZ_TIER1_3	FTLZ_TIER1_4	FTLZ_TIER2_1	FTLZ_TIER2_2	FTLZ_TIER2_3	FTLZ_TIER2_4	
0,0	0,0	0,0	0,0	0,0	0,0	0,0	0,0	
FTLZ_TIER3_1	FTLZ_TIER3_2	FTLZ_TIER3_3	FTLZ_TIER3_4	FTLZ_TIER4_1	FTLZ_TIER4_2	FTLZ_TIER4_3	FTLZ_TIER4_4	
0,0	0,0	0,0	0,0	0,0	0,0	0,0	157,2	
FTLZ_TIER5_1	FTLZ_TIER5_2	FTLZ_TIER5_3	FTLZ_TIER5_4	FTLZ_TIER6_1	FTLZ_TIER6_2	FTLZ_TIER6_3	FTLZ_TIER6_4	250
0,0	26,4	0,0	65,1	0,0	28,7	0,0	0,0	
FTLZ_TIER7_1	FTLZ_TIER7_2	FTLZ_TIER7_3	FTLZ_TIER7_4	FTLZ_TIER8_1	FTLZ_TIER8_2	FTLZ_TIER8_3	FTLZ_TIER8_4	
0,0	5,9	0,0	0,0	0,0	0,0	0,0	0,0	

The same stack configuration was evaluated using internal lashing arrangement. Several load limits were exceeded – lashing forces of all loaded lashing assemblies, container post load of the 1st and 2nd tiers and uplifting force of the 4th tier. The cargo was reduced until all the operational loads remain below the limits, obtaining the stack configuration from Figure 7.2. The maximum cargo capacity for internal lashing for a 8-tier high stack with 2-tier high lashing bridge (for this loading and stiffness values) is 158.0 tons.

The obtained stack has 4 fully loaded containers in the base, 1 partially loaded container in the 5th tier (24.0 tons) and 3 empty boxes at the top. The vertical height of the stack’s gravity center (V_{cg}) is 7.88 meters. The cargo capacity for this configuration is limited by the container post load in the port side of the door end of the 1st tier container (FPOST_TIER1_1), as shown in Table 7.2. The same stack was analyzed by changing the vertical clearance of the twist locks from 15 mm to 25 mm, representing a FAL. No considerable changes were observed in the obtained results, corroborating to the outcomes of (Wolf, Darie and Rathje, Rule Development for Container Stowage on Deck 2011).

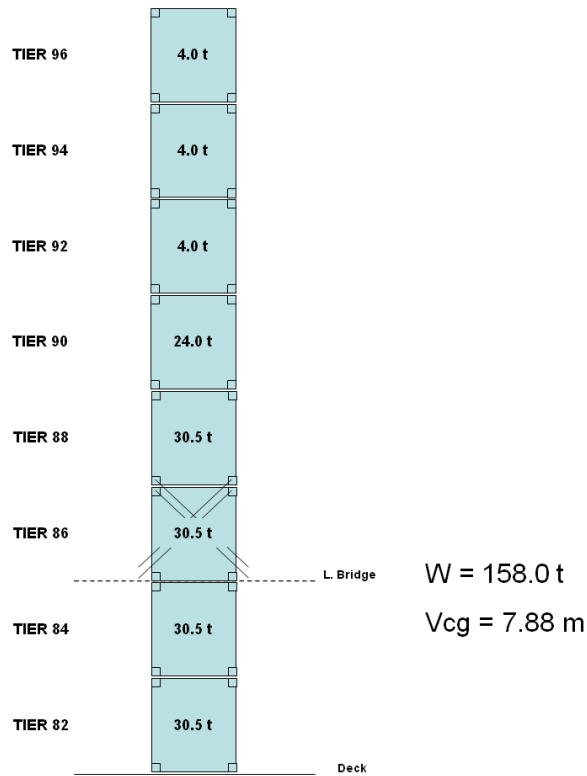


Figure 7.2 - Maximum cargo capacity for 8-tier high stack with 2-tier high lashing bridge, using internal lashing arrangement.

Table 7.2 – Numerical results of the maximum cargo capacity for 8-tier high stack with 2-tier high lashing bridge, using internal lashing arrangement.

RESULT (kN)								LIMIT (kN)
FLASH_TIER3_1	FLASH_TIER3_2	FLASH_TIER3_3	FLASH_TIER3_4	FLASH_TIER4_1	FLASH_TIER4_2	FLASH_TIER4_3	FLASH_TIER4_4	230
207,0	0,0	186,9	0,0	213,0	0,0	186,5	0,0	
FRACK_TIER1_DOOR	FRACK_TIER1_FRONT	FRACK_TIER2_DOOR	FRACK_TIER2_FRONT	FRACK_TIER3_DOOR	FRACK_TIER3_FRONT	FRACK_TIER4_DOOR	FRACK_TIER4_FRONT	150
-46,2	-82,0	16,7	-19,3	75,4	42,4	-109,3	-108,4	
FRACK_TIER5_DOOR	FRACK_TIER5_FRONT	FRACK_TIER6_DOOR	FRACK_TIER6_FRONT	FRACK_TIER7_DOOR	FRACK_TIER7_FRONT	FRACK_TIER8_DOOR	FRACK_TIER8_FRONT	848
-51,5	-49,3	-22,1	-18,9	-13,3	-8,4	-4,1	-4,1	
FPOST_TIER1_1	FPOST_TIER1_2	FPOST_TIER1_3	FPOST_TIER1_4	FPOST_TIER2_1	FPOST_TIER2_2	FPOST_TIER2_3	FPOST_TIER2_4	250
842,7	61,7	734,6	117,7	748,4	17,6	674,2	45,6	
FPOST_TIER3_1	FPOST_TIER3_2	FPOST_TIER3_3	FPOST_TIER3_4	FPOST_TIER4_1	FPOST_TIER4_2	FPOST_TIER4_3	FPOST_TIER4_4	848
630,5	0,0	806,9	0,0	201,6	0,0	186,3	0,0	
FPOST_TIER5_1	FPOST_TIER5_2	FPOST_TIER5_3	FPOST_TIER5_4	FPOST_TIER6_1	FPOST_TIER6_2	FPOST_TIER6_3	FPOST_TIER6_4	250
97,7	0,0	51,4	0,0	42,4	0,0	34,2	0,0	
FPOST_TIER7_1	FPOST_TIER7_2	FPOST_TIER7_3	FPOST_TIER7_4	FPOST_TIER8_1	FPOST_TIER8_2	FPOST_TIER8_3	FPOST_TIER8_4	848
17,9	0,0	8,9	8,2	0,0	0,0	0,0	0,0	
FTLZ_TIER1_1	FTLZ_TIER1_2	FTLZ_TIER1_3	FTLZ_TIER1_4	FTLZ_TIER2_1	FTLZ_TIER2_2	FTLZ_TIER2_3	FTLZ_TIER2_4	250
0,0	0,0	0,0	0,0	0,0	0,0	0,0	0,0	
FTLZ_TIER3_1	FTLZ_TIER3_2	FTLZ_TIER3_3	FTLZ_TIER3_4	FTLZ_TIER4_1	FTLZ_TIER4_2	FTLZ_TIER4_3	FTLZ_TIER4_4	848
0,0	0,0	0,0	0,0	0,0	0,0	0,0	218,7	
FTLZ_TIER5_1	FTLZ_TIER5_2	FTLZ_TIER5_3	FTLZ_TIER5_4	FTLZ_TIER6_1	FTLZ_TIER6_2	FTLZ_TIER6_3	FTLZ_TIER6_4	250
0,0	40,8	0,0	29,6	0,0	43,6	0,0	0,0	
FTLZ_TIER7_1	FTLZ_TIER7_2	FTLZ_TIER7_3	FTLZ_TIER7_4	FTLZ_TIER8_1	FTLZ_TIER8_2	FTLZ_TIER8_3	FTLZ_TIER8_4	848
0,0	6,5	0,0	0,0	0,0	0,0	0,0	0,0	

7.1.2. 6-Tier High Stack with 1-Tier High Lashing Bridge

Using external lashing arrangement, the maximum cargo capacity for a 6-tier high stack with 1-tier high lashing bridge was 136.0 tons (W_{stack}), with a vertical height of the stack gravity center (V_{cg}) of 6.62 meters. The obtained stack has 4 fully loaded containers at the base, 1 intermediate container of 10.0 tons at the 5th tier and 1 empty box at the top (Figure 7.3).

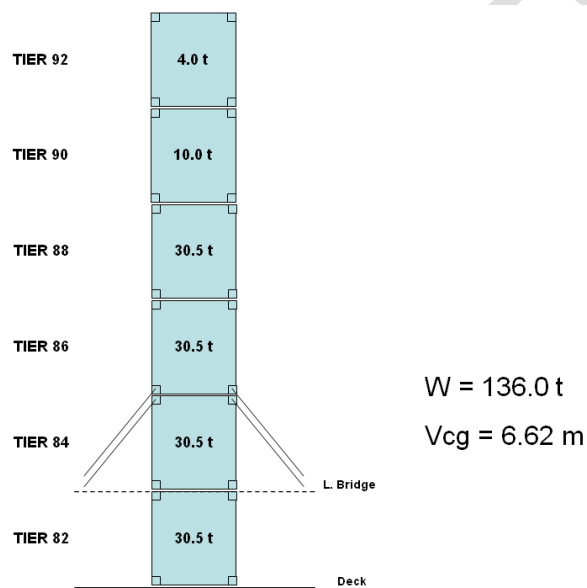


Figure 7.3 – Maximum cargo capacity for 6-tier high stack with 1-tier high lashing bridge, using external lashing arrangement.

The cargo capacity was limited by the lashing force at the uplifted corner (FLASH_TIER3_4) – bottom corner at the port side of the front end of the 3rd tier container (Table 7.3).

The same stack configuration was evaluated using internal lashing arrangement. All the evaluated operational loads were below the limits, with the container post load at the 1st tier as the load closest to the limit (FPOST_TIER1_1), as shown in Table 7.4.

Cargo was added to the 5th tier and the limits were exceeded. Thus, the maximum cargo capacity for internal lashing for a 6-tier high stack with 1-tier high lashing bridge (for this loading and stiffness values) is 136.0 tons, the same than for external lashing (Figure 7.4). The same stack was analyzed by changing the vertical clearance of the twist locks from 15

mm to 25 mm, representing a FAL. No considerable changes were observed in the obtained results.

Table 7.3 – Numerical results of the maximum cargo capacity for 6-tier high stack with 1-tier high lashing bridge, using external lashing arrangement.

RESULT (kN)								LIMIT (kN)
FLASH_TIER2_1	FLASH_TIER2_2	FLASH_TIER2_3	FLASH_TIER2_4	FLASH_TIER3_1	FLASH_TIER3_2	FLASH_TIER3_3	FLASH_TIER3_4	
0,0	147,7	0,0	95,3	0,0	163,6	0,0	226,4	230
FRACK_TIER1_DOOR	FRACK_TIER1_FRONT	FRACK_TIER2_DOOR	FRACK_TIER2_FRONT	FRACK_TIER3_DOOR	FRACK_TIER3_FRONT	FRACK_TIER4_DOOR	FRACK_TIER4_FRONT	
-53,9	-42,0	18,8	11,5	-126,1	-125,6	-62,2	-59,4	150
FRACK_TIER5_DOOR	FRACK_TIER5_FRONT	FRACK_TIER6_DOOR	FRACK_TIER6_FRONT					
-19,0	-15,2	-4,1	-4,1					848
FPOST_TIER1_1	FPOST_TIER1_2	FPOST_TIER1_3	FPOST_TIER1_4	FPOST_TIER2_1	FPOST_TIER2_2	FPOST_TIER2_3	FPOST_TIER2_4	
388,0	311,1	580,9	122,1	295,1	269,9	579,3	72,7	
FPOST_TIER3_1	FPOST_TIER3_2	FPOST_TIER3_3	FPOST_TIER3_4	FPOST_TIER4_1	FPOST_TIER4_2	FPOST_TIER4_3	FPOST_TIER4_4	
198,4	0,0	215,6	0,0	62,7	0,0	55,9	4,9	
FPOST_TIER5_1	FPOST_TIER5_2	FPOST_TIER5_3	FPOST_TIER5_4	FPOST_TIER6_1	FPOST_TIER6_2	FPOST_TIER6_3	FPOST_TIER6_4	
18,1	0,0	8,7	8,6	0,0	0,0	0,0	0,0	
FTLZ_TIER1_1	FTLZ_TIER1_2	FTLZ_TIER1_3	FTLZ_TIER1_4	FTLZ_TIER2_1	FTLZ_TIER2_2	FTLZ_TIER2_3	FTLZ_TIER2_4	250
0,0	0,0	0,0	0,0	0,0	0,0	0,0	0,0	
FTLZ_TIER3_1	FTLZ_TIER3_2	FTLZ_TIER3_3	FTLZ_TIER3_4	FTLZ_TIER4_1	FTLZ_TIER4_2	FTLZ_TIER4_3	FTLZ_TIER4_4	
0,0	0,0	0,0	84,6	0,0	0,0	0,0	20,4	
FTLZ_TIER5_1	FTLZ_TIER5_2	FTLZ_TIER5_3	FTLZ_TIER5_4	FTLZ_TIER6_1	FTLZ_TIER6_2	FTLZ_TIER6_3	FTLZ_TIER6_4	
0,0	0,0	0,0	0,0	0,0	0,0	0,0	0,0	

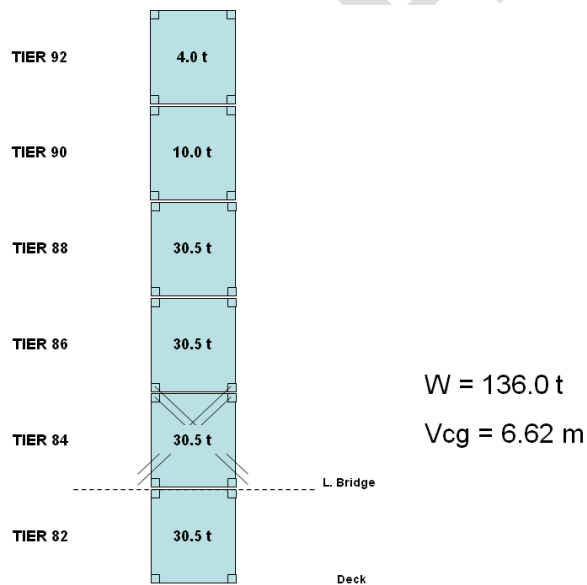


Figure 7.4 – Maximum cargo capacity for 6-tier high stack with 1-tier high lashing bridge, using internal lashing arrangement.

Table 7.4 – Numerical results of the maximum cargo capacity for 6-tier high stack with 1-tier high lashing bridge, using internal lashing arrangement.

RESULT (kN)								LIMIT (kN)
FLASH_TIER2_1	FLASH_TIER2_2	FLASH_TIER2_3	FLASH_TIER2_4	FLASH_TIER3_1	FLASH_TIER3_2	FLASH_TIER3_3	FLASH_TIER3_4	230
199,4	0,0	192,0	0,0	204,7	0,0	187,2	49,7	
FRACK_TIER1_DOOR	FRACK_TIER1_FRONT	FRACK_TIER2_DOOR	FRACK_TIER2_FRONT	FRACK_TIER3_DOOR	FRACK_TIER3_FRONT	FRACK_TIER4_DOOR	FRACK_TIER4_FRONT	150
-2,0	-60,3	57,2	1,9	-127,3	-126,1	-62,6	-59,8	
FRACK_TIER5_DOOR	FRACK_TIER5_FRONT	FRACK_TIER6_DOOR	FRACK_TIER6_FRONT					
-19,4	-15,2	-4,1	-4,1					
FPOST_TIER1_1	FPOST_TIER1_2	FPOST_TIER1_3	FPOST_TIER1_4	FPOST_TIER2_1	FPOST_TIER2_2	FPOST_TIER2_3	FPOST_TIER2_4	848
770,1	13,3	797,1	4,0	650,5	0,0	851,6	0,0	
FPOST_TIER3_1	FPOST_TIER3_2	FPOST_TIER3_3	FPOST_TIER3_4	FPOST_TIER4_1	FPOST_TIER4_2	FPOST_TIER4_3	FPOST_TIER4_4	
211,8	0,0	206,8	0,0	62,3	0,0	57,4	3,1	
FPOST_TIER5_1	FPOST_TIER5_2	FPOST_TIER5_3	FPOST_TIER5_4	FPOST_TIER6_1	FPOST_TIER6_2	FPOST_TIER6_3	FPOST_TIER6_4	
17,9	0,0	8,9	8,2	0,0	0,0	0,0	0,0	
FTLZ_TIER1_1	FTLZ_TIER1_2	FTLZ_TIER1_3	FTLZ_TIER1_4	FTLZ_TIER2_1	FTLZ_TIER2_2	FTLZ_TIER2_3	FTLZ_TIER2_4	250
0,0	0,0	0,0	0,0	0,0	0,0	0,0	0,0	
FTLZ_TIER3_1	FTLZ_TIER3_2	FTLZ_TIER3_3	FTLZ_TIER3_4	FTLZ_TIER4_1	FTLZ_TIER4_2	FTLZ_TIER4_3	FTLZ_TIER4_4	
0,0	0,0	0,0	186,1	0,0	14,2	0,0	12,6	
FTLZ_TIER5_1	FTLZ_TIER5_2	FTLZ_TIER5_3	FTLZ_TIER5_4	FTLZ_TIER6_1	FTLZ_TIER6_2	FTLZ_TIER6_3	FTLZ_TIER6_4	
0,0	0,0	0,0	0,0	0,0	0,0	0,0	0,0	

7.1.3. 4-Tier High Stack with no Lashing Bridge

Using external lashing arrangement, the maximum cargo capacity for a 4-tier high stack with no lashing bridge (lashing plates connected directly to the deck or hatch cover) was 95.5 tons (W_{stack}), with a vertical height of the stack gravity center (V_{cg}) of 4.59 meters. The obtained stack has 3 fully loaded containers at the base and 1 empty box at the top (Figure 7.5).

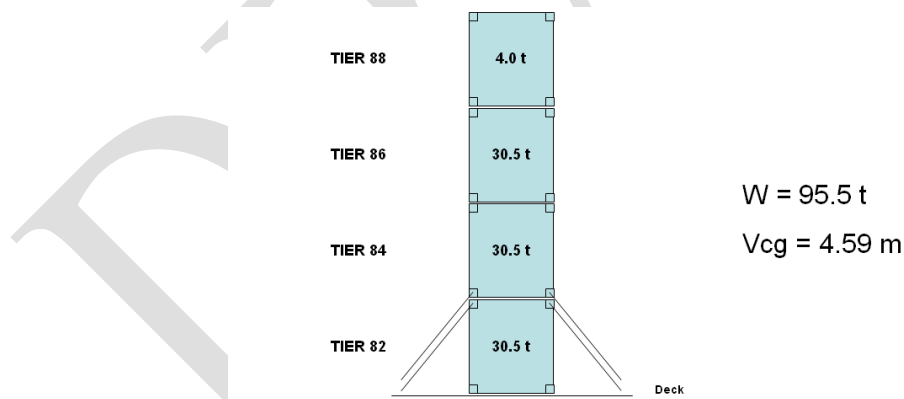


Figure 7.5 – Maximum cargo capacity for 4-tier high stack with no lashing bridge, using external lashing arrangement.

The cargo capacity was limited by the lashing force at the uplifted corner (FLASH_TIER2_4) – bottom corner at the port side of the front end of the 2nd tier container (Table 7.5).

Table 7.5 – Numerical results of the maximum cargo capacity for 4-tier high stack with no lashing bridge, using external lashing arrangement.

RESULT (kN)								LIMIT (kN)
FLASH_TIER1_1	FLASH_TIER1_2	FLASH_TIER1_3	FLASH_TIER1_4	FLASH_TIER2_1	FLASH_TIER2_2	FLASH_TIER2_3	FLASH_TIER2_4	
0,0	101,4	0,0	46,9	0,0	115,3	0,0	227,0	230
FRACK_TIER1_DOOR	FRACK_TIER1_FRONT	FRACK_TIER2_DOOR	FRACK_TIER2_FRONT	FRACK_TIER3_DOOR	FRACK_TIER3_FRONT	FRACK_TIER4_DOOR	FRACK_TIER4_FRONT	
-19,6	1,7	-104,3	-96,8	-40,1	-38,5	-4,1	-4,1	150
FPOST_TIER1_1	FPOST_TIER1_2	FPOST_TIER1_3	FPOST_TIER1_4	FPOST_TIER2_1	FPOST_TIER2_2	FPOST_TIER2_3	FPOST_TIER2_4	848
214,8	234,9	451,9	35,8	133,7	20,0	130,3	21,6	
FPOST_TIER3_1	FPOST_TIER3_2	FPOST_TIER3_3	FPOST_TIER3_4	FPOST_TIER4_1	FPOST_TIER4_2	FPOST_TIER4_3	FPOST_TIER4_4	
18,1	0,0	8,5	8,9	0,0	0,0	0,0	0,0	
FTLZ_TIER1_1	FTLZ_TIER1_2	FTLZ_TIER1_3	FTLZ_TIER1_4	FTLZ_TIER2_1	FTLZ_TIER2_2	FTLZ_TIER2_3	FTLZ_TIER2_4	250
0,0	0,0	0,0	0,0	0,0	0,0	0,0	0,0	
FTLZ_TIER3_1	FTLZ_TIER3_2	FTLZ_TIER3_3	FTLZ_TIER3_4	FTLZ_TIER4_1	FTLZ_TIER4_2	FTLZ_TIER4_3	FTLZ_TIER4_4	
0,0	0,0	0,0	0,0	0,0	0,0	0,0	0,0	

The same stack configuration was evaluated using internal lashing arrangement. All the evaluated operational loads were below the limits, with a considerable safety margin. More cargo was added to the stack and the maximum cargo capacity using internal lashing arrangement was 107.5 tons. The stack has 3 fully loaded containers at the base and 1 partially loaded container at the top, with 16.0 tons. The vertical position of the stack gravity center (V_{cg}) is 5.21 meters (Figure 7.6). The obtained results for this configuration are shown in Table 7.6.

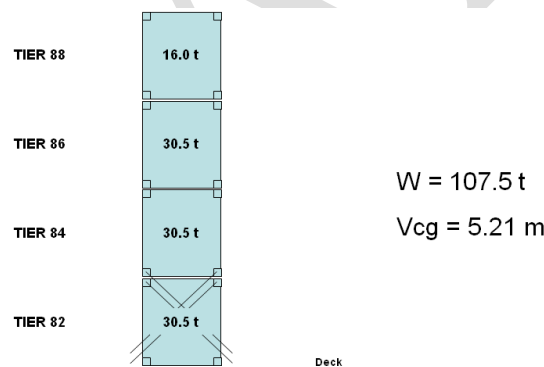


Figure 7.6 – Maximum cargo capacity for 4-tier high stack with no lashing bridge, using internal lashing arrangement.

Table 7.6 – Numerical results of the maximum cargo capacity for 4-tier high stack with no lashing bridge, using internal lashing arrangement.

RESULT (kN)								LIMIT (kN)
FLASH_TIER1_1	FLASH_TIER1_2	FLASH_TIER1_3	FLASH_TIER1_4	FLASH_TIER2_1	FLASH_TIER2_2	FLASH_TIER2_3	FLASH_TIER2_4	
159,5	0,0	179,3	0,0	193,7	0,0	200,2	128,3	230
FRACK_TIER1_DOOR	FRACK_TIER1_FRONT	FRACK_TIER2_DOOR	FRACK_TIER2_FRONT	FRACK_TIER3_DOOR	FRACK_TIER3_FRONT	FRACK_TIER4_DOOR	FRACK_TIER4_FRONT	
44,0	-42,2	-130,7	-123,3	-66,1	-56,6	-16,6	-16,6	150
FPOST_TIER1_1	FPOST_TIER1_2	FPOST_TIER1_3	FPOST_TIER1_4	FPOST_TIER2_1	FPOST_TIER2_2	FPOST_TIER2_3	FPOST_TIER2_4	848
601,5	2,4	840,3	0,0	216,8	0,0	203,9	0,0	
FPOST_TIER3_1	FPOST_TIER3_2	FPOST_TIER3_3	FPOST_TIER3_4	FPOST_TIER4_1	FPOST_TIER4_2	FPOST_TIER4_3	FPOST_TIER4_4	
71,0	0,0	42,0	27,9	0,0	0,0	0,0	0,0	
FTLZ_TIER1_1	FTLZ_TIER1_2	FTLZ_TIER1_3	FTLZ_TIER1_4	FTLZ_TIER2_1	FTLZ_TIER2_2	FTLZ_TIER2_3	FTLZ_TIER2_4	250
0,0	0,0	0,0	0,0	0,0	0,0	0,0	126,4	
FTLZ_TIER3_1	FTLZ_TIER3_2	FTLZ_TIER3_3	FTLZ_TIER3_4	FTLZ_TIER4_1	FTLZ_TIER4_2	FTLZ_TIER4_3	FTLZ_TIER4_4	
0,0	10,2	0,0	0,0	0,0	0,0	0,0	0,0	

7.2. Linear Cargo Distribution

To compare the cargo capacity of the different lashing arrangements using a more realistic case, the container stacks were arranged with 2 fully loaded containers in the base and a linear distribution up to the top. The stack weight was adjusted to have all the operational loads below the limits for the external lashing arrangement.

7.2.1. 8-Tier High Stack with 2-Tier High Lashing Bridge

Using external lashing arrangement, the obtained stack weight was 160.0 tons (W_{stack}), with a vertical height of the stack gravity center (V_{cg}) of 8.80 meters. The obtained stack is shown in Figure 7.7.

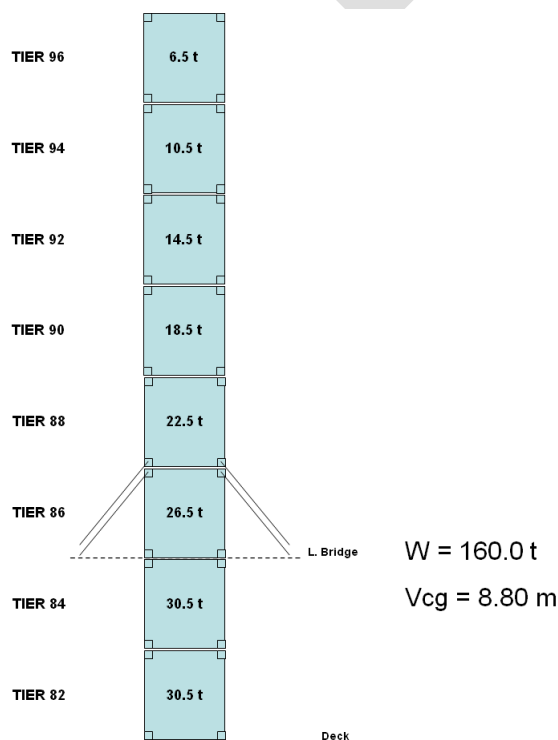


Figure 7.7 – Configuration for 8-tier high stack with 2-tier high lashing bridge and external lashing.

The cargo capacity was limited by the lashing force at the uplifted corner (FLASH_TIER4_4) – bottom corner at the port side of the front end of the 4th tier container – and by the uplifting force at the same corner (FTLZ_TIER4_4), as shown in Table 7.7.

Table 7.7 - Numerical results for 8-tier high stack and 2-tier high lashing bridge with linear cargo distribution, using external lashing arrangement.

RESULT (kN)								LIMIT (kN)
FLASH_TIER3_1	FLASH_TIER3_2	FLASH_TIER3_3	FLASH_TIER3_4	FLASH_TIER4_1	FLASH_TIER4_2	FLASH_TIER4_3	FLASH_TIER4_4	
0,0	174,6	0,0	137,9	0,0	191,2	0,0	225,7	230
FRACK_TIER1_DOOR	FRACK_TIER1_FRONT	FRACK_TIER2_DOOR	FRACK_TIER2_FRONT	FRACK_TIER3_DOOR	FRACK_TIER3_FRONT	FRACK_TIER4_DOOR	FRACK_TIER4_FRONT	
-68,4	-75,6	-14,2	-3,0	55,7	42,4	-129,8	-130,1	150
FRACK_TIER5_DOOR	FRACK_TIER5_FRONT	FRACK_TIER6_DOOR	FRACK_TIER6_FRONT	FRACK_TIER7_DOOR	FRACK_TIER7_FRONT	FRACK_TIER8_DOOR	FRACK_TIER8_FRONT	
-87,5	-87,1	-52,6	-48,1	-25,6	-19,6	-6,7	-6,7	848
FPOST_TIER1_1	FPOST_TIER1_2	FPOST_TIER1_3	FPOST_TIER1_4	FPOST_TIER2_1	FPOST_TIER2_2	FPOST_TIER2_3	FPOST_TIER2_4	
559,7	292,1	690,7	153,6	481,4	235,0	607,0	102,1	
FPOST_TIER3_1	FPOST_TIER3_2	FPOST_TIER3_3	FPOST_TIER3_4	FPOST_TIER4_1	FPOST_TIER4_2	FPOST_TIER4_3	FPOST_TIER4_4	250
371,8	228,3	726,8	107,1	286,8	0,0	377,4	0,0	
FPOST_TIER5_1	FPOST_TIER5_2	FPOST_TIER5_3	FPOST_TIER5_4	FPOST_TIER6_1	FPOST_TIER6_2	FPOST_TIER6_3	FPOST_TIER6_4	
186,3	0,0	169,1	0,0	82,1	0,0	73,5	0,0	
FPOST_TIER7_1	FPOST_TIER7_2	FPOST_TIER7_3	FPOST_TIER7_4	FPOST_TIER8_1	FPOST_TIER8_2	FPOST_TIER8_3	FPOST_TIER8_4	
28,9	0,0	15,9	12,1	0,0	0,0	0,0	0,0	
FTLZ_TIER1_1	FTLZ_TIER1_2	FTLZ_TIER1_3	FTLZ_TIER1_4	FTLZ_TIER2_1	FTLZ_TIER2_2	FTLZ_TIER2_3	FTLZ_TIER2_4	848
0,0	0,0	0,0	0,0	0,0	0,0	0,0	0,0	
FTLZ_TIER3_1	FTLZ_TIER3_2	FTLZ_TIER3_3	FTLZ_TIER3_4	FTLZ_TIER4_1	FTLZ_TIER4_2	FTLZ_TIER4_3	FTLZ_TIER4_4	250
0,0	0,0	0,0	0,0	0,0	0,0	0,0	241,9	
FTLZ_TIER5_1	FTLZ_TIER5_2	FTLZ_TIER5_3	FTLZ_TIER5_4	FTLZ_TIER6_1	FTLZ_TIER6_2	FTLZ_TIER6_3	FTLZ_TIER6_4	
0,0	63,2	0,0	159,1	0,0	45,8	0,0	32,2	
FTLZ_TIER7_1	FTLZ_TIER7_2	FTLZ_TIER7_3	FTLZ_TIER7_4	FTLZ_TIER8_1	FTLZ_TIER8_2	FTLZ_TIER8_3	FTLZ_TIER8_4	
0,0	6,5	0,0	0,0	0,0	0,0	0,0	0,0	

The same stack configuration was analyzed using internal lashing arrangement. Several load limits were exceeded and cargo was removed, from top to bottom, until all the operational loads were below the limits. The obtained stack configuration has 144.0 tons (W_{stack}) and a vertical height of the gravity center (V_{cg}) of 7.77 meters (Figure 7.8).

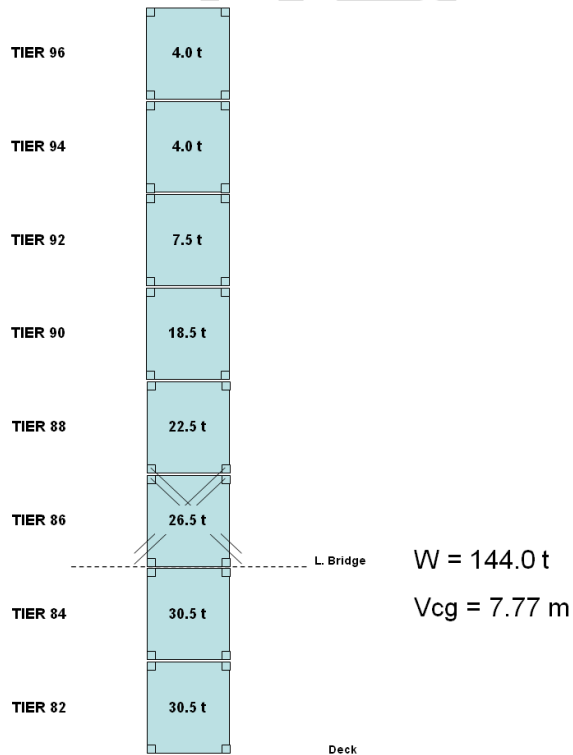


Figure 7.8 – Configuration for 8-tier high stack with 2-tier high lashing bridge and internal lashing.

weather deck

The cargo capacity for this configuration is limited by the uplifting force in the starboard side of the front end of the 4th tier container (FTLZ_TIER4_4), as shown in Table 7.8.

Table 7.8 – Numerical results for 8-tier high stack and 2-tier high lashing bridge using internal lashing arrangement.

RESULT (kN)								LIMIT (kN)
FLASH_TIER3_1	FLASH_TIER3_2	FLASH_TIER3_3	FLASH_TIER3_4	FLASH_TIER4_1	FLASH_TIER4_2	FLASH_TIER4_3	FLASH_TIER4_4	230
184,3	0,0	168,6	0,0	189,7	0,0	168,0	0,0	
FRACK_TIER1_DOOR	FRACK_TIER1_FRONT	FRACK_TIER2_DOOR	FRACK_TIER2_FRONT	FRACK_TIER3_DOOR	FRACK_TIER3_FRONT	FRACK_TIER4_DOOR	FRACK_TIER4_FRONT	150
-46,5	-73,2	17,4	-11,2	72,7	46,8	-96,8	-95,8	
FRACK_TIER5_DOOR	FRACK_TIER5_FRONT	FRACK_TIER6_DOOR	FRACK_TIER6_FRONT	FRACK_TIER7_DOOR	FRACK_TIER7_FRONT	FRACK_TIER8_DOOR	FRACK_TIER8_FRONT	150
-53,5	-51,5	-25,8	-22,8	-13,3	-8,5	-4,1	-4,1	
FPOST_TIER1_1	FPOST_TIER1_2	FPOST_TIER1_3	FPOST_TIER1_4	FPOST_TIER2_1	FPOST_TIER2_2	FPOST_TIER2_3	FPOST_TIER2_4	848
752,8	52,8	659,3	103,3	658,6	9,1	613,8	15,8	
FPOST_TIER3_1	FPOST_TIER3_2	FPOST_TIER3_3	FPOST_TIER3_4	FPOST_TIER4_1	FPOST_TIER4_2	FPOST_TIER4_3	FPOST_TIER4_4	848
549,7	0,0	758,1	0,0	184,2	0,0	209,3	0,0	
FPOST_TIER5_1	FPOST_TIER5_2	FPOST_TIER5_3	FPOST_TIER5_4	FPOST_TIER6_1	FPOST_TIER6_2	FPOST_TIER6_3	FPOST_TIER6_4	848
105,9	0,0	68,6	0,0	42,5	0,0	34,2	0,0	
FPOST_TIER7_1	FPOST_TIER7_2	FPOST_TIER7_3	FPOST_TIER7_4	FPOST_TIER8_1	FPOST_TIER8_2	FPOST_TIER8_3	FPOST_TIER8_4	848
17,9	0,0	9,0	8,1	0,0	0,0	0,0	0,0	
FTLZ_TIER1_1	FTLZ_TIER1_2	FTLZ_TIER1_3	FTLZ_TIER1_4	FTLZ_TIER2_1	FTLZ_TIER2_2	FTLZ_TIER2_3	FTLZ_TIER2_4	250
0,0	0,0	0,0	0,0	0,0	0,0	0,0	0,0	
FTLZ_TIER3_1	FTLZ_TIER3_2	FTLZ_TIER3_3	FTLZ_TIER3_4	FTLZ_TIER4_1	FTLZ_TIER4_2	FTLZ_TIER4_3	FTLZ_TIER4_4	250
0,0	0,0	0,0	0,0	0,0	0,0	0,0	243,1	
FTLZ_TIER5_1	FTLZ_TIER5_2	FTLZ_TIER5_3	FTLZ_TIER5_4	FTLZ_TIER6_1	FTLZ_TIER6_2	FTLZ_TIER6_3	FTLZ_TIER6_4	250
0,0	32,2	0,0	61,3	0,0	36,4	0,0	1,9	
FTLZ_TIER7_1	FTLZ_TIER7_2	FTLZ_TIER7_3	FTLZ_TIER7_4	FTLZ_TIER8_1	FTLZ_TIER8_2	FTLZ_TIER8_3	FTLZ_TIER8_4	250
0,0	6,6	0,0	0,0	0,0	0,0	0,0	0,0	

7.2.2. 6-Tier High Stack with 1-Tier High Lashing Bridge

Using external lashing arrangement, the obtained stack weight was 128.0 tons (W_{stack}), with a vertical height of the stack gravity center (V_{cg}) of 6.82 meters. The obtained stack is shown in Figure 7.9.

Table 7.9 – Numerical results for 6-tier high stack and 1-tier high lashing bridge with linear cargo distribution, using external lashing arrangement.

RESULT (kN)								LIMIT (kN)
FLASH_TIER2_1	FLASH_TIER2_2	FLASH_TIER2_3	FLASH_TIER2_4	FLASH_TIER3_1	FLASH_TIER3_2	FLASH_TIER3_3	FLASH_TIER3_4	230
0,0	137,9	0,0	91,7	0,0	152,5	0,0	221,6	
FRACK_TIER1_DOOR	FRACK_TIER1_FRONT	FRACK_TIER2_DOOR	FRACK_TIER2_FRONT	FRACK_TIER3_DOOR	FRACK_TIER3_FRONT	FRACK_TIER4_DOOR	FRACK_TIER4_FRONT	150
-49,4	-31,4	21,4	23,7	-114,9	-114,9	-68,8	-64,9	
FRACK_TIER5_DOOR	FRACK_TIER5_FRONT	FRACK_TIER6_DOOR	FRACK_TIER6_FRONT					150
-33,3	-26,5	-8,8	-8,8					
FPOST_TIER1_1	FPOST_TIER1_2	FPOST_TIER1_3	FPOST_TIER1_4	FPOST_TIER2_1	FPOST_TIER2_2	FPOST_TIER2_3	FPOST_TIER2_4	848
387,1	260,6	565,2	96,7	296,3	217,8	579,8	69,9	
FPOST_TIER3_1	FPOST_TIER3_2	FPOST_TIER3_3	FPOST_TIER3_4	FPOST_TIER4_1	FPOST_TIER4_2	FPOST_TIER4_3	FPOST_TIER4_4	848
208,6	0,0	260,8	0,0	107,2	0,0	98,2	0,0	
FPOST_TIER5_1	FPOST_TIER5_2	FPOST_TIER5_3	FPOST_TIER5_4	FPOST_TIER6_1	FPOST_TIER6_2	FPOST_TIER6_3	FPOST_TIER6_4	848
37,9	0,0	21,2	15,7	0,0	0,0	0,0	0,0	
FTLZ_TIER1_1	FTLZ_TIER1_2	FTLZ_TIER1_3	FTLZ_TIER1_4	FTLZ_TIER2_1	FTLZ_TIER2_2	FTLZ_TIER2_3	FTLZ_TIER2_4	250
0,0	0,0	0,0	0,0	0,0	0,0	0,0	0,0	
FTLZ_TIER3_1	FTLZ_TIER3_2	FTLZ_TIER3_3	FTLZ_TIER3_4	FTLZ_TIER4_1	FTLZ_TIER4_2	FTLZ_TIER4_3	FTLZ_TIER4_4	250
0,0	0,0	0,0	124,1	0,0	21,1	0,0	76,7	
FTLZ_TIER5_1	FTLZ_TIER5_2	FTLZ_TIER5_3	FTLZ_TIER5_4	FTLZ_TIER6_1	FTLZ_TIER6_2	FTLZ_TIER6_3	FTLZ_TIER6_4	250
0,0	7,0	0,0	0,0	0,0	0,0	0,0	0,0	

The cargo capacity was limited by the lashing force at the uplifted corner (FLASH_TIER3_4) – bottom corner at the port side of the front end of the 3rd tier container – as shown in Table 7.9.

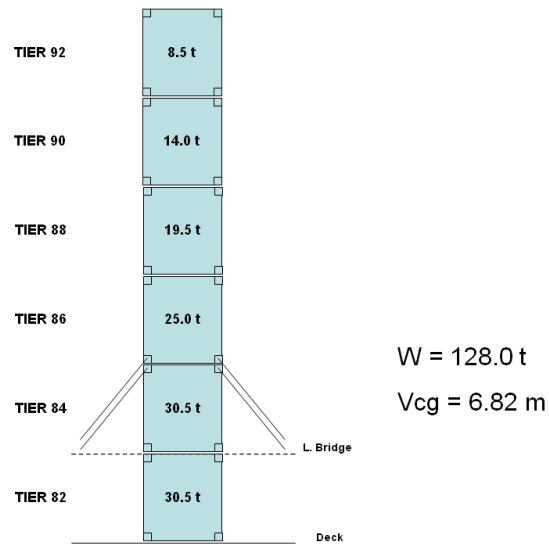


Figure 7.9 – Configuration for 6-tier high stack with 1-tier high lashing bridge and external lashing.

The same stack configuration was analyzed using internal lashing arrangement. The container post load at the starboard side of the front end of the 2nd tier container (FPOST_TIER2_3) and the uplifting force at the port side of the door end of the 3rd tier container (FTLZ_TIER3_4) were exceeded. It was necessary to remove 2 tons of cargo from the uppermost container to have all the loads below the limits. The obtained stack configuration has 126.0 tons (W_{stack}) and a vertical height of the gravity center (V_{cg}) of 6.68 meters (Figure 7.10). The results are shown in Table 7.10.

Table 7.10 – Numerical results for 6-tier high stack and 1-tier high lashing bridge using internal lashing arrangement.

RESULT (kN)								LIMIT (kN)
FLASH_TIER2_1	FLASH_TIER2_2	FLASH_TIER2_3	FLASH_TIER2_4	FLASH_TIER3_1	FLASH_TIER3_2	FLASH_TIER3_3	FLASH_TIER3_4	230
184,2	0,0	190,8	0,0	188,9	0,0	185,7	52,9	
FRACK_TIER1_DOOR	FRACK_TIER1_FRONT	FRACK_TIER2_DOOR	FRACK_TIER2_FRONT	FRACK_TIER3_DOOR	FRACK_TIER3_FRONT	FRACK_TIER4_DOOR	FRACK_TIER4_FRONT	150
0,4	-40,6	57,4	17,8	-112,3	-112,0	-65,3	-61,0	
FRACK_TIER5_DOOR	FRACK_TIER5_FRONT	FRACK_TIER6_DOOR	FRACK_TIER6_FRONT					848
-29,2	-23,6	-6,7	-6,7					
FPOST_TIER1_1	FPOST_TIER1_2	FPOST_TIER1_3	FPOST_TIER1_4	FPOST_TIER2_1	FPOST_TIER2_2	FPOST_TIER2_3	FPOST_TIER2_4	250
713,2	0,0	759,5	0,0	581,6	0,0	845,8	0,0	
FPOST_TIER3_1	FPOST_TIER3_2	FPOST_TIER3_3	FPOST_TIER3_4	FPOST_TIER4_1	FPOST_TIER4_2	FPOST_TIER4_3	FPOST_TIER4_4	
195,8	0,0	240,6	0,0	91,9	0,0	89,0	0,0	
FPOST_TIER5_1	FPOST_TIER5_2	FPOST_TIER5_3	FPOST_TIER5_4	FPOST_TIER6_1	FPOST_TIER6_2	FPOST_TIER6_3	FPOST_TIER6_4	250
28,9	0,0	15,9	12,1	0,0	0,0	0,0	0,0	
FTLZ_TIER1_1	FTLZ_TIER1_2	FTLZ_TIER1_3	FTLZ_TIER1_4	FTLZ_TIER2_1	FTLZ_TIER2_2	FTLZ_TIER2_3	FTLZ_TIER2_4	250
0,0	0,0	0,0	0,0	0,0	0,0	0,0	0,5	
FTLZ_TIER3_1	FTLZ_TIER3_2	FTLZ_TIER3_3	FTLZ_TIER3_4	FTLZ_TIER4_1	FTLZ_TIER4_2	FTLZ_TIER4_3	FTLZ_TIER4_4	
0,0	0,0	0,0	224,2	0,0	18,0	0,0	66,1	
FTLZ_TIER5_1	FTLZ_TIER5_2	FTLZ_TIER5_3	FTLZ_TIER5_4	FTLZ_TIER6_1	FTLZ_TIER6_2	FTLZ_TIER6_3	FTLZ_TIER6_4	250
0,0	0,9	0,0	0,0	0,0	0,0	0,0	0,0	

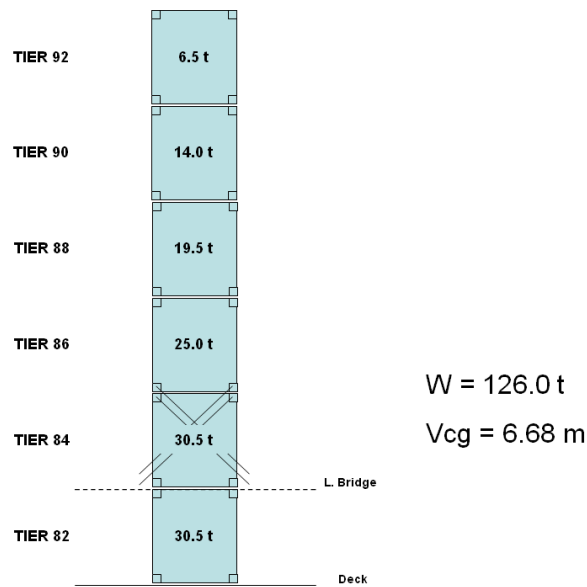


Figure 7.10 – Configuration for 6-tier high stack with 1-tier high lashing bridge and internal lashing.

7.2.3. 4-Tier High Stack with no Lashing Bridge

Using external lashing arrangement, the obtained stack weight was 92.0 tons (W_{stack}), with a vertical height of the stack gravity center (V_{cg}) of 4.69 meters. The obtained stack is shown in Figure 7.11.

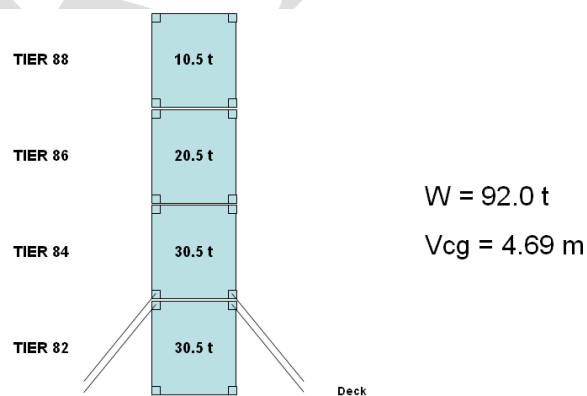


Figure 7.11 – Configuration for 4-tier high stack with no lashing bridge and external lashing.

The cargo capacity was limited by the lashing force at the uplifted corner (FLASH_TIER2_4) – bottom corner at the port side of the front end of the 2nd tier container – as shown in Table 7.11.

The same stack configuration was evaluated using internal lashing arrangement. All the evaluated operational loads were below the limits, with a considerable safety margin. More cargo was added to the stack, and the obtained configuration is the maximum cargo capacity using internal lashing arrangement ($W_{stack} = 107.5$ tons) from section 7.1.3.

Table 7.11 – Numerical results for 4-tier high stack and no lashing bridge using external lashing arrangement.

RESULT (kN)								LIMIT (kN)
FLASH_TIER1_1	FLASH_TIER1_2	FLASH_TIER1_3	FLASH_TIER1_4	FLASH_TIER2_1	FLASH_TIER2_2	FLASH_TIER2_3	FLASH_TIER2_4	230
0,0	97,3	0,0	44,0	0,0	110,6	0,0	226,6	
FRACK_TIER1_DOOR	FRACK_TIER1_FRONT	FRACK_TIER2_DOOR	FRACK_TIER2_FRONT	FRACK_TIER3_DOOR	FRACK_TIER3_FRONT	FRACK_TIER4_DOOR	FRACK_TIER4_FRONT	150
-18,2	7,4	-96,8	-95,5	-43,3	-36,7	-10,9	-10,9	
FPOST_TIER1_1	FPOST_TIER1_2	FPOST_TIER1_3	FPOST_TIER1_4	FPOST_TIER2_1	FPOST_TIER2_2	FPOST_TIER2_3	FPOST_TIER2_4	848
222,0	205,8	436,1	33,5	138,0	0,3	136,3	0,0	
FPOST_TIER3_1	FPOST_TIER3_2	FPOST_TIER3_3	FPOST_TIER3_4	FPOST_TIER4_1	FPOST_TIER4_2	FPOST_TIER4_3	FPOST_TIER4_4	250
47,0	0,0	26,0	20,1	0,0	0,0	0,0	0,0	
FTLZ_TIER1_1	FTLZ_TIER1_2	FTLZ_TIER1_3	FTLZ_TIER1_4	FTLZ_TIER2_1	FTLZ_TIER2_2	FTLZ_TIER2_3	FTLZ_TIER2_4	250
0,0	0,0	0,0	0,0	0,0	0,0	0,0	0,0	
FTLZ_TIER3_1	FTLZ_TIER3_2	FTLZ_TIER3_3	FTLZ_TIER3_4	FTLZ_TIER4_1	FTLZ_TIER4_2	FTLZ_TIER4_3	FTLZ_TIER4_4	250
0,0	0,0	0,0	0,0	0,0	0,0	0,0	0,0	

7.3. Additional Calculation

For small stacks of light containers, it is possible to have a lashing arrangement where lashing assemblies are connected only to the bottom corners of the 2nd tier container. In order to compare the performance of external and internal lashing for this configuration, a 4-tier high stack with no lashing bridge was modelled using external lashing arrangement (Figure 7.12). The stack is composed by 2 fully loaded containers at the base and a linear weight distribution up to the top, with a stack weight of 90.5 tons and a vertical position of the stack gravity center of 4.62 meters.

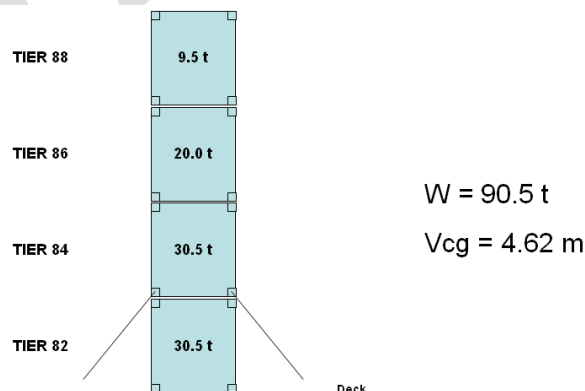


Figure 7.12 – Top lashed 4-tier high stack with no lashing bridge and external lashing.

Once again, the cargo capacity was limited by the lashing force at the uplifted corner (FLASH_TIER2_4) – bottom corner at the port side of the front end of the 2nd tier container – as shown in Table 7.12.

Table 7.12 – Numerical results for 4-tier high stack and no lashing bridge using external lashing arrangement for top lashed configuration.

RESULT (kN)								LIMIT (kN)
				FLASH_TIER2_1	FLASH_TIER2_2	FLASH_TIER2_3	FLASH_TIER2_4	230
				0,0	179,3	0,0	225,1	
FRACK_TIER1_DOOR	FRACK_TIER1_FRONT	FRACK_TIER2_DOOR	FRACK_TIER2_FRONT	FRACK_TIER3_DOOR	FRACK_TIER3_FRONT	FRACK_TIER4_DOOR	FRACK_TIER4_FRONT	150
-29,3	-17,9	-93,8	-92,5	-40,9	-34,7	-9,8	-9,8	
FPOST_TIER1_1	FPOST_TIER1_2	FPOST_TIER1_3	FPOST_TIER1_4	FPOST_TIER2_1	FPOST_TIER2_2	FPOST_TIER2_3	FPOST_TIER2_4	848
205,3	191,3	427,8	0,0	128,3	3,3	129,8	0,0	
FPOST_TIER3_1	FPOST_TIER3_2	FPOST_TIER3_3	FPOST_TIER3_4	FPOST_TIER4_1	FPOST_TIER4_2	FPOST_TIER4_3	FPOST_TIER4_4	
42,5	0,0	23,3	18,4	0,0	0,0	0,0	0,0	
FTLZ_TIER1_1	FTLZ_TIER1_2	FTLZ_TIER1_3	FTLZ_TIER1_4	FTLZ_TIER2_1	FTLZ_TIER2_2	FTLZ_TIER2_3	FTLZ_TIER2_4	250
0,0	0,0	0,0	0,0	0,0	0,0	0,0	0,0	
FTLZ_TIER3_1	FTLZ_TIER3_2	FTLZ_TIER3_3	FTLZ_TIER3_4	FTLZ_TIER4_1	FTLZ_TIER4_2	FTLZ_TIER4_3	FTLZ_TIER4_4	
0,0	0,0	0,0	0,0	0,0	0,0	0,0	0,0	

The same stack was analyzed using internal lashing arrangement and the lashing assembly connected to the starboard side of the door end of the 2nd tier container was overloaded. Cargo was removed from the stack, keeping a linear distribution, and the stack configuration with maximum cargo ($W_{stack} = 85.3$ tons) and loads below the limits is shown in Figure 7.13. The obtained results are shown in Table 7.13.

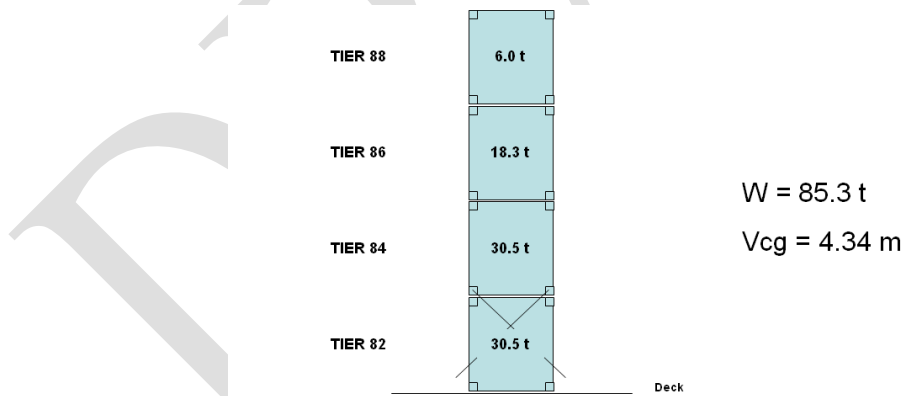


Figure 7.13 – Top lashed 4-tier high stack with no lashing bridge and internal lashing.

Table 7.13 – Numerical results for 4-tier high stack and no lashing bridge using internal lashing arrangement for top lashed configuration.

RESULT (kN)								LIMIT (kN)
				FLASH_TIER2_1	FLASH_TIER2_2	FLASH_TIER2_3	FLASH_TIER2_4	
				229,2	0,0	188,9	106,3	230
FRACK_TIER1_DOOR	FRACK_TIER1_FRONT	FRACK_TIER2_DOOR	FRACK_TIER2_FRONT	FRACK_TIER3_DOOR	FRACK_TIER3_FRONT	FRACK_TIER4_DOOR	FRACK_TIER4_FRONT	
12,7	-96,6	-83,3	-76,6	-31,9	-27,5	-6,2	-6,2	150
FPOST_TIER1_1	FPOST_TIER1_2	FPOST_TIER1_3	FPOST_TIER1_4	FPOST_TIER2_1	FPOST_TIER2_2	FPOST_TIER2_3	FPOST_TIER2_4	
399,6	8,8	454,6	0,0	108,2	0,0	94,3	12,0	848
FPOST_TIER3_1	FPOST_TIER3_2	FPOST_TIER3_3	FPOST_TIER3_4	FPOST_TIER4_1	FPOST_TIER4_2	FPOST_TIER4_3	FPOST_TIER4_4	
26,9	0,0	14,0	12,1	0,0	0,0	0,0	0,0	
FTLZ_TIER1_1	FTLZ_TIER1_2	FTLZ_TIER1_3	FTLZ_TIER1_4	FTLZ_TIER2_1	FTLZ_TIER2_2	FTLZ_TIER2_3	FTLZ_TIER2_4	250
0,0	0,0	0,0	0,0	0,0	0,0	0,0	0,0	
FTLZ_TIER3_1	FTLZ_TIER3_2	FTLZ_TIER3_3	FTLZ_TIER3_4	FTLZ_TIER4_1	FTLZ_TIER4_2	FTLZ_TIER4_3	FTLZ_TIER4_4	
0,0	0,0	0,0	0,0	0,0	0,0	0,0	0,0	

8. ADDITIONAL STUDIES

It was observed in section 5.6 the influence of the lashing stiffness – equivalent stiffness from the association of the lashing assembly and lashing bridge – over the operational loads acting on lashing equipments and containers stowed on weather deck.

The stiffness values used in the calculations were taken from (GL 2012). According them, the lashing assembly stiffness should be evaluated by tensile tests and the obtained value used for the design of cargo stowage. When experiments are not possible to be performed, the rule based method can be used for the lashing assembly stiffness determination. For the lashing bridge, the maximum deflection values required by the rules should be checked during design and classification stages. However, even respecting this criterion, lashing bridge stiffness values can be widely different.

The lashing assembly and the lashing bridge designs used on the container ship studied in section 5 were analyzed using numerical calculation by FEM and the obtained values were compared to the rule based approach.

8.1. Lashing Assembly Stiffness

The lashing assembly was evaluated using the software *ANSYS Mechanical* for the pre-processing, solution and results post-processing. The numerical model is composed by the turnbuckle, lashing rod, rod head and corner casting (Figure 8.1).

The lashing positioning and the corner casting geometry represent the top side of a bottom lashed HQ container, using the lashing plans available on the CSM of the ship. The corner casting is manufactured in a type of structural steel much softer than the lashing assembly. Thus, plastic deformations may occur in the corner casting when pressure load is applied by the rod head. These plastic deformations can have influence on the overall stiffness of the lashing assembly, which motivated the modelling of the corner casting as an elasto-plastic material with 10% of hardening. The lashing rod, turnbuckle and rod head are manufactured

in high tensile steel and were modelled as linear elastic materials. The material properties can be seen in Table 8.1.

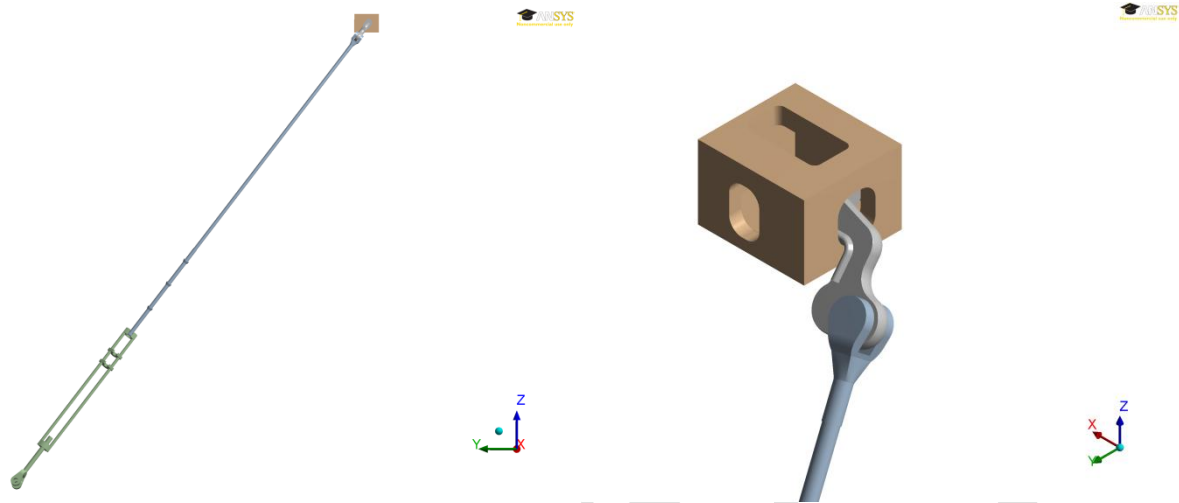


Figure 8.1 – Lashing assembly geometry.

Constraint equations were used on the interface between the lashing rod and the turnbuckle, coupling the displacements both in the normal and in the tangential direction of these regions (bonded contact). For the interface between the lashing rod and the rod head, contact elements were modelled in order to have freedom of rotation without friction (frictionless contact). In the interface between the rod head and the corner casting (Figure 8.1), constraint equations were used to couple the normal and tangential displacements of the surfaces, assuming no relative deformation between the bodies after the lashing pre-tension application.

Table 8.1 – Material properties for the lashing assembly analysis.

<i>Part</i>	<i>Young's Modulus (GPa)</i>	<i>Poisson's Coefficient</i>	<i>Yield Stress (MPa)</i>	<i>Tangent Modulus (GPa)</i>
Lashing Assembly	205	0.3	675	-
Corner Casting	205	0.3	235	20.5

The corner casting and the rod head were modelled using second order tetrahedral elements (*SOLID187*) while the lashing rod and the turnbuckle were modelled using first order solid elements (*SOLID185*). The mesh is composed by 85,960 elements and 77,771 nodes.

The corner casting had its displacements fixed at the faces which are welded to the container frames. A pilot node was linked by rigid elements (*MPC184*) to the base of the turnbuckle, and an axial displacement was applied at this point (local Z axis in Figure 8.2) until the lashing force limit was achieved. The lateral displacements of the pilot node (X and Y local axes in Figure 8.2) were constrained. The numerical analysis was performed using large deflections theory.

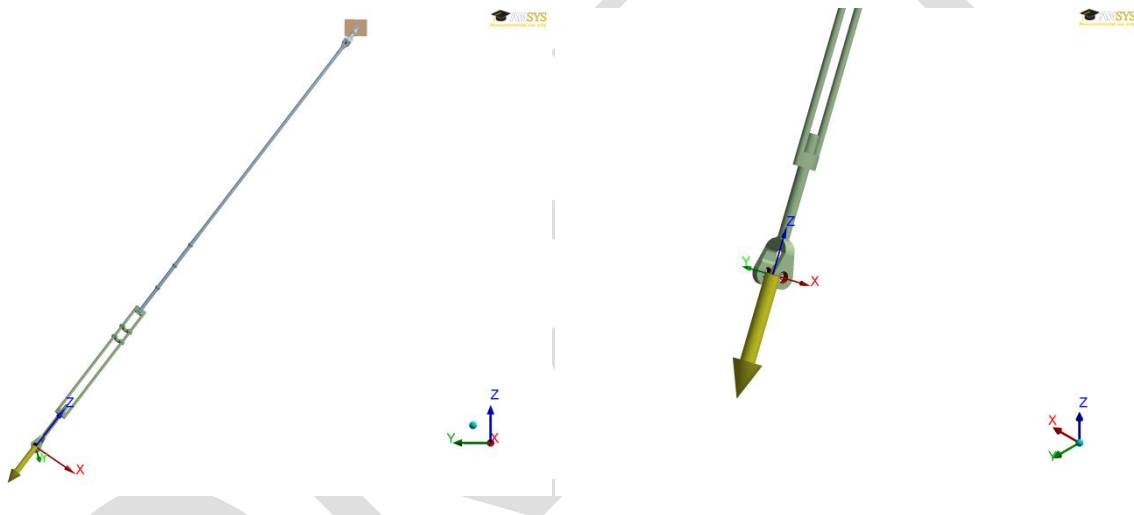


Figure 8.2 – Axial displacement applied in the base of the turnbuckle.

The axial force reaction at the pilot node connected to the turnbuckle was measured during the analysis and a Force x Deformation curve was generated (Figure 8.3). From the slope of the curve, the numerical value of the lashing assembly stiffness (k_{rod}) was obtained as 19.5 kN/mm. In the beginning of the curve, an accommodation region with can be observed. Constant slope is observed beyond the pre-tension value (around 5 kN).

The overall length of the lashing assembly (L_{rod}) is 3940.4 mm and the diameter of the lashing rod (D_{rod}) is 23 mm, which gives a cross sectional area (A_{rod}) of 415.5 mm². According the Equation (4-1), the equivalent modulus of elasticity (E_{rod}) is obtained as 184 GPa.

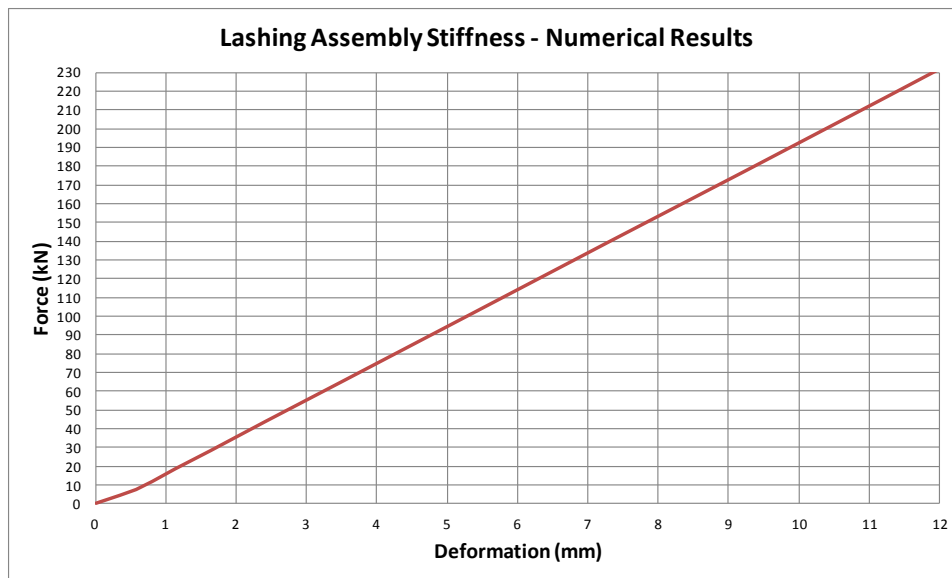


Figure 8.3 – Force x Deformation curve of the lashing assembly.

8.2. Lashing Bridge Stiffness

Two lashing bridge designs used on the studied container ship – 1-tier high and 2-tier high lashing bridge (Figure 8.4) – were modelled using the software *Poseidon*. The designs were modelled using beam elements, and the cross-sectional properties of each profile were inputted into the software. A linear static calculation was performed to obtain the displacement values on the lashing plate positions due to the lashing forces applied, considering the ship rolling to the starboard.

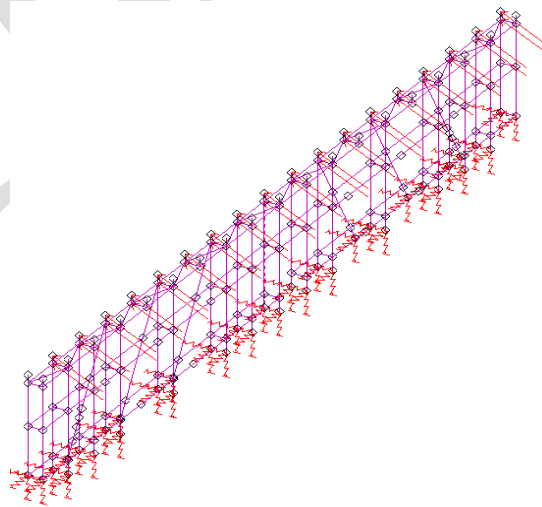


Figure 8.4 – FE model of the 2-tier high lashing bridge.

The deflection values were measured in two steps: first, the loads were applied in the direction of the lashing assemblies connected to the door end of the bay; later, in the direction of the lashing assemblies connected to the front end of the bay.

On each position of a lashing plate connected to the containers of the bay, a force correspondent to 61% of the service working load (*SWL*) was applied, according (GL 2012). This hypothesis assumes all lashing assemblies loaded, but with different load forces, with an average value of 140.3 kN (0.61 x 230 kN) on the direction of the lashing assembly.

The lashing bridge stiffness (k_{bridge}) was calculated for each case dividing the *SWL* by the average value of the measured deformations on the direction of the applied forces, according to Equation (8-1).

$$k_{bridge} = \frac{1}{N} \sum_{i=1}^N \frac{SWL}{u_F^i} \quad (8-1)$$

Table 8.2 – Numerical result of the 1-tier high lashing bridge stiffness.

<i>Lashing Position</i>	<i>Average Value</i>	<i>Standard Deviation</i>
	k_{bridge} (kN/mm)	k_{bridge} (kN/mm)
2 nd Tier – Port Side – Door End	31.66	8.18
3 rd Tier – Port Side – Door End	29.13	7.23
2 nd Tier – Port Side – Front End	33.41	7.12
3 rd Tier – Port Side – Front End	29.79	5.34
Overall	31.00	7.09

The obtained lashing bridge stiffness values (k_{bridge}) are presented in Table 8.2 for 1-tier high lashing bridge and in Table 8.3 for 2-tier high lashing bridge and correspond, respectively, to 31.0 kN/mm and 19.6 kN/mm.

Table 8.3 – Numerical result of the 2-tier high lashing bridge stiffness.

<i>Lashing Position</i>	<i>Average Value</i>	<i>Standard Deviation</i>
	k_{bridge} (kN/mm)	k_{bridge} (kN/mm)
3 rd Tier – Port Side – Door End	20.50	6.25
4 th Tier – Port Side – Door End	20.00	6.63
3 rd Tier – Port Side – Front End	19.58	3.19
4 th Tier – Port Side – Front End	18.51	2.75
Overall	19.65	4.97

9. CONCLUSIONS

The main objectives established in section 1.2 were achieved during this study. The parameters which influence the operational loads acting on container stacks stowed on weather deck using external lashing arrangement were identified in section 5. A simplified method to take into account the influence of the vertical clearance of locks on the load sharing between lashing assemblies and twist locks was proposed in section 6. The cargo capacity for different lashing arrangements – internal and external – was compared for different stack configurations in section 7. And, in section 8, the stiffness values for the lashing assemblies and lashing bridges from a real case were evaluated using numerical simulation and compared to the values suggested by (GL 2012), which were used in the present study.

The lashing stiffness and the vertical clearance were identified as the most significant stack parameters affecting the operational loads. The simplified method from section 6, to account the influence of the clearance on the lashing force, as a function of the lashing stiffness, can be used on the rules for classification and construction from GL (GL 2012), in order to permit the use of external lashing arrangement, which at this time is not permitted by this classification society.

The cargo capacities of internal and external lashing arrangements were compared in section 7 using two methodologies: the maximum cargo capacity, without taking into account the cargo distribution; linear cargo distribution, representing a case more close to a real application. For some cases external lashing arrangement was found more interesting than internal lashing, while for others it was the opposite.

External lashing was verified as more interesting than internal lashing for the 8-tier high stack with 2-tier high lashing bridge. Changing the lashing configuration from internal to external, the maximum cargo capacity is increased in 9.5% (section 7.1.1). Considering 16 rows in a bay and 11 bays with the same configuration, the ship's capacity using external lashing can be increased in 2,640 tons. When a linear distribution is used, the cargo capacity is increased from internal to external lashing arrangement in 11.1% (section 7.2.1).

For the 6-tier high stack with 1-tier high lashing bridge there was no significant difference between the lashing arrangements. The maximum cargo capacity was the same for both cases (section 7.1.2), and adopting a linear cargo distribution the capacity is increased from internal to external lashing in 1.6% (section 7.2.2).

In the other hand, internal lashing arrangement was found more interesting than external lashing for the 4-tier high stack with no lashing bridge. The maximum cargo capacity from internal to external lashing is decreased in 11.2% (section 7.1.3). When a linear cargo distribution was adopted, the cargo capacity is reduced in 14.4% from internal to external lashing (section 7.2.3).

For large container ships, stacking containers up to 8 or 9 tiers up, external lashing is an interesting arrangement. It supports higher stack weights and allows heavier containers stacked up in the stack, which is very interesting for the shipping companies. The use of this solution can contribute to increase maritime container efficiency and the economy of scale.

The lashing stiffness values from a real case evaluated in section 8 are considerably different from the rule based values suggested by (GL 2012). The numerically calculated value of the equivalent modulus of elasticity of the lashing rod (E_{rod}), 184 GPa, is 31% greater than the rule base value proposed by (GL 2012), 140 GPa, and 90% greater than the value proposed by (ABS 2010), 97.1 GPa.

The average values for the lashing bridge stiffness (k_{bridge}) obtained in section 8.2 are 35% greater than the rule based values proposed by (GL 2012), for the case of 1-tier high, and 114% greater for the case of 2-tier high lashing bridge.

The lashing stiffness values proposed by (GL 2012) must be reviewed and possibly updated. Other lashing assemblies designs must be evaluated experimentally and numerically and different lashing bridge designs can be evaluated numerically using more detailed FE models.

9.1. Future Work

The rule based design approach presented in section 6 shall be verified and compared to numerical results. Other analytical methods to take into account the dependence of the lashing force on the vertical clearance can be developed both for use in design synthesis (by ship owners and shipyards) in design analysis (by classification societies).

The cargo capacity comparison between internal and external lashing arrangements shall be performed again using the stiffness values taken from the real case or using updated values on the classification rules. The lashing stiffness affects the load sharing between twist locks and lashing assemblies and can affect the cargo capacity results.

The possible interference between lashing rods connected to adjacent stacks using external lashing arrangement, when stacks are subjected to relative longitudinal displacement, must be carefully verified using numerical simulation and experimental tests. This phenomenon can be a drawback of the external lashing arrangement.

DRAFT

10. ACKNOWLEDGEMENTS

This thesis was developed in the frame of the European Master Course in “Integrated Advanced Ship Design” named “EMSHIP” for “European Education in Advanced Ship Design”, Ref.: 159652-1-2009-1-BE-ERA MUNDUS-EMMC.

The studies presented here were developed during a 4 months internship at the Research and Rule Development Department of Germanischer Lloyd SE, in Hamburg – Germany. Even during this short time it was possible to learn about the rule development process and contribute to research activities of a well known classification society. I would like to thank the whole department, in the name of the head of department Mr. Arne Schulz-Heimbeck, and especially Mr. Viktor Wolf, who supervised my work, corrected my mistakes and was always available for my doubts and questions.

This master thesis concludes the studies performed in the framework of the EMSHIP program. Much more than a master course, this international experience is an opportunity to learn about different cultures. In my case, during the 18 months of the master course, I had the opportunity of living in 4 countries and travelling around other 9, understanding different regional aspects, customs and socioeconomic conditions. Besides the European teachers we had, visiting professors from North and South America, Japan, Bangladesh and Turkey shared their knowledge and experience with us, contributing to the success of the course. As a Brazilian citizen, a developing country, I will take all this knowledge and use it to contribute on the development of my country.

I thank all my colleagues, friends from all over the world I made during this period and my teachers for the great experience I had; my family – my father Antonio, my mother Regina, my sisters Monica and Fabiana and my nephew and godson Enrico, the joy of the family – for the unconditional support during my whole life and my studies; and my fiancé and future wife Angelica, who was with me during this great time, helping me, supporting me, taking care of me and enjoying this experience abroad with me.

DRAFT

11. BIBLIOGRAPHY

ABS. *Guide for Certification of Container Securing Systems*. Houston, USA: American Bureau of Shipping, 2010.

Cargotec. "Flexilash." *Cargotec Solutions*. 2005. <http://www.cargotec.com/en-global/PS/Lashing-equipment/Container-lashing-systems/Flexilash/Pages/default.aspx> (accessed January 13, 2013).

Containertech. "Container Ship types." *Containertech Main Page*. 2008. <http://www.containertech.no/no/SEcontainershiptypes.htm> (accessed January 13, 2013).

DNV. "Container Securing." In *Classification Notes*, No. 32.2. Høvik, Norway: Det Norske Veritas, 2011.

Ebeling, Charles W. "Evolution of a Box." *Invention & Technology*, Winter 2009: Volume 3, Issue 4.

GL. "Stowage and Lashing of Containers." In *Rules for Classification and Construction*. Hamburg, Germany: Germanischer Lloyd SE, 2012.

Hanjin. "Service Network." *Hanjin Shipping*. 2013. http://www.hanjin.com/hanjin/CUP_HOM_1100.do?sessLocale=en# (accessed January 13, 2013).

IACS. "No. 45 Guidelines for Container Corner Fittings." *International Association of Classification Societies*. 2004. http://www.iacs.org.uk/document/public/publications/guidelines_and_recommendations/pdf/REC_45_pdf191.pdf (accessed January 13, 2013).

LR. "Cargo Securing Arrangements." In *Rules and Regulations for the Classification of Ships*, Part 3, Chapter 14. London, United Kingdom: Lloyd's Register, 2011.

Maersk. "International shipping between Asia & Europe with Triple-E." *The Worlds Largest Ship is the Maersk Line Triple-E class vessel*. 2013. <http://www.worldslargestship.com/shipping/> (accessed January 13, 2013).

MARIN. *Lashing @ Sea 19717-20-TM*. Executive Summary, Wageningen, The Netherlands: Maritime Research Institute Netherlands, 2009.

Murdoch, Erich, and David Tozer. *A Master's Guide to Container Securing*. London, United Kingdom: Lloyd's Register; The Standard P&I Club.

Rathje, Helge, Ionel Darie, and Daniel Schnorrer. "Seaborne Container Losses and Damages." *Schiffbautechnische Gesellschaft*. Hamburg, Germany, 2008.

Schellin, Thomas E., Helge Rathje, and Adrian Kahl. "High-Frequency Ship Response Assessment of Large Containerships." *International Journal of Offshore and Polar Engineering (ISSN 1053-5381)*, Vol. 22, No. 2, June 2012: 115-122.

SEC. *Products & Services*. Catalogue, Bremen, Germany: Ship's Equipment Centre GmbH, 2007.

Souza, Vinicius Aguiar de, Levent Kirkayak, Katsuyuki Suzuki, Hideyuki Ando, and Hidetoshi Sueoka. "Experimental and numerical analysis of container stack dynamics." *Ocean Engineering*, 2012: *Ocean Engineering* 39 (2012) 24–42.

Transportation Research Board. "The Intermodal Container Era." *TR News*, September-October 2006: 5-9.

US Army. "Port And Inland Waterways Modernization: Preparing For Post-Panamax Vessels." *IWR - U.S. Army Engineer Institute for Water Resources*. 2013. http://www.iwr.usace.army.mil/index.php?option=com_content&view=article&catid=44:project-stories&id=820:ports-and-waterways-expansion-study&Itemid=4 (accessed January 13, 2013).

Wikipedia. "List of largest containerships." *Wikipedia*. 2013. http://en.wikipedia.org/wiki/List_of_largest_container_ships (accessed January 13, 2013).

Wolf, Viktor, and Helge Rathje. "Motion Simulation of Container Stacks on Deck." *SNAME Annual Meeting and Ship Production Symposium Proceedings*. Society of Naval Architects and Marine Engineers, 2009. 1: 277-285.

Wolf, Viktor, Ionel Darie, and Helge Rathje. "Rule Development for Container Stowage on Deck." *International Conference on Marine Structures*. Hamburg, Germany: MARSTRUCT, 2011.

WSC. "Trade Statistics." *World Shipping Council*. 2013.
<http://www.worldshipping.org/about-the-industry/global-trade/trade-statistics> (accessed January 13, 2013).

DRAFT

DRAFT

12. APPENDIX I – TRADE STATISTICS

Table 12.1 – Top 20 exporters of containerized cargo from 2009 and 2010 (WSC 2013).

RANK	EXPORTER	2009 TEUS (MILLIONS)	2010 TEUS (MILLIONS)
1	China	26.1	31.3
2	United States	10.2	11.2
3	Japan	4.8	5.7
4	South Korea	4.5	5.2
5	Taiwan, China	2.9	3.4
6	Thailand	3.0	3.4
7	Germany	2.6	3.0
8	Indonesia	2.7	3.0
9	Malaysia	2.2	2.5
10	Brazil	2.3	2.3
11	India	1.6	1.9
12	Vietnam	1.3	1.6
13	Saudi Arabia	1.1	1.6
14	Italy	1.5	1.6
15	Turkey	1.4	1.6
16	Netherlands	1.4	1.6
17	Canada	1.4	1.5
18	United Kingdom	1.4	1.5
19	France	1.2	1.3
20	Hong Kong	1.2	1.3
World Total		99.8	114.3

Note: TEUs are fully loaded.

Table 12.2 – Top 20 importers of containerized cargo from 2009 and 2010 (WSC 2013).

RANK	IMPORTER	2009 TEUS (MILLIONS)	2010 TEUS (MILLIONS)
1	United States	15.0	17.6
2	China	11.2	12.0
3	Japan	5.4	6.1
4	South Korea	3.9	4.5
5	Germany	2.4	2.8
6	Other Arabian Gulf	2.3	2.7
7	United Kingdom	2.3	2.5
8	Indonesia	2.1	2.5
9	Taiwan	2.2	2.5
10	Hong Kong	2.3	2.5
11	Western Africa	2.5	2.4
12	United Arab Emirates	2.0	2.1
13	Malaysia	1.7	2.1
14	Thailand	1.6	2.0
15	Vietnam	1.8	2.0
16	India	1.7	2.0
17	Brazil	1.3	1.9
18	Australia	1.5	1.8
19	Italy	1.6	1.8
20	Netherlands	1.3	1.7
World Total		99.7	114.3

Note: TEUs are fully loaded.

Table 12.3 – Top 20 European Union exporters of containerized cargo from 2010 (WSC 2013).

RANK	EXPORTER	2010 TEUS
1	Germany	3,036,978
2	Italy	1,635,234
3	Netherlands	1,585,773
4	United Kingdom	1,469,172
5	France	1,328,393
6	Spain	1,201,957
7	Belgium	1,104,244
8	Sweden	597,604
9	Finland	584,255
10	Austria	452,709
11	Portugal	288,368
12	Denmark	267,874
13	Poland	225,379
14	Greece	195,839
15	Ireland	184,360
16	Czech Republic	162,134
17	Romania	151,761
18	Baltics (Estonia, Latvia and Lithuania)	105,315
19	Hungary	85,934
20	Bulgaria	63,195
EU Total		14,846,543

Note: TEUs are fully loaded.




Table 12.4 – Top 20 European Union importers of containerized cargo from 2010 (WSC 2013).

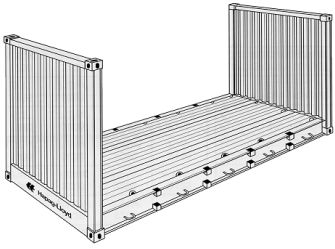
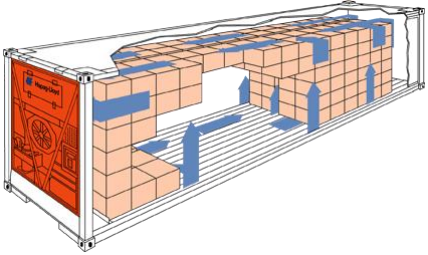
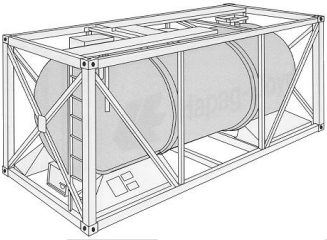

RANK	IMPORTER	2010 TEUS
1	Germany	2,841,570
2	United Kingdom	2,513,450
3	Italy	1,766,774
4	Netherlands	1,656,708
5	France	1,547,080
6	Belgium	1,464,825
7	Spain	1,433,358
8	Poland	555,338
9	Sweden	371,186
10	Czech Republic	310,237
11	Denmark	254,702
12	Greece	238,948
13	Austria	237,873
14	Finland	236,095
15	Baltics (Estonia, Latvia and Lithuania)	222,293
16	Portugal	207,965
17	Ireland	203,872
18	Romania	163,165
19	Hungary	161,881
20	Slovak Republic	144,099
EU Total		16,779,910

Note: TEUs are fully loaded.

13. APPENDIX II – CONTAINER TYPES

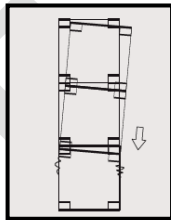
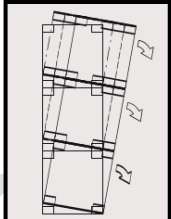
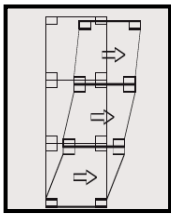
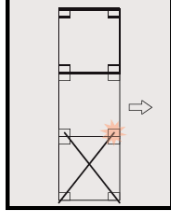


Table 13.1 – Container types.

<i>Type</i>	<i>Image</i>	<i>Characteristics</i>
Dry Van Box		<ul style="list-style-type: none"> • The most common type • Corrugated steel walls with plate thickness \geq 1.6mm • Timber base and steel or glass reinforce plastic top • Their frame consists of side and end rails and corner pillars, fitted with corner castings • The front end is approximately 4.5 times stiffer than the door end (racking stiffness)
Curtain Wall		<ul style="list-style-type: none"> • Similar to dry van boxes • Fabric side walls that can be opened to facilitate easy cargo handling
Open Top		<ul style="list-style-type: none"> • Similar to dry van boxes • Walls made by corrugated steel • Roof consists of removable bows and a removable tarpaulin

Flat Rack		<ul style="list-style-type: none"> • Floor structure with a high loading capacity • End walls can be fixed or folded flat for ease of transportation when empty • The structure must have equivalent strength to a dry van box
Reefer		<ul style="list-style-type: none"> • They usually have the same construction than dry van boxes • Usually they have their own refrigeration unit, with and air or water-cooled heat exchanger • They have their own data logger to record temperature
Tank		<ul style="list-style-type: none"> • Steel skeletal framework within which the tank is housed • Steel framework must have equivalent strength to a dry van box • The tank has its own design and strength criteria and it may be a pressure vessel
Bulk		<ul style="list-style-type: none"> • Bulk containers have three loading hatches in the roof • On the door side, there are two discharge hatches, which are sometimes equipped with short discharge tubes for guiding the bulk cargo

14. APPENDIX III – OPERATIONAL LOAD LIMITS

Table 14.1 – Operational load limits for containers and lashing components according (GL 2012).

<i>Load</i>	<i>Limit</i>	<i>Scheme</i>
Container Post Load	848 kN	
Uplifting Force	250 kN	
Racking Force (End Walls)	150 kN	
Lashing Force	230 kN	
Vertical Twist Lock Force	250 kN	
Lateral Twist Lock Force	210 kN	

DRAFT

15. APPENDIX IV – DESIGN CRITERIA WORKFLOW

